SCUOLA DI DOTTORATO
UNIVERSITÀ DEGLI STUDI DI MILANO-BICOCCA

Department of Medicine and Surgery

PhD program in Translational and

Molecular Medicine XXXIII cycle

# ActivinA as a key modulator of B-Cell Precursor Acute Lymphoblastic Leukemia Cell motility and vesiculation within the bone marrow niche

Giulia Cricrì

registration number: 796749

Tutor: Prof. Andrea Biondi

Co-tutor: Dr. Giovanna D'Amico

Dr. Erica Dander

Coordinator: Prof. Andrea Biondi

**ACADEMIC YEAR**

2019/2020

# Table of Contents

# 1. Introduction

## 1.1. B-Cell Precursor Acute Lymphoblastic Leukemia

B-Cell Precursor Acute Lymphoblastic Leukemia (BCP-ALL) is a hematologic heterogenous malignancy caused by a defective development of normal lymphoblasts in mature lymphocytes which are also overproduced within bone marrow (BM), peripheral blood (PB) and other organs. Traditionally, BCP-ALL is likely to arise from lymphoid progenitor cells and it has been classified into precursor T (or T-cell), precursor B (BCP), and B-cell (Burkitt) phenotypes, which are then further subdivided according to recurrent karyotypic abnormalities, including aneuploidy and translocations. Although BCP-ALL occurs in both children and adults, the incidence is respectively of 3-4 cases per 100,000 and 1 case per 100,000 each year. Therefore, patients are predominantly children with peak prevalence between the ages of 2 and 5 years[1]. Over the past five decades, this fatal disease has been transformed to one with a 5-year survival rate exceeding 85% among children receiving protocol-directed treatment in most developed countries. However, relapse still occurs in 10-15% of patients, and death due to the relapsed BCP-ALL remains one of the leading causes of childhood cancer-related mortality[2].

### 1.1.1. Clinical Features

BCP-ALL is a clonal and lymphoid malignant disease, initiated by lymphoblasts committed to the B cell lineage and characterized by their uncontrolled accumulation in the BM. Since these immature lymphoid blasts progressively occupy and alter the BM niche where normal hematopoietic stem cells (HSCs) reside, many of the common symptoms of the disease are typical of BM failure such as bruising or bleeding due to thrombo-cytopenia, pallor and fatigue from anemia, and infection caused by neutropenia. Malignant blasts can also infiltrate extramedullary sites such as lymph nodes, spleen, liver by causing lymphadenopathy, splenomegaly, hepatomegaly as well as the central nervous system (CNS) with cranial nerve deficits and meningismus. In general, BM aspirate of BCP-ALL patients is characterized by a high white blood cell count (more than 20%); less than 20% of lymphoblasts is in fact associated with lymphoma diagnosis. However, morphology, cytogenetics, and immunophenotype are proposed to be the specific clinical features for an accurate diagnosis and risk stratification of BCP-ALL[3]

### 1.1.2. Pathobiology

Currently, only ionizing radiation is an established causal exposure for childhood leukemia, as supported by evidence indicating an appropriate relationship between cancer incidence and atomic bombs survivors[4]. Epidemiological studies provide insights that BCP-ALL can result from an abnormal immune response to one or more common infections (viral or bacterial) in susceptible children which received minimal exposure to infection during infancy and present a persistent in utero-generated pre-leukemic clone plus a variable degree of genetic susceptibility[5]. So far, the precise pathogenetic events leading to BCP-ALL development are unknown. In only a few cases (<5%), inherited and predisposing genetic syndromes such as Down's syndrome, Bloom's syndrome, ataxia-telangiectasia, and Nijmegen breakage syndrome, seems to be associated with an increased risk of childhood BCP-ALL. Since pediatric BCP-ALL is defined as a genetically heterogeneous disease, many studies focused on its mutational landscape and revealed three major categories of genetic alterations: chromosomal translocations, duplications or deletions of large segments of DNA, and point mutations in oncogenes or tumor suppressors[6]. Translocations frequently involve specific transcription-factor genes regulating multiple key cellular pathways such as lymphoid development, tumor suppression, cytokine receptors, kinase and Ras signaling, and chromatin remodeling. About 25% of BCP-ALL cases in children harbors the TEL-AML1 fusion gene, generated by the t(12;21)(p13;q22) translocation. The presence of this

fusion protein in B-cell progenitors leads to the alteration of their self-renewal and differentiation capacities[7]. The BCR–ABL1 fusion protein, characterized by t(9;22)(q34;q11) translocation or the Philadelphia chromosome, occurs in 3% of pediatric BCP-ALL and alters signaling pathways that control the proliferation, survival, and self-renewal of HSCs[8]. The translocation t(1;19)(q23;p13) resulting in the TCF3-PBX1 fusion occurs in approximately 5% of childhood patients and interferes with hematopoietic differentiation[9]. Rearrangements of the mixed-lineage leukemia (MLL) gene, which is located at chromosome 11q23 and occurs in 80 % of infants, create fusion proteins that mediate aberrant self-renewal of hematopoietic progenitors[10]. Also changes in chromosome number such as hyperdiploidy and hypodiploidy can contribute to leukemogenesis. Hyperdiploidy with gain of at least five chromosomes is present in 30% of patients with childhood BCP-ALL and is associated with favorable outcome whereas hypodiploidy with less than 44 chromosomes occurs in 1% of patients and is a negative prognostic factor[11]. Despite chromosomal aberrations are the hallmark of BCP-ALL, additional cooperating genetic alterations are required to induce leukemia. These are typical of a group of patients characterized by a gene expression profile similar to (Philadelphia) Ph-positive BCP-ALL and include: deletions of lymphoid transcription factors (IKZF1, PAX5, EBF1)[12], kinase-activating mutations as rearrangements involving ABL1, JAK2, PDGFRB, CRLF2 and EPOR, activating mutations of IL7R and FLT3 and deletion of SH2B3, which encodes the JAK2-negative

regulator LNK[13]. Thus, most of the childhood BCP-ALL cases are likely to arise from the interplay of these series of genetic alterations which have important prognostic significance and are used in risk stratification.

### 1.1.3. Established Treatments

Treatment regimens in childhood BCP-ALL consist of at least four phases[14]. Induction therapy is the early phase of treatment which is given immediately after diagnosis and consists in the restore of normal blood cell production by use of multiple cancer chemotherapeutic drugs such as steroids (prednisolone or dexamethasone), vincristine, and asparaginase with or without anthracycline (doxorubicin or daunorubicin). More than 95% of pediatric patients achieved complete remission after 4–6 weeks of this regimen. However, despite the induction therapy has decreased the mortality rate in induction to 2–3%, some children still have severe adverse events including infection[5]. After induction therapy, subsequent consolidation/intensification and re-induction segments begin to eradicate residual leukemic cells resistant to standard chemotherapy in patients who are in remission by morphologic criteria. Various combinations of cytotoxic agents are used such as mercaptopurine, thioguanine, methotrexate, cyclophosphamide, etoposide and cytarabine. This phase is followed by the extracompartment therapy, such as CNS preventive therapy because of the high rate of children with BCP-ALL which suffers from disease recurrence originating from

the CNS. CNS relapse rate can be reduced through the introduction of cranial irradiation, intrathecal chemotherapy with methotrexate alone or in combination with other drugs (cytarabine, hydrocortisone). At the end-consolidation phase, patients receive an antimetabolite-based maintenance therapy to further stabilize remission by suppressing the re-emergence of a drug-resistant clone through continuing reduction of residual leukemic cells. The current standard of maintenance therapy lasts 2-3 years and provides the use of antimetabolite drugs including methotrexate and mercaptopurine.

### 1.1.4. Individualized medicine: potential of therapeutic advances

With these aggressive treatment regimens and precise risk stratification based on the biological features of leukemic cells, the long-term survival rate for pediatric BCP-ALL is now approaching 85%. However, diverse molecular and genetic alterations occur in children with leukemia as revealed by next-generation sequencing. Therefore, it is unlikely that a single agent can be effective for all patients. By characterizing the immunophenotype and genotype of each patient's leukemia, targeted therapy can be expected to lead to improvements in remission and survival as part of individualized treatment strategies. The successes from tyrosine kinase inhibition (TKIs) in chronic myeloid leukemia have been translated to Ph-positive BCP-ALL, and second and third generation TKIs are being

studied for use in high-risk Ph-like disease. Other signaling pathways, such as PI3K/AKT/mTOR pathway, are also promising targets for small molecule inhibition[15]. In addition to targeting intracellular pathways, several immunotherapeutic approaches proved to be highly effective for both relapsed and refractory patients with survival rates superior to those observed with conventional chemotherapy, although longer follow-up is necessary. One of the most important agents in this regard is blinatumomab, a bi-specific antibody that binds to CD19, the most widely expressed B-lineage specific antigen, and CD3 (present on T cells), causing the direct activation of T cells against B lymphoblasts. CAR (Chimeric Antigen Receptor)-T therapy involves a similar mechanism in which autologous T cells are genetically engineered to couple an anti-CD19 domain to intracellular T cell signaling domains, thus redirecting cytotoxic T cells to CD19-expressing cells to induce an antileukemic immune response[10]. Finally, existing agents, such as bortezomib, decitabine and ruxolitinib that are well tolerated in the treatment of various malignancies resulted to be highly active also in BCP-ALL. However, several pediatric patients still experience resistance to conventional chemotherapy. For this reason, further studies are warranted to investigate new therapeutic targets in order to improve outcome disease.

## 1.2. The hematopoietic stem cell niche

The HSC microenvironment, or niche, is critical in regulating the biology of hematopoiesis. More than 50 years ago, Schofield suggested that HSCs reside in this sanctuary niche which provides a critical regulatory milieu responsible for orchestrating their differentiation into the different types of mature blood cells throughout life[16]. These cells are primitive, pluripotent progenitors that differentiate, in part, in response to environmental signals that mediate homeostatic maintenance of the entire hematopoietic system, as well as when increased blood cell production is required in times of enhanced demand, such as in response to infection or enhanced blood cell destruction. BM niche is also responsible for regulating HSCs cell cycle activity and self-renewing cell divisions, by keeping stem cells in the G0 phase of the cell cycle in a stage of quiescence to preserve their function and limit damage associated with cell replication[17] but also by inducing their switch from a quiescent to a proliferative status in response to a broad range of systemic signals[18]. Thus, HSCs critically depend on short and long-range instructive cues from the BM niche for many aspects of their biology, including survival, self-renewal, differentiation and retention, due to the dynamic regulation of the switch between quiescence/proliferation and anchoring/mobilization.

Among all niche residents, HSCs are quite rare, comprising ~0.001% of total BM cells. The remaining cells are hematopoietic progenitors at various stages of maturity, nearly mature blood cells and non-hematopoietic cells that provide key regulatory

signals in the hematopoietic niche. HSCs are known to reside in two distinct microenvironmental niches within the BM, an “osteoblastic (endosteal)” niche and a “vascular” niche, which have been demonstrated to work in concert[19].

In the vascular niche, most HSCs localize adjacent to sinusoidal blood vessels, where they are in close contact with endothelial cells (ECs) which are necessary sources of the stem cell factor (SCF) and soluble stromal-cell-derived factor 1 (also known as CXCL12) required for HSC maintenance in the niche[20]. ECs have been proposed to exclusively express E-selectin in the BM and E-selectin blockade in mice improves HSC survival upon chemotherapeutic agents or irradiation treatment[21] Also Jagged-1 deletion in ECs was shown to compromise self-renewal and maintenance of HSCs[22].

Non-myelinating Schwann cells (Nes+) regulate the hibernation and activation of HSCs, by keeping HSCs quiescent through activation of latent-TGF-β1 found in the surrounding microenvironment[23].

Recent findings have identified a direct HSC regulation by megakaryocytes. Ablation of megakaryocytes leads to cell cycle entry of quiescent HSC, suggesting that this cellular population contributes to maintaining HSC quiescence. This interaction was reported as being mediated by soluble factors such as TGF-b1 which promotes HSCs quiescence *in vivo*[24]. Megakaryocytes are also a source of CXCL4 which negatively regulates HSC proliferation, reduces HSC numbers, and decreases

engraftment. An increase in HSC number, proliferation, and repopulating activity was observed in CXCL4 knockout mice[25]. Megakaryocytes can also promote the regeneration and expansion of HSCs after myeloablation by synthesizing FGF1, a cytokine that acts on HSCs to promote regeneration after injury[26].

In the osteoblastic niche, HSCs reside near the endosteal bone surface which has long been recognized as the principal component of the hematopoietic niche, with osteoblasts, osteoclasts, adipocytes and mesenchymal stromal cells (MSCs) all influencing HSC fate selection[27].

Osteoblast lineage cells located on the endosteal surface immobilize HSCs by the binding of integrin α4β1 to VCAM1, which reduces apoptosis and induces HSC quiescence[28]. Similarly, CXCL12 and angiopoietin-1 secreted by osteoblasts prevent HSC mobilization from the niche and promotes cell quiescence[29,30]. Osteoblasts are also closely coupled to HSC proliferation, as increases in the osteoblast population lead to concomitant increases in HSC numbers[31,32]. This expansion of the HSC compartment seems to be mediated by osteoblastic Notch signaling[32], as osteoblastic expression of Notch ligands leads to proliferation of both short-term and long-term HSCs[33]. Other factors involved in the osteoblast lineage regulation of HSC numbers include osteopontin which limits HSCs expansion[34], thrombopoietin[35] and angiopoietin which both contribute to HSCs quiescence[29].

Osteoclasts, large multinucleated cells derived from hematopoietic progenitors that are primarily responsible for resorbing bone matrix during bone remodeling, are also involved in the maintenance and fate selection of HSCs. Whereas osteoblast secretion of CXCL12 encourages HSC retention in the BM microenvironment, osteoclast activity has the effect of mobilizing hematopoietic progenitors by enzymatically cleaving CXCL12[36], indicating a competitive balance between osteoblasts and osteoclasts in the regulation of HSCs. Importantly, the bone resorption mediated by osteoclast activity releases high levels of $Ca^{2+}$ near the endosteal surface, enabling HSCs which possess $Ca^{2+}$ receptors (CaR) not only to navigate to the BM, but also to lodge in the vicinity of the endosteal bone surface itself[37].

Sharing the BM niche with osteoblasts and osteoclasts, adipocytes have been involved in HSC behavior. Interestingly, although adipocytes have been traditionally considered as negative regulators of the HSC niche regulation[38], more recent data point to them as key players during hematopoietic regeneration. Indeed, adipocytes were demonstrated as the major sources of SCF after irradiation and essential for hematopoietic recovery[39], suggesting that BM adipogenesis after irradiation represents a fast and efficient response to promote emergency hematopoietic regeneration. BM adipocytes secrete a variety of factors, and some of these have HSC regulatory activity such as leptin. Leptin-deficient and leptin receptor-deficient mice impair hematopoiesis, BM hypocellularity and myeloid skewing[40].

The physical and functional separation of the different niches and the cells residing within them provides further evidence that local changes in BM composition can have differential, yet substantial, effects on HSCs and hematopoiesis.

However, many other cell types that are present in the BM contribute to the microenvironment, including immune cells which provide an “immune niche” that is involved in the regulation of HSC homeostasis and emergency hematopoiesis[41]. Lymphocytes have been suggested to influence hematopoiesis, potentially through direct cellular interactions with the HSCs. Natural killer cells have been suggested to play a negative role in HSC differentiation[42], activated T cells have a positive regulatory role on normal hematopoiesis[43], regulatory T cells (T-regs) suppress colony formation and myeloid differentiation of HSCs[44]. Furthermore, T-regs confer immune-privilege to the HSC niche, protecting HSCs from immune destruction[45].

Macrophages were recently found to be another indispensable cellular participant needed for HSC retention in the BM. They promote HSC retention by regulating the expression of CXCL12 by Nestin–GFP+ MSCs via a soluble factor secreted by CD169+ macrophages[46]. Recent studies have suggested that this factor was oncostatin M[47]. Additionally, a separate subpopulation of macrophages expressing high levels of α-smooth muscle actin and cyclooxygenase 2 synthesizes prostaglandin E2, which increases CXCL12 expression in Nestin-GFP+ MSCs[48] and

CXCR4 expression on HSCs[49], thus improving the survival and maintenance of HSCs in the BM.

Neutrophils have been reported to support niche activity by enhancing the capacity of pre-osteoblastic cells to produce osteopontin, an important retention factor for HSC in the marrow[50]. Interestingly, adrenergic stimulation of neutrophils through the β3 receptor induces production of prostaglandin E2, a well-known support factor for hematopoiesis[51]. The BM is one of the tissues in which aged neutrophils are cleared in larger numbers by tissue-resident macrophages to generate homeostatic signals that modulate the BM niche[52]. Homeostatic clearance in this organ is important not only to control neutrophil number but to generate undefined signals that down-regulate the number of niche cells and, consequently, the amount of CXCL12 in the marrow, thereby promoting HSC egress into blood. Consistently, the number of CXCL12-producing reticular cells and osteoblasts in the BM increase when neutrophils are experimentally depleted, indicating that neutrophils preserve niche function, preventing excessive mobilization of HSC into blood.

### 1.2.1. Mesenchymal contribution to the niche

MSC co-localization with sites of hematopoiesis indicates that these cells are essential niche components with a pivotal role in regulating HSC homeostasis[53]. MSCs were first described in 1968 by Friedenstein as a population of adherent cells present in the BM, which exhibit a fibroblast-like morphology and the ability to differentiate *in vitro* into mesodermal lineages including bone, cartilage and adipose tissue[54]. In addition to generating cells of several connective tissue lineages, MSCs also give rise to the hematopoietic supportive stroma that constitutes the hematopoietic microenvironment in adult BM. The ability of MSCs to regulate hematopoiesis is mediated by the production of growth factors involved in the homing, proliferation and differentiation of HSCs including CXCL12 and stem cell factor (SCF)[55]. Nestin+ MSCs expressing high CXCL12 levels have been identified by Mendez-Ferrer group in mouse BM as niche key elements and act in a perivascular location in proximity with HSCs to participate to the prenatal development of the HSC niche. The deletion of these perivascular Nestin-GFP+ cells is associated with depletion of HSCs, highlighting their fundamental role in the niche as a key component of the HSC-supportive BM microenvironment[56]. Additionally, knockout of MSCs severely reduced the maintenance of hematopoietic progenitors and the ability of HSCs to home to the BM, further emphasizing the critical role that MSCs have in HSC health and maintenance.

Apart from being involved in supporting HSCs maintenance in the adult BM, MSCs possess immunomodulatory functions.

Particularly, they can robustly interact with cells of the innate and adaptive immune system to suppress their immune cell responses through their specific secretome, which consists of various growth factors and immunomodulatory factors [57]. On MSCs interaction, T cells and DCs polarize, respectively, toward a regulatory and anti-inflammatory DC2 phenotype leading to an immunologic tolerance state[58]. Interestingly, MSCs possess characteristics similar to those of these immune cells and they can transform into a pro-inflammatory MSC1 or an anti-inflammatory MSC2 subpopulation, depending on pro- or anti-inflammatory differentiation-related factors within the environment the microenvironment[59] . Moreover, MSCs regulate the polarization of monocytes (M0) toward M1 and M2 macrophages after sensing the surrounding microenvironment, thus contributing to deliver both anti- and pro-inflammatory signals.

Finally, MSCs are key elements in the BM where they participate in niche activities to support HSC function, including quiescence, self-renewal, differentiation and apoptosis. Interestingly, under leukemic conditions, BM MSCs are both altered in cellular nature by leukemic cells and serve as an active component of leukemogenesis by selectively supporting leukemic cells over normal HSCs, leading to the concept of the “leukemic niche”.

## 1.3. The leukemic hematopoietic stem cell niche

HSCs are constantly exposed to both intrinsic and extrinsic stresses, which can cause DNA damage and lead to mutations if not properly resolved. These mutations accumulate with age and can result in malignant transformation. These transformed cells, referred to as leukemic stem cells (LSC), are known to share many biological characteristics with HSCs, including strong self-renewal capacities and multilineage differentiation. Functionally, LSC are characterized by the ability to initiate and propagate leukemia, thereby recreating the primary malignancy and its full heterogeneity[60]. Taken together with the fact that normal hematopoiesis is impaired in patients with hematological malignancies, it has been postulated that HSCs are expelled from their niche by LSCs and the resultant LSC microenvironment supports leukemogenesis. Accordingly, several reports describe morphological and functional changes of BM stromal cells in patients with various hematological diseases such as primary myelofibrosis (PMF), myelodysplastic syndrome (MDS), and acute myelogenous leukemia (AML)[61]. Murine models of these diseases provide mechanistic insights into the creation and function of malignant niches. For instance, in the MLL-AF9-induced murine AML model has been reported that AML disrupts sympathetic nerves, leading to an expansion of phenotypic MSCs primed for osteoblastic differentiation[62]. Such lesion is accompanied by the reduction of $NG2^+$ periarteriolar cells and the decreased expression of HSC maintenance factors such as CXCL12 and SCF, which could

underlie the impaired hematopoiesis in AML. In a murine myeloproliferative neoplasm (MPN) model, generated by Janus kinase 2 (Jak2)$^{V617F}$ knock-in, neuropathy results in the Nes-GFP$^{+}$MSC reduction that is preceded by Schwann cell death triggered by mutant HSC-producing IL-1β[63]. In the case of inducible BCR-ABL transgenic chronic myelogenous leukemia (CML) mice, direct contact of leukemic cells with MSCs allows the latter cells to expand their osteoblastic lineage cell (OBCs), characterized by alteration of several cytokine signaling pathways, including chemokine ligand 3 (CCL3) and thrombopoietin (TPO) over-production[64]. These remodeled OBCs have compromised capacity to support HSCs, while LSCs are maintained in such environment.

In the context of BCP-ALL, the effect of stromal cells on leukemic blasts appears to be recapitulating normal physiological cell–cell adhesion through adhesive receptors like integrins in normal hematopoietic progenitors. The very late antigen-4 (VLA-4) integrin expressed on leukemic blasts interacts with stromal ligands such as vascular cell adhesion molecule 1 (VCAM-1) to promote leukemic blast survival, proliferation and protection from drug-induced cell death[65]. In addition to adhesive cell-cell interactions, growth factors and cytokines produced by BM stromal cells enhance leukemia growth and progression. The exact role of these mediators in leukemic cell survival is not well known, but probably they form complex and dynamic networks in which leukemic blasts and stromal cells complement each other's cytokine expression, as shown in several co-culture models of

BCP-ALL. *In vitro*, leukemic cell lines co-cultured with stromal cells that are high producers of TGF-β and BMP-6, express TGF-β inducible early gene 1 (TIEG1), resulting in inhibition of proliferation and protection from chemotherapy, thus suggesting a role for these two mediators in stroma-mediated escape from treatment[66]. BM stroma skew leukemic cells towards a proliferative and survival IL-3 and IL-7-producing phenotype by production of stromal CXCL12[67].

Intriguingly, several studies have implicated a previously unrecognized link between microenvironment and cancer metabolism. Hypoxic BCP-ALL cells may resist the therapeutic effect by overexpression of the oxygen-regulated component hypoxia-inducible transcription factor alpha (HIF-1α) leading to the upregulation of glucose transporter GLUT thereby increasing the rate of glycolysis[68]. Furthermore, a high level of asparagine secretion by MSCs has been shown to cause asparaginase resistance of BCP-ALL cells that reside in MSC niches, and this protective effect correlated with levels of asparagine synthetase expression in MSCs[69]. Although the microenvironment plays a crucial role in protecting leukemic cells, recent studies have shown that leukemic cells could also induce the stroma to alter the BM niche, suggesting a bi-directional influence in the microenvironment. Xenotransplantation of BCP-ALL cell lines has been shown to disrupt the normal BM microenvironment[70,71]

Particularly, these cells cause severe damage of the vasculature and endosteum-lining cells and lead to the formation of abnormal

niches primarily formed by the mutated cells, which highly express SCF but produce low levels of CXCL12. In these aberrant niches, both the numbers and the traffic of normal HSCs are reduced. This process has been proposed as a mechanism by which normal hematopoiesis could be impaired even in the presence of a low tumor burden. In the same xenotransplant model, chemotherapy has been shown to induce the formation of transient niches consisting of small foci of surviving BCP-ALL cells and nestin$^{+}$ LepR$^{+}$ NG2$^{+}$ stromal cells with properties of MSCs (multipotent sphere formation, *in vitro* differentiation). Formation of these structures require CCL3 and TGFb1 produced by BCP-ALL cells and have been proposed to protect BCP-ALL cells from chemotherapy-induced apoptosis. Moreover, contact of MSCs derived from leukemic patients (ALL-MSC) with leukemic blasts causes upregulation of several chemokines such as CCL2, CCL22, CXCL8 and CXCL1, thus acting as mediators for leukemic niche alterations through the reduction of healthy HSC homing to BM niche[72]. Leukemic cells not only occupy the HSC niche but can affect the expression of key chemokine and cytokine in the BM, remodeling it into a self-reinforcing malignant microenvironment at the expense of normal hematopoiesis[73]. Collectively, leukemic cells and their microenvironment are regulated by an interdependent network which plays a key role for disease progression.

### 1.3.1. Pathological leukemia-stroma connectivity as a hallmark of cancer

When leukemic cells are engrafted in the stem cell niche, they profoundly disrupt hematopoietic stroma creating abnormal malignant niches which compete for $CD34^+$ homing and finally cause an abnormal progenitor cell function, even in early phases of the disease[70]. Moreover, BM stromal cells can also protect leukemic cells providing an environment conducive to survival and development of relapsing leukemic clones[74]. Although the microenvironment plays a crucial role in protecting leukemic cells, recent studies have shown that leukemic cells could also induce the stroma to cause alterations in the BM niche, suggesting a bi-directional influence in the microenvironment[75]. Beside several studies emphasized the relevance of cell-to-cell contacts between leukemic and stromal cellular populations[76], recent reports[77,78] suggested that soluble factors such as cytokines were shown to contribute to the leukemia development and to the acquisition of chemoresistance in leukemic cells[79,80]. In addition, recent studies have shown that exosomes and microvesicles (EVs) produced by leukemic cells induce cellular changes in stroma, suggesting that they act as mediators for leukemic niche alterations[81,82]. Hence, the altered niche can provide distinct cross-talk interactions between normal HSCs and LSCs to reinforce the pro-leukemic microenvironment.

## 1.4. ActivinA, a TGF-β superfamily member

Among the soluble molecules regulating microenvironmental effects, the role of TGF-β family members as tumor-promoters has been described in several solid tumors. Activins are found either as homodimers or heterodimers of βA or/and βB subunits linked with disulfide bonds. There are three functional isoforms of activins: ActivinA (βAβA), ActivinB (βBβB) and ActivinAB (βAβB). ActivinA, a cytokine belonging to the human transforming growth factor-β (TGF-β) family, represents the most extensively investigated protein among the family of activins. Initially, it was identified as inducer of follicle-stimulating hormone secretion but extensive research over the past decades illuminated fundamental roles for ActivinA in essential biologic processes such as hematopoiesis, embryonic development, stem cell maintenance and pluripotency, tissue repair and fibrosis[83]. ActivinA elicits these diverse biological responses by signaling via type I and type II receptor serine kinases. Activin expresses the type II receptors activin receptor type 2A (ACVR2A) and ACVR2B, the type I receptors ACVR1 (also known as ALK2), ACVR1B (also known as ALK4) and ACVR1C (also known as ALK7). Activin signaling occurs through the binding with two type I (that is, signal-propagating) and two type II (that is, activator) receptor molecules to assemble the heterotetrameric required to allow type II receptors to phosphorylate the cytoplasmic domains of the type I receptors which then propagate the signal. Upon activation, the type I receptor kinases phosphorylate the receptor-regulated SMADS

(R-SMADs), SMAD2 and SMAD3, enabling the formation of a heterocomplex with the common-SMAD 4 (co-SMAD). Subsequently, the SMAD complexes translocate and accumulate into the nucleus where they act as transcription factors regulating the expression of target genes by cooperating with other cofactors. Activin signaling can be inhibited by SMAD7 in competition with R-SMADs for the binding and activation of type I receptors which are then internalized and degraded through the recruitment of E3 ubiquitin ligases[83]. Considering the crucial roles that ActivinA plays in these biological processes, its mode of action is tightly regulated by a plethora of molecules. Follistatin (FS) represents the major inhibitor of ActivinA as it binds to ActivinA with high affinity and neutralizes its functions by preventing ActivinA interaction with its type II receptors. Inhibins compete for binding to the type II receptors but can also bind directly to activins with variable affinities. The pseudoreceptor BMP and activin membrane-bound inhibitor homolog (BAMBI) restrains ActivinA signaling by interacting with the type I receptors and inhibiting the formation of the receptor signaling complex. Furthermore, overexpression of Cripto, the co-receptor for nodal ligands inhibits ActivinA signaling by binding ActivinA receptors. Still, small-molecule inhibitors such as SB-431542 and SB-505124 against the ALK4 and ALK7 activin type I receptors have been developed to be used as therapeutics to block specifically ALK4 and ALK7-induced SMAD signaling pathways since these exogeneous antagonists have no effect on numerous other protein kinases[84].

Similar to TGF-β, ActivinA can influence the development and progression of cancer by regulating the innate and adaptative immune responses to tumors. ActivinA and its signaling pathway components are expressed by a wide variety of immune cells, including macrophages, dendritic cells (DCs), T and B lymphocytes and natural killer (NK) cells. ActivinA exerts pro-inflammatory effects on resting cells and during the onset of immune responses, while at later time points or during stimulation of activated cells, ActivinA exhibits immunosuppressive functions. Pertinent to cancer, ActivinA exerts both pro-tumorigenic functions, promoting immunosuppressive activities of macrophages and T-regs and anti-tumorigenic effects boosting CD4+ and CD8+ T effector responses and dendritic cell (DC) antigen presenting functions[85]. Intriguingly, these divergent effects of ActivinA depend on the type of cancer and the context of the immune response. ActivinA attenuates cytokine and chemokine production by stimulated DCs, thereby inhibiting the ability of DC to activate T cells[86]. It has been further demonstrated that ActivinA, produced by the Th2 subpopulation of T cells, markedly induces in macrophages the expression of arginase-1 (anti-inflammatory M2 marker) and decreases the interferon (IFN)-γ-induced expression of inducible nitric oxide (NO) synthase (pro-inflammatory M1 marker)[87]. This indicates that ActivinA is involved in polarization of macrophages towards an M2 phenotype, a phenomenon that is also frequently associated with a tumor-promotive microenvironment[88]. Finally, ActivinA attenuates several functions of human NK cells, such as

IFN-γ production, proliferation and phenotypic maturation, further suggesting it has immunosuppressive properties[89].

Like most other cytokines, ActivinA is pleiotropic and affects different cell types within the hemopoietic system. Probably the most well-studied and most prominent activities are those related to the erythroid and B-lymphocyte lineages. *In vivo* studies suggest that ActivinA enhances erythropoiesis since its administration to rodents causes an increase in erythroid precursors, circulating red blood cells, and reticulocyte release[90]; by contrast, the molecule is apparently inhibitory to the generation of B-lineage cells in which it induces cell cycle arrest and a shift towards the G0/G1 cell cycle. ActivinA role as negative regulator of B cell development has been confirmed by the fact that elevated expression of ActivinA in primary BM cultures is associated with lack of pre-B-cell production which is enhanced following ActivinA inhibition by follistatin[91]. Moreover, treatment of B-cell precursors with ActivinA causes halting of the cell growth at an earlier differentiation stage compared with cells not treated with this cytokine[92]. Such discriminating effects and the confinement of ActivinA to specific sites within the hemopoietic microenvironment imply a role for this factor in the organization of the hemopoietic system into functional domains that differ in their cell type composition.

Deregulated expression of components of the activin signaling axis have been found in a broad range of malignancies. ActivinA can directly promote or inhibit cancer cell growth depending on

the type of cancer cells involved. In cancer of the breast, liver and colon, activin signals inhibit tumor cell growth and tumor tissue express decreased levels of ActivinA, increased levels of ActivinA antagonists or demonstrate a loss of functional ActivinA receptors or SMAD proteins[93–95]. However, some other tumors, such as oral squamous cell carcinoma (OSCC), esophageal and malignant pleural mesothelioma, gain resistance to the growth-inhibitory effect of ActivinA. In these malignancies, ActivinA can even stimulate tumor cell proliferation and aggressiveness[96,97]. In addition, ActivinA can also indirectly affect tumor growth by suppressing the antitumor immune responses of immune cells which reside within the tumor microenvironment. The high circulating levels of ActivinA in cancer patients suggest that it could be involved in tumor progression[98]. In lung adenocarcinoma, ActivinA is overexpressed in tumor tissue compared with normal lung tissue, and this overexpression of ActivinA is correlated with worse prognosis in stage I disease[99]. The effects of activinA on cancer cells lead to increased migration through induction of EMT, as well as angiogenesis and cancer cell invasiveness to ultimately accelerate the metastatic process[100]. So far, several works have demonstrated the pro-tumoral role of ActivinA in solid cancer development, mainly through enhancement of cell migration and invasion. Although several studies established clear roles for the ActivinA signalling pathway in aspects of the pathogenesis of solid tumours, the involvement of the ActivinA signalling pathway in hematologic malignancies has not been explored.

## 1.5. The role of EVs as mediators of cellular crosstalk

The term EVs, coined by the International Society for Extracellular Vesicles (ISEV), categorizes vesicles based on their biogenesis or release pathway, and includes exosomes, microvesicles and apoptotic bodies[101].

*Biogenesis*. Exosomes are 30-150 nm diameter membranous vesicles of endocytic origin and homogenous with respect to shape, whereas microvesicles (151-700 nm in diameter) and apoptotic bodies (701-1000 nm in diameter) are large membranous vesicles that are shed directly from the cell plasma-membrane and heterogenous in shape. The release of EVs may be constitutive or consequent to cell activation by soluble agonists, by physical or chemical stress such as the oxidative stress hypoxia, and by shear stress. In detail, exosomes, which were firstly described by Johnstone and Stahl research groups in 1983[102,103], are actively secreted through the receptor-mediated endocytosis; when the receptor-bound molecule reaches the early endosomes, these cell compartments can mature into late endosomes and their inward budding results in the progressive accumulation of intraluminal vesicles (ILVs) inside the multivesicular bodies (MVBs). These MVBs can partake the a) degradative pathway where they fuse with lysosomes and degrade their content or b) the exocytic pathway where MVBs can fuse with the plasma-membrane and release their content into the extracellular milieu. Once that ILVs are released

externally, they are named exosomes. So far, which kind of mechanism governs the transition of the MVBs to degradative or exocytic pathway remains uncharacterized[104]. Regarding the microvesicles, they are mainly produced via outward blebbing of small plasma-membrane protrusions which loose contact with cytoskeleton and consequently detach from the cell surface. In addition to the cytoskeleton reorganization, also specific calcium-dependent enzymes contribute to microvesicle formation by modifying the asymmetric phospholipid distribution of plasma-membranes[105]. Lastly, apoptotic bodies are membrane vesicles which are condensed remnants of the shrinking apoptotic cells and are released via blebbing of the plasma-membrane during the late stages of cell death[106]. EVs, including exosomes and microvesicles, are very difficult to distinguish from each other but, basically, they are both nanosized particles limited by lipid bilayer membrane extracellular structures and they are usually spherical in shape. Where are they? Thinking about the human body, EVs can be found in several biofluids such as urine, saliva, milk, cerebrospinal fluid, blood, and plasma because cells constantly secrete and release EVs into their surroundings. The reason for EVs being present everywhere resides in the fact that almost all living organisms on the earth shed vesicles into the extracellular environment. Indeed, EVs secretion and EV-mediated communication are evolutionary conserved phenomena: from simple organisms [archaea[107] or Gram-negative and Gram-positive bacteria[108,109]] to complex multicellular organism. EVs have been identified also in all four eukarya subdomains:

Protista[110], fungi[111,112], plantae[113], animalia[114]. This highly conserved biological release of membrane-bound vesicles in prokaryotes and eukaryotes attributes EVs the important role of mediators of communication between cells, orchestrating different physio-pathological cellular processes, including immune responses, tissue regeneration, blood coagulation, neurodegenerative diseases and tumorigenesis[115]. Notably, functions of EVs in physiological and pathological processes depend on their content that can be delivered to recipient cells in both autocrine and paracrine fashion.

*Protein Composition*. Accumulating evidences demonstrated that EVs can carry a range of molecules, such as proteins, lipids, metabolites, and nucleic acids including messenger RNA (mRNA), microRNAs (miRNAs) and other classes of small RNA (sRNA) as well as DNA reflective of their cellular origin[116] (*Extracellular vesicles: Exosomes, microvesicles, and friends*). Obviously, the discovery of this cargo has drawn an increasing amount of attention among researchers, due to its significant impact on the phenotype of recipient cells. Comprehensive research has been done on the vast repertoire of molecules that can be packaged within EVs. Commonly found proteins in exosomes are those associated with the mechanisms responsible for MVBs biogenesis such as tetraspanins (CD63, CD81, CD9), including proteins associated with the endosomal pathway (Alix, TSG101); additionally, cytosolic proteins which participate in membrane fusion events, such as Rabs (small GTPases), are also often detected; moreover, exosomes are

heavily enriched in membrane trafficking and fusion proteins such as annexins; other exosomal proteins include cell-type-specific proteins (MHC-II, CD86), signaling molecules, oncogenic molecules, integrins and adhesion molecules, lipid rafts components (flotillins)[106]. Contrary to exosomes, the protein composition of microvesicles is less well defined. Proteins abundant in microvesicles are matrix metalloproteinases (MMP2 and ADAM), enzymes, membrane trafficking and fusion proteins, and those localized to centrosome, ribosome, nucleolus, cytoplasm and mitochondria[117].

*DNA Composition*. Between the several messages that can be sent via EVs and then dispatched into the extracellular space to be horizontally transferred to recipient cells there are also nucleic acids. EVs were shown to contain different fractions of single-stranded genomic DNA (ssDNA) fragments that recapitulate genomic aberrations such as oncogene amplifications in the primary tumor[118]. However, Thakur et al. demonstrated that the majority of EV-associated DNA is double-stranded and reflects the oncogenic mutational status of the respective parental cell[119]. EVs can also mediate intercellular communication by carrying mitochondrial DNA (mtDNA) which can be, therefore, shuttled between cells. Strong research efforts have uncovered that, within the physical and functional cross-talk that take places between multiple cell types, transfer involving mitochondria is particularly provocative because of the crucial functions of the organelle in the regulation of cellular energetic metabolism and in the control of apoptosis. In their work, Guescini et al.

demonstrated that migration of mtDNA can occur via exosomes derived from astrocytes and glioblastoma cells to modify host cell fate[120].

*mRNA Composition*. Additionally, many studies revealed that horizontal vesicle-mediated transfer of distinct RNA species between cells allows dissemination of genetically encoded messages, which may modify the function of recipient cells. Ratajczak et al. showed that small vesicles derived from murine embryonic stem cell (ESCs) express mRNA for several pluripotent transcriptional factors and that these vesicles have functional activity. Indeed, when these vesicles enter in close contact with target cells, they release their mRNA molecules which can be translated into the corresponding proteins[121]. Also, the research conducted by Valadi and colleagues demonstrated that mRNAs can have biologically active functions when they are transferred through the vesicles. They showed that exosomes contain both mRNA and other classes of small non-coding RNA, including miRNA and that these components are delivered to target cells, resulting in protein translation. Recently, it has been shown that EV-mediated transfer of genetic information under the form of RNA can reflect the mutational status of the parental cell from which the EVs originate[122]. A further study on the use of mRNA in exosomes was conducted by Rolfo et al. to identify genetic mutations in nano-sized vesicles derived from plasma of patients with non-small cell lung cancer patients (NSCLC) [123]. Analysis of RNA from EVs by a deep sequencing approach demonstrated that, in addition to mRNA, EVs harbor selective

patterns of small non-coding RNA species, including RNA transcripts overlapping with protein coding regions, repeat sequences, structural RNAs, tRNA fragments, vault RNA, Y-RNA, small interfering RNAs and also small regulatory miRNAs[124].

*miRNA Composition*. Discovery of miRNA cargo carrying EVs adds a new dimension to our understanding of complex gene regulatory networks, due to their altering effects on the transcriptome in recipient cells. Interestingly, in depth analysis of the content of EVs revealed that it has a different profile as compared to the miRNA content of the cells from which it is derived. Several highly abundant cellular miRNAs, such as miR-29a and miR-31, are in fact less abundant in shuttle miRNAs and vice versa. As such, miRNAs uptake by EVs and their subsequent delivery into the extracellular space are not random processes but a selective loading mechanism by which cells incorporate miRNA molecules into EVs[124]. So far, many studies focused on investigating the role that EVs play in cell-to-cell signaling, often hypothesizing that delivery of their miRNA cargo molecules will explain biological effects. It has been proposed that EV-mediated delivery of miRNAs is a powerful mechanism to influence the physiology of target cells, by directly reducing the stability and thus preventing translation of specific target mRNAs into functional proteins. Based on current research, EV-associated miRNAs play a fundamental biologic role in the regulation of normal physiological processes such as coagulation, antigen presentation, metabolism, pregnancy,

facilitation of the immune response, cell apoptosis and senescence as well as aberrant pathological processes including cancer via altered gene regulatory networks or via epigenetic programming[125]. However, molecular and functional characterization of EVs-associated miRNAs has been well described in pathological processes in which they can act as oncogenes or tumor suppressor genes respectively up-regulating and down-regulating the down-stream effector and thereby leading to the initiation, and progression of different malignancies by affecting several cancer-related processes, including proliferation, apoptosis, invasion, and angiogenesis[126]. A great number of dysregulated miRNAs has been discovered in EVs derived from many solid tumor cells, such as breast cancer, melanoma and lung cancer. In breast cancer, it has been reported that exosomal miR-122 promotes metastasis via reprogramming glucose metabolism, in the premetastatic niche. Inhibition of miR-122 decreases the incidence of metastasis, through restoring the glucose uptake in distant organs, such as the brain and lungs[127]. Moreover, it has been shown that pharmacologic inhibition of BRAFV600 in malignant melanoma cell alters the microRNA cargo in the vesicular secretome, with an increase of miR-211-5p, linked to the activation of survival pathway [128]. Increasing evidence shows that tumor-derived exosomal miRNAs can also be taken up by normal cell types that surround the tumor, an outcome that helps shape the tumor microenvironment, in order to trigger tumor vascularization, which is a major hallmark of cancer, and even to confer upon

normal recipient cells the transformed characteristics of a cancer cell. Accordingly, exosomal miR-21 released by transforming lung cancer cells, induce vascular endothelial growth factor (VEGF) production and promote angiogenesis, through a STAT3 dependent mechanism, in nearby normal bronchial cells[129]. Further, tumor released exosomal miRNAs have been postulated to re-shape the local tumor environment into a more favorable niche for tumor growth, invasion and spread of metastasis. For example, miR-21 containing exosomes have been indicated that significantly enhance the migration and invasion of recipient esophageal cancer cells, by targeting programmed cell death4 (PDCD4) and activating its downstream c-Jun N-terminal kinase (JNK) signaling pathway[130]. Tumor exosomal miRNAs transfer is believed to be effective also on the drug response. Qin and coworkers reported that exosomes derived from cisplatin resistant lung cancer cells, characterized by prominent low expression of miR-100-5p, are capable of inducing drug resistance in recipient cells, through exosomal miR-100-5p-dependent manner[131]. Collectively, these studies indicate that EVs, regardless of tumor type, can influence the tumor microenvironment in favor of disease progression. Despite the prominent role that EVs play in solid tumor progression, the involvement of these small particles in the pathogenesis of hematologic malignancies has been less investigated. The limited leukemia EVs studies have highlighted a possible role in leukemia development and progression, particularly in the context of chronic lymphocytic leukemia (CLL) and acute myeloid

leukemia (AML). Concerning the CLL malignancy, Yeh et al. showed that CLL plasma exosomes possess an enriched leukemia-associated miRNA signature, including miR-29 family, miR-150, miR-155, and miR-223. Their results indicated that these miRNAs are associated with CLL progression since levels of miRNA-shuttling exosomes were significantly decreased in plasma after treatment of leukemic cells with ibrutinib[132]. Various properties of leukemic cells such as proliferation, survival, adhesion, drug resistance, and metastasis are known to be strongly associated with their microenvironment. Since EVs in tumor microenvironment are attracting more and more attention, they were proposed as a new mechanism of cross-talk. In a study, Paggetti et al. indicated that exosomes derived from CLL cells transfer miR-146a and miR-451 which induce an inflammatory phenotype in the target stromal cells and transform them into cancer-associated fibroblasts (CAFs), resulting in increased proliferation, secretion of inflammatory cytokines, and metastasis which in turn help to provide suitable conditions for progression of leukemic cells[133]. Another functional study has revealed that exosomes containing miR-19b and miR-20a released from AML resistant cells can interact with their sensitive counterparts and transfer their chemo-resistance, by inducing overexpression of multidrug resistance protein 1 (MRP-1)[134].

*Diagnostic and therapeutic potential of EVs*. Overall, with the natural ability of EVs to concomitantly signal via many forms of cellular material (proteins, lipids, and nuclei acids) both locally and systematically, some research groups have investigated

ways to exploit these vesicles as potential diagnostic and therapeutic agents in cancer patients[135]. Hence, exosomes may provide a potential utility as biomarkers to monitor the emergence, progression and prognosis of cancer, as well as the efficacy of treatment regimens. Although few, studies have revealed exosomes can be readily detected in higher concentrations both in tumor tissue and many bodily fluids of cancer patients. The fact that exosomes are reflective of disease state and can be easily found in biofluids make these small particles an ideal candidate for a non-invasive biomarker of tumor progression[136]. Additionally, such EVs can have therapeutic potential as gene therapy tools since they represent vehicles that are well tolerated, bioavailable, targetable to specific tissues, resistant to metabolic processes, and membrane permeable. Therefore, EVs may be used to efficiently deliver chemotherapeutics compounds to target recipient cells.

## 1.6. Scope of the Thesis

ActivinA is a key protein for the regulation of normal B cell lymphopoiesis, highly produced by BM stroma components. Several studies on solid malignancies showed that ActivinA is an important regulator of carcinogenesis. Indeed, it can directly modulate growth, migration and drug response of cancer cells. In addition, it can also enhance tumor progression by regulating important aspects of crosstalk within the tumor microenvironment.

The general aim of the thesis was to study the role of ActivinA in the leukemic BM niche. In particular, in the first part of the thesis, we characterized the role of ActivinA in the leukemia-stroma crosstalk, by investigating the impact of this molecule in the modulation of the functional activities of both BCP-ALL cells and MSCs. In the second part, we analyzed the potential role of ActivinA to influence BCP-ALL cell vesiculation thereby contributing to leukemic propagation.

# References


1. Chiarini F, Lonetti A, Evangelisti C, et al. Advances in understanding the acute lymphoblastic leukemia bone marrow microenvironment: From biology to therapeutic targeting. Biochimica et Biophysica Acta - Molecular Cell Research 2016;1863(3):449–463.
2. Bhojwani D, Yang JJ, Pui CH. Biology of childhood acute lymphoblastic leukemia. *Pediatric Clinics of North America* 2015;62(1):47–60.
3. Alvarnas JC, Co-Chair /, Hopkins J, et al. Acute Lymphoblastic Leukemia NCCN Guidelines ® NCCN Acute Lymphoblastic Leukemia Panel Members. 2015. 1258 p.
4. Preston DL, Kusumi S, Tomonaga M, et al. Supplement: Cancer Incidence in Atomic Bomb Survivors. Radiation Effects Research Foundation, Hiroshima and Nagasaki. 68–97 p.
5. O'Connor D, Bate J, Wade R, et al. Infection-related mortality in children with acute lymphoblastic leukemia: An analysis of infectious deaths on UKALL2003. Blood 2014;124(7):1056–1061.
6. Roberts KG, Mullighan CG. Genomics in acute lymphoblastic leukaemia: insights and treatment implications. Nature Reviews Clinical Oncology 2015;12(6):344–357.
7. Hong D, Gupta R, Ancliff P, et al. Initiating and Cancer-Propagating Cells in TEL-AML1-Associated Childhood Leukemia. Source: Science, New Series 2008;319(5861):336–339.
8. Ren R. Mechanisms of BCR-ABL in the pathogenesis of chronic myelogenous leukaemia. *Nature Reviews Cancer* 2005;5(3):172–183.
9. Kamps MP. E2A-Pbxl Induces Growth, Blocks Differentiation, and Interacts with Other Homeodomain Proteins Regulating Normal Differentiation.
10. Vrooman LM, Silverman LB. Treatment of Childhood Acute Lymphoblastic Leukemia: Prognostic Factors and Clinical Advances. *Current Hematologic Malignancy Reports* 2016;11(5):385–394.
11. Holmfeldt L, Wei L, Diaz-Flores E, et al. The genomic landscape of hypodiploid acute lymphoblastic leukemia. Nature Genetics 2013;45(3):242–252.
12. Mullighan CG, Goorha S, Radtke I, et al. Genome-wide analysis of genetic alterations in acute lymphoblastic leukaemia. Nature 2007;446(7137):758–764.
13. Roberts KG, Morin RD, Zhang J, et al. Genetic Alterations Activating Kinase and Cytokine Receptor Signaling in High-Risk Acute Lymphoblastic Leukemia. Cancer Cell 2012;22(2):153–166.
14. Cooper SL, Brown PA. Treatment of pediatric acute lymphoblastic leukemia. *Pediatric Clinics of North America* 2015;62(1):61–73.
15. Heikamp EB, Pui CH. Next-Generation Evaluation and Treatment of Pediatric Acute Lymphoblastic Leukemia. Journal of Pediatrics 2018;20314-24.e2.
16. R Shofield. The relationship between the spleen colony-forming cell and the haemopoietic stem cell. Blood Cells [Epub ahead of print].

17. Bakker ST, Passegué E. Resilient and resourceful: Genome maintenance strategies in hematopoietic stem cells. *Experimental Hematology* 2013;41(11):915–923.
18. Pietras EM, Warr MR, Passegué E. Cell cycle regulation in hematopoietic stem cells. Journal of Cell Biology 2011;195(5):709–720.
19. Perry JM, Li L. Disrupting the Stem Cell Niche: Good Seeds in Bad Soil. *Cell* 2007;129(6):1045–1047.
20. Kiel MJ, Yilmaz ÖH, Iwashita T, Yilmaz OH, Terhorst C, Morrison SJ. SLAM family receptors distinguish hematopoietic stem and progenitor cells and reveal endothelial niches for stem cells. Cell 2005;121(7):1109–1121.
21. Winkler IG, Barbier V, Nowlan B, et al. Vascular niche E-selectin regulates hematopoietic stem cell dormancy, self renewal and chemoresistance. Nature Medicine 2012;18(11):1651–1657.
22. Poulos MG, Guo P, Kofler NM, et al. Endothelial Jagged-1 Is necessary for homeostatic and regenerative hematopoiesis. Cell Reports 2013;4(5):1022–1034.
23. Yamazaki S, Ema H, Karlsson G, et al. Nonmyelinating schwann cells maintain hematopoietic stem cell hibernation in the bone marrow niche. Cell 2011;147(5):1146–1158.
24. Yamazaki S, Iwama A, Takayanagi S, Eto K, Ema H, Nakauchi H. TGF-β as a candidate bone marrow niche signal to induce hematopoietic stem cell hibernation. Blood 2009;113(6):1250–1256.
25. Bruns I, Lucas D, Pinho S, et al. Megakaryocytes regulate hematopoietic stem cell quiescence through CXCL4 secretion. Nature Medicine 2014;20(11):1315–1320.
26. Zhao M, Perry JM, Marshall H, et al. Megakaryocytes maintain homeostatic quiescence and promote post-injury regeneration of hematopoietic stem cells. Nature Medicine 2014;20(11):1321–1326.
27. Kiel MJ, Morrison SJ. Uncertainty in the niches that maintain haematopoietic stem cells. *Nature Reviews Immunology* 2008;8(4):290–301.
28. Frisch BJ, Porter RL, Calvi LM. Hematopoietic niche and bone meet.
29. Tie2/Angiopoietin-1 Signaling Regulates Hematopoietic Stem Cell Quiescence in the Bone Marrow Niche.
30. Tzeng YS, Li H, Kang YL, Chen WG, Cheng W, Lai DM. Loss of Cxcl12/Sdf-1 in adult mice decreases the quiescent state of hematopoietic stem/progenitor cells and alters the pattern of hematopoietic regeneration after myelosuppression. Blood 2011;117(2):429–439.
31. Zhang J, Niu C, Ye L, et al. Identification of the haematopoietic stem cell niche and control of the niche size. Nature 2003;425(6960):836–841.
32. Calvi LM, Adams GB, Weibrecht KW, et al. Osteoblastic cells regulate the haematopoietic stem cell niche. Nature 2003;425(6960):841–846.
33. Weber JM, Calvi LM. Notch signaling and the bone marrow hematopoietic stem cell niche. *Bone* 2010;46(2):281–285.

34. Stier S, Ko Y, Forkert R, et al. Osteopontin is a hematopoietic stem cell niche component that negatively regulates stem cell pool size. Journal of Experimental Medicine 2005;201(11):1781–1791.
35. Fox N, Priestley G, Papayannopoulou T, Kaushansky K. Thrombopoietin expands hematopoietic stem cells after transplantation. Journal of Clinical Investigation 2002;110(3):389–394.
36. Kollet O, Dar A, Shivtiel S, et al. Osteoclasts degrade endosteal components and promote mobilization of hematopoietic progenitor cells. Nature Medicine 2006;12(6):657–664.
37. Adams GB, Chabner KT, Alley IR, et al. Stem cell engraftment at the endosteal niche is specified by the calcium-sensing receptor. Nature 2006;439(7076):599–603.
38. Naveiras O, Nardi V, Wenzel PL, Hauschka P v., Fahey F, Daley GQ. Bone-marrow adipocytes as negative regulators of the haematopoietic microenvironment. Nature 2009;460(7252):259–263.
39. Zhou BO, Yu H, Yue R, et al. Bone marrow adipocytes promote the regeneration of stem cells and haematopoiesis by secreting SCF. Nature Cell Biology 2017;19(8):891–903.
40. Claycombe K, King LE, Fraker PJ. A role for leptin in sustaining lymphopoiesis and myelopoiesis.
41. Mercier FE, Ragu C, Scadden DT. The bone marrow at the crossroads of blood and immunity. *Nature Reviews Immunology* 2012;12(1):49–60.
42. Degliantoni G, Murphy M, Kobayashi M, Francis MK, Perussia B, Trinchieri G. NATURAL KILLER (NK) CELL-DERIVED HEMATOPOIETIC COLONY-INHIBITING ACTIVITY AND NK CYTOTOXIC FACTOR Relationship with Tumor Necrosis Factor and Synergism with Immune Interferon.
43. Sharara LI, Andersson Å, Guy-Grand D, Fischer A, Disanto JP. Deregulated TCRαβ T cell population provokes extramedullary hematopoiesis in mice deficient in the common γ chain. European Journal of Immunology 1997;27(4):990–998.
44. Urbieta M, Barao I, Jones M, et al. Hematopoietic progenitor cell regulation by CD4+CD25+ T cells. Blood 2010;115(23):4934–4943.
45. Fujisaki J, Wu J, Carlson AL, et al. In vivo imaging of T reg cells providing immune privilege to the haematopoietic stem-cell niche. Nature 2011;474(7350):216–220.
46. Chow A, Lucas D, Hidalgo A, et al. Bone marrow CD169+ macrophages promote the retention of hematopoietic stem and progenitor cells in the mesenchymal stem cell niche. Journal of Experimental Medicine 2011;208(2):761–771.
47. Albiero M, Poncina N, Ciciliot S, et al. Bone marrow macrophages contribute to diabetic stem cell mobilopathy by producing oncostatin M. Diabetes 2015;64(8):2957–2968.
48. Ludin A, Itkin T, Gur-Cohen S, et al. Monocytes-macrophages that express α-smooth muscle actin preserve primitive hematopoietic cells in the bone marrow. Nature Immunology 2012;13(11):1072–1082.

49. Hoggatt J, Singh P, Sampath J, Pelus LM. Prostaglandin E2 enhances hematopoietic stem cell homing, survival, and proliferation. Blood 2009;113(22):5444–5455.
50. Kawano Y, Fukui C, Shinohara M, et al. G-CSF-induced sympathetic tone provokes fever and primes antimobilizing functions of neutrophils via PGE 2 Key Points • G-CSF-induced sympathetic tone provokes fever and modulates microenvironment via PGE 2 production by bone marrow Gr-1 high neutrophils [Epub ahead of print].
51. Frisch BJ, Porter RL, Gigliotti BJ, et al. In vivo prostaglandin E2 treatment alters the bone marrow microenvironment and preferentially expands short-term hematopoietic stem cells. Blood 2009;114(19):4054–4063.
52. Casanova-Acebes M, Pitaval C, Weiss LA, et al. XRhythmic modulation of the hematopoietic niche through neutrophil clearance. Cell 2013;153(5):1025.
53. Mesenchymal progenitor cells localize within hematopoietic sites throughout ontogeny [Epub ahead of print].
54. Friedenstein A, Petrakova K, Kurolesova A, Frolova G. Heterotopic of bone marrow. Analysis of precursor cells for osteogenic and hematopoietic tissues. Transplantation [Epub ahead of print].
55. Greenbaum A, Hsu YMS, Day RB, et al. CXCL12 in early mesenchymal progenitors is required for haematopoietic stem-cell maintenance. Nature 2013;495(7440):227–230.
56. Méndez-Ferrer S, Michurina T v., Ferraro F, et al. Mesenchymal and haematopoietic stem cells form a unique bone marrow niche. Nature 2010;466(7308):829–834.
57. Meisel R, Zibert A, Laryea M, Göbel U, Däubener W, Dilloo D. Human bone marrow stromal cells inhibit allogeneic T-cell responses by indoleamine 2,3-dioxygenase–mediated tryptophan degradation. Blood 2004;103(12):4619–4621.
58. Aggarwal S, Pittenger MF. Human mesenchymal stem cells modulate allogeneic immune cell responses [Epub ahead of print].
59. Waterman RS, Tomchuck SL, Henkle SL, Betancourt AM. A new mesenchymal stem cell (MSC) paradigm: Polarization into a pro-inflammatory MSC1 or an immunosuppressive MSC2 phenotype. PLoS ONE;5(4):.
60. Kreso A, Dick JE. Evolution of the cancer stem cell model. *Cell Stem Cell* 2014;14(3):275–291.
61. Schepers K, Campbell TB, Passegué E. Normal and leukemic stem cell niches: Insights and therapeutic opportunities. *Cell Stem Cell* 2015;16(3):254–267.
62. Hanoun M, Zhang D, Mizoguchi T, et al. Acute myelogenous leukemia-induced sympathetic neuropathy promotes malignancy in an altered hematopoietic stem cell Niche. Cell Stem Cell 2014;15(3):365–375.
63. Arranz L, Sánchez-Aguilera A, Martín-Pérez D, et al. Neuropathy of haematopoietic stem cell niche is essential for myeloproliferative neoplasms. Nature 2014;512(1):78–81.

64. Schepers K, Pietras EM, Reynaud D, et al. Myeloproliferative neoplasia remodels the endosteal bone marrow niche into a self-reinforcing leukemic niche. Cell Stem Cell 2013;13(3):285–299.
65. Jacamo R, Chen Y, Wang Z, et al. Reciprocal leukemia-stroma VCAM-1/VLA-4-dependent activation of NF-κB mediates chemoresistance. Blood 2014;123(17):2691–2702.
66. Døsen-Dahl G, Munthe E, Nygren MK, Stubberud H, Hystad ME, Rian E. Bone marrow stroma cells regulate TIEG1 expression in acute lymphoblastic leukemia cells: Role of TGFβ/BMP-6 and TIEG1 in chemotherapy escape. International Journal of Cancer 2008;123(12):2759–2766.
67. Juarez J, Baraz R, Gaundar S, Bradstock K, Bendall L. Interaction of interleukin-7 and interleukin-3 with the CXCL12-induced proliferation of B-cell progenitor acute lymphoblastic leukemia. Haematologica 2007;92(4):450–459.
68. Frolova O, Samudio I, Benito J, et al. Regulation of HIF-1α signaling and chemoresistance in acute lymphocytic leukemia under hypoxic conditions of the bone marrow microenvironment. Cancer Biology and Therapy 2012;13(10):858–870.
69. Iwamoto S, Mihara K, Downing JR, Pui CH, Campana D. Mesenchymal cells regulate the response of acute lymphoblastic leukemia cells to asparaginase. Journal of Clinical Investigation 2007;117(4):1049–1057.
70. Colmone A, Amorim M, Pontier AL, Wang S, Jablonski E, Sipkins DA. Leukemic Cells Create Bone Marrow Niches That Disrupt the Behavior of Normal Hematopoietic Progenitor Cells. Science 2008;322(5909):1861–1865.
71. Duan C-W, Shi J, Chen J, et al. Leukemia Propagating Cells Rebuild an Evolving Niche in Response to Therapy. Cancer Cell 2014;25(6):778–793.
72. de Rooij B, Polak R, van den Berk LCJ, Stalpers F, Pieters R, den Boer ML. Acute lymphoblastic leukemia cells create a leukemic niche without affecting the CXCR4/CXCL12 axis. *Haematologica* 2017;102(10):e389–e393.
73. Zhang B, Ho YW, Huang Q, et al. Altered Microenvironmental Regulation of Leukemic and Normal Stem Cells in Chronic Myelogenous Leukemia. Cancer Cell 2012;21(4):577–592.
74. Li Z-W, Dalton WS. Tumor microenvironment and drug resistance in hematologic malignancies. Blood Reviews 2006;20(6):333–342.
75. Kim J-A, Shim J-S, Lee G-Y, et al. Microenvironmental Remodeling as a Parameter and Prognostic Factor of Heterogeneous Leukemogenesis in Acute Myelogenous Leukemia. Cancer Research 2015;75(11):2222–2231.
76. Manabe A, Coustan-Smith E, Behm F, Raimondi S, Campana D. Bone marrow-derived stromal cells prevent apoptotic cell death in B-lineage acute lymphoblastic leukemia. Blood [Epub ahead of print].
77. Vilchis-Ordoñez A, Contreras-Quiroz A, Vadillo E, et al. Bone Marrow Cells in Acute Lymphoblastic Leukemia Create a Proinflammatory

Microenvironment Influencing Normal Hematopoietic Differentiation Fates. BioMed Research International 2015;20151–14.
78. Enciso J, Mayani H, Mendoza L, Pelayo R. Modeling the pro-inflammatory tumor microenvironment in acute lymphoblastic leukemia predicts a breakdown of hematopoietic-mesenchymal communication networks. Frontiers in Physiology;7(AUG):
79. Tabe Y, Konopleva M. Role of Microenvironment in Resistance to Therapy in AML. Current Hematologic Malignancy Reports 2015;10(2):96–103.
80. Doepfner KT, Spertini O, Arcaro A. Autocrine insulin-like growth factor-I signaling promotes growth and survival of human acute myeloid leukemia cells via the phosphoinositide 3-kinase/Akt pathway. Leukemia 2007;21(9):1921–1930.
81. Huan J, Hornick NI, Goloviznina NA, et al. Coordinate regulation of residual bone marrow function by paracrine trafficking of AML exosomes. Leukemia 2015;29(12):2285–2295.
82. Huan J, Hornick NI, Shurtleff MJ, et al. RNA Trafficking by Acute Myelogenous Leukemia Exosomes. Cancer Research 2013;73(2):918–929.
83. Chen W, ten Dijke P. Immunoregulation by members of the TGFβ superfamily. Nature Reviews Immunology 2016;16(12):723–740.
84. Harrison CA, Gray PC, Vale WW, Robertson DM. Antagonists of activin signaling: Mechanisms and potential biological applications. *Trends in Endocrinology and Metabolism* 2005;16(2):73–78.
85. Antsiferova M, Werner S. The bright and the dark sides of activin in wound healing and cancer. *Journal of Cell Science* 2012;125(17):3929–3937.
86. Robson NC, Phillips DJ, Mcalpine T, et al. Activin-A: a novel dendritic cell-derived cytokine that potently attenuates CD40 ligand-specific cytokine and chemokine production [Epub ahead of print].
87. Ogawa K, Funaba M, Chen Y, Tsujimoto M. Activin A Functions as a Th2 Cytokine in the Promotion of the Alternative Activation of Macrophages. The Journal of Immunology 2006;177(10):6787–6794.
88. Mantovani A, Sozzani S, Locati M, Allavena P, Sica A. Macrophage polarization: tumor-associated macrophages as a paradigm for polarized M2 mononuclear phagocytes.
89. Robson NC, Wei H, McAlpine T, Kirkpatrick N, Cebon J, Maraskovsky E. Activin-A attenuates several human natural killer cell functions. Blood 2009;113(14):3218–3225.
90. Shiozaki M, Sakai R, Tabuchi M, Eto Y, Kosaka M, Shibai H. Invivo treatment with erythroid differentiation factor (EDF / activin a) increases erythroid precursors (CFU-E and BFU-E) in mice. Biochemical and Biophysical Research Communications 1989;165(3):1155–1161.
91. Shav‐Tal Y, Zipori D. The Role of Activin A in Regulation of Hemopoiesis. Stem Cells 2002;20(6):493–500.
92. SHOHAM T, PARAMESWARAN R, SHAV-TAL Y, BARDA-SAAD M, ZIPORI D. The Mesenchymal Stroma Negatively Regulates B Cell

Lymphopoiesis through the Expression of Activin A. Annals of the New York Academy of Sciences 2003;996(1):245–260.
93. Burdette JE, Jeruss JS, Kurley SJ, Lee EJ, Woodruff TK. Activin A mediates growth inhibition and cell cycle arrest through Smads in human breast cancer cells. Cancer Research 2005;65(17):7968–7975.
94. Hempen PM, Zhang L, Bansal RK, et al. Evidence of Selection for Clones Having Genetic Inactivation of the Activin A Type II Receptor (ACVR2) Gene in Gastrointestinal Cancers 1. 994–999 p.
95. Grusch M, Drucker C, Peter-Vörösmarty B, et al. Deregulation of the activin/follistatin system in hepatocarcinogenesis. Journal of Hepatology 2006;45(5):673–680.
96. Bufalino A, Cervigne NK, de Oliveira CE, et al. Low miR-143/miR-145 Cluster Levels Induce Activin A Overexpression in Oral Squamous Cell Carcinomas, Which Contributes to Poor Prognosis. PLOS ONE 2015;10(8):e0136599.
97. Taylor C, Loomans HA, le Bras GF, et al. Activin a signaling regulates cell invasion and proliferation in esophageal adenocarcinoma. Oncotarget 2015;6(33):34228–34244.
98. Loumaye A, de Barsy M, Nachit M, et al. Circulating Activin A predicts survival in cancer patients. Journal of Cachexia, Sarcopenia and Muscle 2017;8(5):768–777.
99. Hoda MA, Rozsas A, Lang E, et al. High circulating activin A level is associated with tumor progression and predicts poor prognosis in lung adenocarcinoma. Oncotarget 2016;7(12):13388–13399.
100. Bashir M, Damineni S, Mukherjee G, Kondaiah P. Activin-a signaling promotes epithelial–mesenchymal transition, invasion, and metastatic growth of breast cancer. npj Breast Cancer;1.
101. Ramirez MI, Amorim MG, Gadelha C, et al. Technical challenges of working with extracellular vesicles. *Nanoscale* 2018;10(3):881–906.
102. Pan B-T, Johnstone RM. Fate of the transferrin receptor during maturation of sheep reticulocytes in vitro: Selective externalization of the receptor. Cell 1983;33(3):967–978.
103. Harding C, Heuser J, Stahl P. Receptor-mediated endocytosis of transferrin and recycling of the transferrin receptor in rat reticulocytes. Journal of Cell Biology 1983;97(2):329–339.
104. Mathivanan S, Ji H, Simpson RJ. Exosomes: Extracellular organelles important in intercellular communication. *Journal of Proteomics* 2010;73(10):1907–1920.
105. Cocucci E, Meldolesi J. Ectosomes and exosomes: Shedding the confusion between extracellular vesicles. *Trends in Cell Biology* 2015;25(6):364–372.
106. Mathivanan S, Ji H, Simpson RJ. Exosomes: Extracellular organelles important in intercellular communication. *Journal of Proteomics* 2010;73(10):1907–1920.
107. Soler N, Marguet E, Verbavatz J-M, Forterre P. Virus-like vesicles and extracellular DNA produced by hyperthermophilic archaea of the order Thermococcales. Research in Microbiology 2008;159(5):390–399.

108. Knox KW, Vesk M, Work E. Relation Between Excreted Lipopolysaccharide Complexes and Surface Structures of a Lysine-Limited Culture of Escherichia coli. Journal of Bacteriology 1966;92(4):1206–1217.
109. Lee E-Y, Choi D-Y, Kim D-K, et al. Gram-positive bacteria produce membrane vesicles: Proteomics-based characterization of Staphylococcus aureus-derived membrane vesicles. PROTEOMICS 2009;9(24):5425–5436.
110. Tatischeff I, Bomsel M, de Paillerets C, et al. Dictyostelium discoideum cells shed vesicles with associated DNA and vital stain Hoechst 33342. Cellular and Molecular Life Sciences (CMLS) 1998;54(5):476–487.
111. Albuquerque PC, Nakayasu ES, Rodrigues ML, et al. Vesicular transport in *Histoplasma capsulatum* : an effective mechanism for trans-cell wall transfer of proteins and lipids in ascomycetes. Cellular Microbiology 2008;10(8):1695–1710.
112. Rodrigues ML, Nimrichter L, Oliveira DL, et al. Vesicular Polysaccharide Export in Cryptococcus neoformans Is a Eukaryotic Solution to the Problem of Fungal Trans-Cell Wall Transport. Eukaryotic Cell 2007;6(1):48–59.
113. Regente M, Corti-Monzón G, Maldonado AM, Pinedo M, Jorrín J, de la Canal L. Vesicular fractions of sunflower apoplastic fluids are associated with potential exosome marker proteins. FEBS Letters 2009;583(20):3363–3366.
114. Wolf P. The Nature and Significance of Platelet Products in Human Plasma. British Journal of Haematology 1967;13(3):269–288.
115. Gangoda L, Boukouris S, Liem M, Kalra H, Mathivanan S. Extracellular vesicles including exosomes are mediators of signal transduction: Are they protective or pathogenic? *Proteomics* 2015;15(2–3):260–271.
116. Raposo G, Stoorvogel W. Extracellular vesicles: Exosomes, microvesicles, and friends. *Journal of Cell Biology* 2013;200(4):373–383.
117. Keerthikumar S, Gangoda L, Liem M, et al. Proteogenomic analysis reveals exosomes are more oncogenic than ectosomes.
118. Balaj L, Lessard R, Dai L, et al. Tumour microvesicles contain retrotransposon elements and amplified oncogene sequences. Nature Communications 2011;2(1):180.
119. Thakur BK, Zhang H, Becker A, et al. Double-stranded DNA in exosomes: A novel biomarker in cancer detection. *Cell Research* 2014;24(6):766–769.
120. Guescini M, Genedani S, Stocchi V, Agnati LF. Astrocytes and Glioblastoma cells release exosomes carrying mtDNA. Journal of Neural Transmission 2010;117(1):1–4.
121. Ratajczak J, Wysoczynski M, Hayek F, Janowska-Wieczorek A, Ratajczak MZ. Membrane-derived microvesicles: Important and underappreciated mediators of cell-to-cell communication. *Leukemia* 2006;20(9):1487–1495.

122. Kunz F, Kontopoulou E, Reinhardt K, et al. Detection of AML-specific mutations in pediatric patient plasma using extracellular vesicle–derived RNA. Annals of Hematology 2019;98(3):595–603.
123. Reclusa P, Laes JF, Malapelle U, et al. EML4-ALK translocation identification in RNA exosomal cargo (ExoALK) in NSCLC patients: A novel role for liquid biopsy. *Translational Cancer Research* 2019;8S76–S78.
124. Nolte'T Hoen ENM, Buermans HPJ, Waasdorp M, Stoorvogel W, Wauben MHM, 'T Hoen PAC. Deep sequencing of RNA from immune cell-derived vesicles uncovers the selective incorporation of small non-coding RNA biotypes with potential regulatory functions. Nucleic Acids Research 2012;40(18):9272–9285.
125. Yang Q, Diamond MP, Al-Hendy A. The emerging role of extracellular vesicle-derived miRNAs: implication in cancer progression and stem cell related diseases.
126. Zhang B, Pan X, Cobb GP, Anderson TA. microRNAs as oncogenes and tumor suppressors. Developmental Biology 2007;302(1):1–12.
127. Fong MY, Zhou W, Liu L, et al. Breast-cancer-secreted miR-122 reprograms glucose metabolism in premetastatic niche to promote metastasis. Nature Cell Biology 2015;17(2):183–194.
128. Lunavat TR, Cheng L, Einarsdottir BO, et al. BRAFV600 inhibition alters the microRNA cargo in the vesicular secretome of malignant melanoma cells. Proceedings of the National Academy of Sciences of the United States of America 2017;114(29):E5930–E5939.
129. Liu Y, Luo F, Wang B, et al. STAT3-regulated exosomal miR-21 promotes angiogenesis and is involved in neoplastic processes of transformed human bronchial epithelial cells. Cancer Letters 2016;370(1):125–135.
130. Liao J, Liu R, Shi YJ, Yin LH, Pu YP. Exosome-shuttling microRNA-21 promotes cell migration and invasion-targeting PDCD4 in esophageal cancer. International Journal of Oncology 2016;48(6):2567–2579.
131. Qin X, Yu S, Zhou L, et al. Cisplatin-resistant lung cancer cell–derived exosomes increase cisplatin resistance of recipient cells in exosomal miR-100–5p-dependent manner. International Journal of Nanomedicine 2017;123721–3733.
132. Yeh Y-Y, Ozer HG, Lehman AM, et al. Characterization of CLL exosomes reveals a distinct microRNA signature and enhanced secretion by activation of BCR signaling [Epub ahead of print].
133. Paggetti J, Haderk F, Seiffert M, et al. Exosomes released by chronic lymphocytic leukemia cells induce the transition of stromal cells into cancer-associated fibroblasts. Blood 2015;126(9):1106–1117.
134. Bouvy C, Wannez A, Laloy J, Chatelain C, Dogné JM. Transfer of multidrug resistance among acute myeloid leukemia cells via extracellular vesicles and their microRNA cargo. Leukemia Research 2017;6270–76.
135. Mirzaei H, Sahebkar A, Jaafari MR, Goodarzi M, Mirzaei HR. Diagnostic and Therapeutic Potential of Exosomes in Cancer: The

Beginning of a New Tale? *Journal of Cellular Physiology* 2017;232(12):3251–3260.

136. Pant S, Hilton H, Burczynski ME. The multifaceted exosome: Biogenesis, role in normal and aberrant cellular function, and frontiers for pharmacological and biomarker opportunities. *Biochemical Pharmacology* 2012;83(11):1484–1494.

# 2. ActivinA: a new leukemia-promoting factor conferring migratory advantage to B-cell precursor-Acute Lymphoblastic Leukemic cells

Federica Portale[1], Giulia Cricrì[1], Silvia Bresolin[2], Monica Lupi[3], Stefania Gaspari[4], Daniela Silvestri[5,6], Barbara Russo[1], Noemi Marino[1], Paolo Ubezio[3], Fabio Pagni[7], Patrizia Vergani[8], Geertruy Te Kronnie[2], Maria Grazia Valsecchi[5], Franco Locatelli[4], Carmelo Rizzari[6], Andrea Biondi[1,6], Erica Dander[1]* and Giovanna D'Amico[1]*

*E.D. and G.D'A. equally contributed to the work

***Haematologica. 2019 Mar;104(3):533-545. doi: 10.3324/haematol.2018.188664***

[1]Centro Ricerca Tettamanti, Pediatric Dep, University of Milano-Bicocca, Fondazione MBBM, Monza; [2]Department of Women's and Children's Health, University of Padova; [3]Department of Oncology, Istituto di Ricerche Farmacologiche Mario Negri IRCCS, Milano; [4]Department of Pediatric Hematology-Oncology, IRCCS Bambino Gesù Children's Hospital, University of Pavia, Rome; [5]Medical Statistics Unit, Department of Clinical Medicine and Prevention, University of Milano-Bicocca; [6]Clinica Pediatrica Ospedale S. Gerardo, Fondazione MBBM, University of Milano-Bicocca, Monza; [7]School of Medicine and Surgery, University of Milano-Bicocca; [8]Department of Obstetrics and Gynecology, University of Milano-Bicocca, Monza (Italy)

## 2.1. Abstract

B-cell precursor-acute lymphoblastic leukemia modulates the bone marrow (BM) niche to become leukemia-supporting and chemoprotective by reprogramming the stromal microenvironment. New therapies targeting the interplay between leukemia and stroma can help improve disease outcome. We identified ActivinA, a TGF-β family member with a well-described role in promoting several solid malignancies, as a factor favoring leukemia that could represent a new potential target for therapy.

ActivinA resulted overexpressed in the leukemic BM and its production was strongly induced in mesenchymal stromal cells (MSCs) after culture with leukemic cells. Moreover, MSCs isolated from BM of leukemic patients showed an intrinsic ability to secrete higher amounts of ActivinA compared to their normal counterpart. The pro-inflammatory leukemic BM microenvironment synergized with leukemic cells to induce stromal-derived ActivinA. Gene expression analysis of ActivinA-treated leukemic cells showed that this protein was able to significantly influence motility-associated pathways. Interestingly, ActivinA promoted random motility and CXCL12-driven migration of leukemic cells, even at suboptimal chemokine concentrations, characterizing the leukemic niche. Conversely, ActivinA severely impaired CXCL12-induced migration of healthy CD34+ cells. This opposite effect can be explained by the ability of ActivinA to increase intracellular calcium only in leukemic cells, boosting cytoskeleton dynamics through a higher rate of actin polymerization. Moreover, by stimulating the invasiveness of the leukemic cells, ActivinA was found to be a

leukemia-promoting factor. Importantly, the ability of ActivinA to enhance BM engraftment and the metastatic potential of leukemic cells was confirmed in a xenograft mouse model of the disease.

Overall, ActivinA was seen to be a key factor in conferring a migratory advantage to leukemic cells over healthy hematopoiesis within the leukemic niche.

## 2.2. Introduction

Acute lymphoblastic leukemia (ALL) is the most frequent childhood malignancy worldwide. B-cell precursor (BCP)-ALL represents about 80% of ALL cases and mainly affects children, with an incidence of 3-4 cases per 100,000 each year[1]. Even though the cure rate exceeds 80% in children, BCP-ALL is the leading cause of cancer-related death in children and young adults[2]. In spite of the notable ameliorations in disease management, the emergence of chemoresistance decreases the probability that therapy will be successful and leads to relapse in more than 20% of treated patients[3]. BCP-ALL cells critically depend on interactions with the bone marrow (BM) microenvironment, which provides essential regulatory cues for proliferation, survival and drug resistance, and such interactions contribute to treatment failure and disease relapse[4]. In particular, mesenchymal stromal cells (MSCs) have been recognized as an essential supportive element of the leukemic hematopoietic microenvironment because of their ability to define exclusive BM niches that sustain leukemic cells to the detriment of normal hematopoiesis and resist chemotherapy[5]. In this complex network, it has been shown that chemokines could contribute to BCP-ALL development by driving the migration of leukemic cells toward protective BM niches, as well as by providing anti-apoptotic signals[6].

ActivinA is a pleiotropic cytokine that belongs to the TGF-β superfamily. It has a broad tissue distribution, being involved in multiple physiological and pathological processes, including

inflammation, metabolism, immune response, and endocrine function. Recent studies have demonstrated that ActivinA is an important regulator of carcinogenesis. Indeed, it can directly modulate cancer cell proliferation and migration. It can also enhance tumor progression by regulating the tumor microenvironment[7]. ActivinA signals through transmembrane serine/threonine kinase receptors. It binds to type II Activin receptors (ACVR2A or ACVR2B), causing recruitment, phosphorylation and activation of type I Activin receptors (ALK2 or ALK4). ActivinA signaling is inhibited by Inhibins, through competitive binding for Activin receptors, and by Follistatin (FST) and Follistatin like-3 (FSTL3), which act as trap molecules[8]. The Activin receptor II ligand trap ACE-011 is currently under investigation in a Phase II clinical trial on Multiple Myeloma[9].

The aim of the current study was to explore the role of ActivinA in the leukemic BM niche, with a particular focus on its supportive role for BCP-ALL cells to the detriment of healthy hematopoiesis.

## 2.3. Experimental procedures

### 2.3.1. Patients' and healthy donors' samples

Bone marrow plasma samples were collected from 125 BCP-ALL patients at diagnosis and from 56 healthy donors (HDs). Primary BCP-ALL cells were isolated at diagnosis from 22 BM aspirates and used for *in vitro* assays. Details of the study cohort are shown in the *Supplementary Materials*. The study was approved by the Institutional Review Board (AIEOP-BFM ALL 2009 protocol; EudraCT-2007-004270-43).

### 2.3.2. Culture of BCP-ALL cell lines

The leukemic cell lines 697, NALM-6, RS4;11, SUP-B15 and REH were cultured as described in the *Supplementary Materials*.

### 2.3.3. Isolation of BM-MSCs

Bone marrow-mesenchymal stromal cells (BM-MSCs) from 15 BCP-ALL patients (ALL-MSCs) and 15 age-matched HDs (HD-MSCs) (Supplemental Table 1) were cultured as described in the *Supplementary Materials*.

### 2.3.4. CB- and BM-CD34+ cell isolation

CD34+ cells were isolated from cord blood (CB) units and HD BM aspirates as described in the *Supplementary Materials*.

### 2.3.5. Co-culture of primary leukemic cells with BM-MSCs

Bone marrow-mesenchymal stromal cells were co-cultured with primary leukemic cells at an MSC:leukemia ratio of 1:30, either in the presence or in the absence of 0.4 μm Transwell inserts (Costar Transwell® Permable Supports, Corning Inc., MA, USA) in DMEM 2% FBS. After 72 hours (h), supernatants were collected and cryopreserved at -80°C for further analyses.

### 2.3.6. ELISA assay for quantification of ActivinA, CXCL12 and pro-inflammatory cytokines

The levels of ActivinA, pro-inflammatory cytokines (IL-1β, IL-6 and TNF-α) and CXCL12 were assessed in BM plasma samples and culture supernatants using commercially available ELISA kits (R&D Systems, USA), according to the manufacturer's instructions.

### 2.3.7. Quantitative RT-PCR

qRT-PCR was performed using LightCycler® 480 (Roche, Basel, Switzerland), as reported in the *Supplementary Materials*.

### 2.3.8. Gene expression profile analysis

Gene expression profile analysis of 697 cells treated or not with ActivinA (50 ng/mL) for 6 h and 24 h was evaluated by GeneChip Human Genome U133 Plus 2.0 arrays (Affymetrix Inc., Santa Clara, CA, USA). Details of the procedure are described in the *Supplementary Materials*.

### 2.3.9. Time-lapse microscopy

Leukemic cells were seeded in Gelatin B-coated wells of an 8-well chamber slide (Ibidi, Martinsried, Germany). Cell tracks were recorded as described in the *Supplementary Materials*.

### 2.3.10. Chemotaxis assays

Both leukemic and healthy $CD34^+$ cells, pretreated or not with ActivinA (24 h stimulation), were tested for chemotaxis in Transwell-based assays (Costar Transwell® Permable Supports, Corning Inc.). Selected experiments were performed using the ALK4 blocker SB431542 (SigmaAldrich, St Louis, MO, USA). Details are described in the *Supplementary Materials*.

### 2.3.11. Invasion assays

The invasive capacity of leukemic cells was evaluated using Matrigel-coated Transwells, as described in the *Supplementary Materials*.

### 2.3.12. Activin Receptor analyses

697 leukemic cell line and primary blasts were analyzed for ALK4, ACVR2A and ACVR2B expression by flow cytometry and qRT-PCR and for ALK2 expression by Western Blot, as described in the *Supplementary Materials*.

### 2.3.13. CXCR4 and CXCR7 staining

Expression of CXCR4 and CXCR7 was analyzed by flow cytometry in 697 cells, pretreated or not with ActivinA (*Supplementary Materials*).

### 2.3.14. Filamentous (F)-actin polymerization assay

F-actin polymerization was analyzed in 697 cells pretreated or not with ActivinA using AlexaFluor 647-labeled phalloidin (Invitrogen, Carlsbad, CA, USA) before and after CXCL12 stimulation as reported in the *Supplementary Materials*.

### 2.3.15. Calcium mobilization

Intracellular calcium mobilization was measured by flow cytometry using the Fluo-4NW Assay (Invitrogen), as reported in the *Supplementary Materials*.

### 2.3.16. B-cell acute lymphoblastic leukemia xenograft model

Female 7-9-week-old NOD-SCID-γchain$^{-/-}$ (NSG) mice (Charles River, Calco, Italy) were intravenously (i.v.) transplanted with $0.5\times10^6$ 697 cells or $10^6$ NALM-6 cells, either pretreated or not with ActivinA for 24 h. Details are described in the *Supplementary Materials*. The study was approved by the Italian Ministry of Health (approval n.64/2014).

### 2.3.17. Statistical analyses

Differences between subgroups were compared with the Mann-Whitney test or Wilcoxon matched-pairs signed rank test in the case of matched values.

## 2.4. Results

### 2.4.1. Stroma-derived ActivinA increased in response to leukemia

It has been demonstrated that ActivinA could exert a pro-tumoral role in several types of cancer both through direct effects on tumoral cells and indirect effects on the tumor microenvironment[7]. Therefore, we first measured ActivinA levels in BM plasma samples from 44 HDs and 108 BCP-ALL patients at disease onset. ELISA assay revealed that ActivinA was significantly increased in the BM plasma of BCP-ALL patients compared to that of HDs (Figure 1A). The median concentration (mc) of ActivinA was 400 pg/mL (range:62.5-7241 pg/mL) in BCP-ALL patients and 273.4 pg/mL (range:62.5-2338 pg/mL) in HDs ($P$<0.05).

To determine whether ActivinA plasma levels at BCP-ALL diagnosis were related with disease outcome/severity, we analyzed 98 patients with available follow-up out of the 108 tested, considering several clinical and biological parameters. In detail, 3- and 4-year event-free survival (EFS) and sensitive quantitative PCR-based minimal residual disease (MRD) at day +33 and +78 and final risk were taken into account[10]. ActivinA levels did not impact on EFS, on PCR-MRD risk, or on patients' final risk stratification (*data not shown*).

It had previously been shown that BM-MSCs exhibit a basal level of ActivinA secretion[11]. In view of the pivotal role of BM-MSCs in sustaining the leukemic niche, we explored the regulation of MSC-derived ActivinA in the context of BCP-ALL. We first

confirmed that MSCs isolated from the BM of HDs (HD-MSCs) were able to constitutively produce the molecule (mc:103.2, range:62.5-526.7 pg/mL). Then, to test whether BCP-ALL cells could modulate MSC-derived ActivinA, we set up co-culture experiments of HD-MSCs with primary leukemic blasts and quantified ActivinA in supernatants after 72 h of culture. Interestingly, we found that primary leukemic cells significantly induced ActivinA in MSCs both through soluble factors (mc:268.1, range:62.5-842.8 pg/mL) and a cell-to-cell contact-mediated mechanism (mc:777.9, range:96.2-1456 pg/mL), with a 2.6 and a 7-fold increase, respectively, compared to the basal condition ($P<0.001$ and $P<0.0001$). Notably, primary BCP-ALL cells secreted either very low or even undetectable levels of ActivinA (Figure 1B).

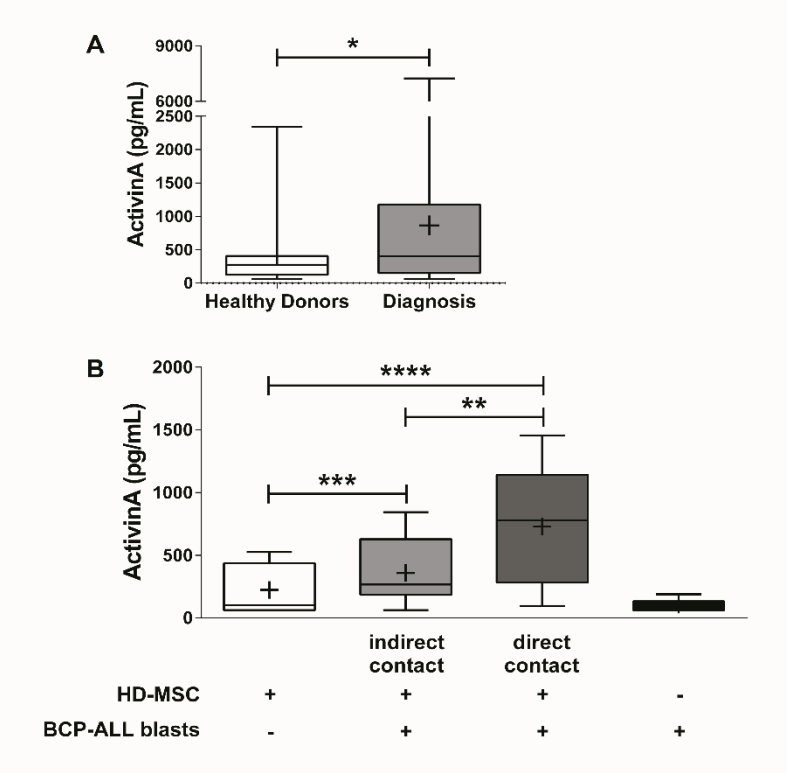


**Figure 1. B-cell precursor-acute lymphoblastic leukemia (BCP-ALL) cells reprogrammed the bone marrow (BM) stroma to produce high levels of ActivinA.**

**(A)** BM plasma levels of ActivinA were assessed by ELISA in healthy donors (HDs) (n=44) and BCP-ALL patients at the onset of the disease (n=108). Each box plot shows the median and the mean (+) and extends from the lowest to the highest value. **P*<0.05: Mann-Whitney test. **(B)** Primary leukemic blasts were either directly co-cultured or separated by a 0.4 µm Transwell insert with HD-mesenchymal stromal cells (MSCs). After 72 hours of culture, supernatants were collected and ActivinA concentration was analyzed by ELISA (n=17 independent co-

cultures). Each box plot shows the median and extends from the lowest to the highest value. **P<0.01, ***$P$<0.001, ****$P$<0.0001: Wilcoxon matched-pairs signed rank test.

### 2.4.2. Leukemic cells expressed ActivinA receptors

To determine whether BCP-ALL cells could be targets of ActivinA, the expression of Activin receptors was assessed on five leukemic cell lines (697, NALM-6, RS4;11, SUP-B15, REH) (Figure 2A) and eighteen primary BCP-ALL blasts by flow cytometry and Western Blot analyses (Figure 2B). Western Blot images are presented in *Supplementary* Figure S1.

Both type I and type II Activin receptors were found to be expressed by all primary blasts and cell lines tested, with a markedly wide range of expression. The expression level of ActivinA receptors in primary BCP-ALL cells was highly patient-specific and was shown to be independent of the commonly investigated leukemia-related genetic alterations.

Taken together, these data suggest that BCP-ALL cells could possibly respond to ActivinA. Moreover, we showed that ActivinA was able to significantly increase the expression of its type I receptors, thus suggesting a positive loop underlying the responsiveness of leukemic cells to ActivinA (*Supplementary* Figure S2).

Subsequent analyses were performed on the 697 and NALM-6 cell lines as their different Activin receptor expression makes them representative of the high inter-patient variability observed.

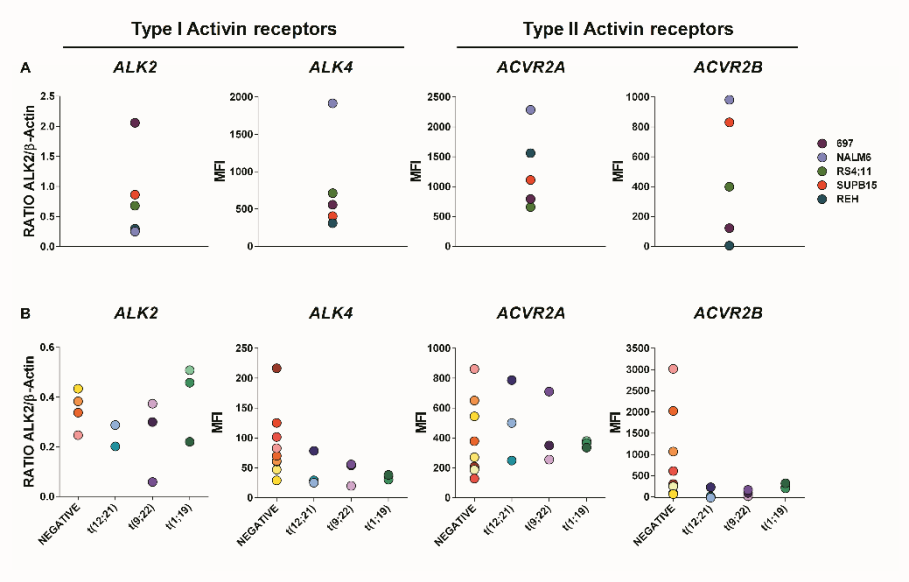


**Figure 2. B-cell precursor-acute lymphoblastic leukemia (BCP-ALL) cells expressed type I and type II ActivinA receptors.**

**(A)** The expression of the type I ActivinA receptors ALK2 and ALK4 and the type II ActivinA receptors ACVR2A and ACVR2B was quantified in five leukemic cell lines (697, NALM-6, RS4;11, SUP-B15, REH) and **(B)** in bone marrow (BM) primary blasts from BCP-ALL patients by Western Blot (ALK2, n=12) and flow cytometry (ALK4, ACVR2A, ACVR2B, n=18). Data are presented as the ratio of ALK2 to β-actin obtained by densitometric analysis and mean fluorescence intensity (MFI) for ALK4, ACVR2A and ACVR2B.

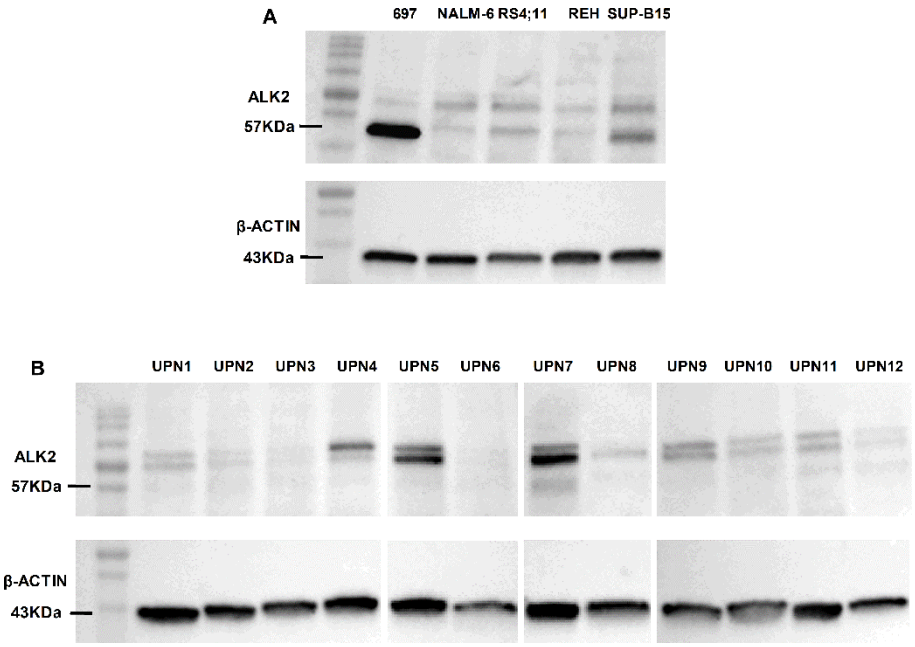


**Supplementary Figure S1. ALK2 was variably expressed by BCP-ALL cell lines and primary BM samples.**

Western Blot analyses of ALK2 in five different BCP-ALL cell lines **(A)** and in primary blasts from twelve BCP-ALL patients **(B)** demonstrate a variable expression of the expected 57 KDa protein isoform. Additional bands with higher molecular weight, possibly derived from the glycosylation of the protein as already described in mouse cells, were further visualized. β-actin levels were used as a loading control.

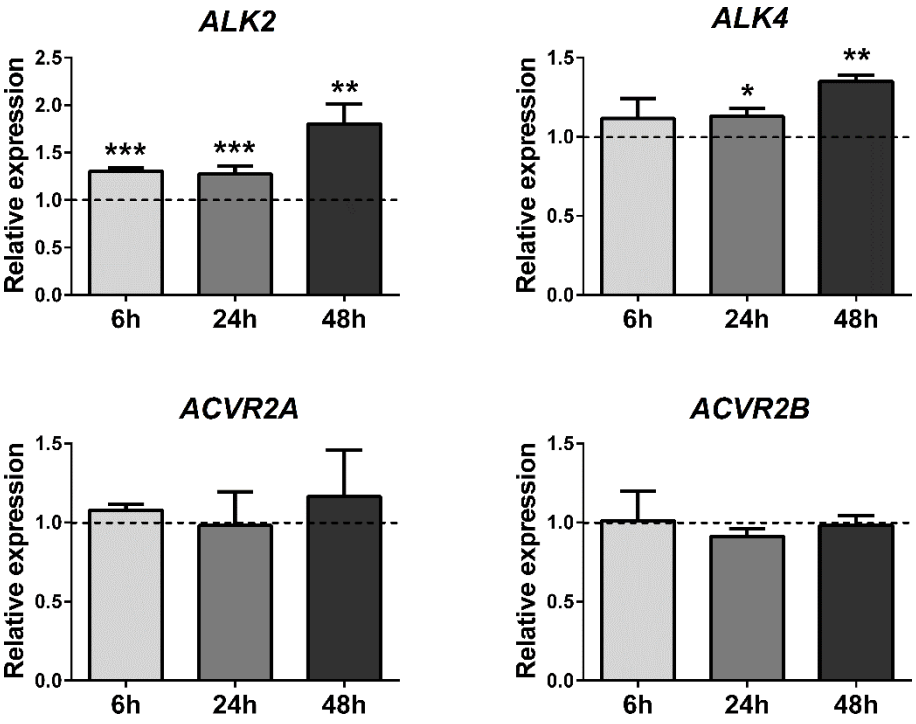


**Supplementary Figure S2. Modulation of ActivinA receptor expression by ActivinA.**

Expression of *ALK2, ALK4, ACVR2A* and *ACVR2B* was assessed in 697 cells treated or not with ActivinA (50 ng/mL) for 6 hours, 24 hours and 48 hours. The data are presented as the mean fold change ± SEM of mRNA levels normalized to *GAPDH* mRNA (endogenous control). The graphs represent the results of three independent experiments.

**P*<0.05, ***P*<0.01, ****P*<0.001: Mann-Whitney test.

### 2.4.3. Gene expression analysis revealed ActivinA involvement in regulating cell motility

For a more in depth analysis of the molecular changes induced by ActivinA in BCP-ALL cells, we performed gene expression profile (GEP) analysis of 697 cells upon stimulation with ActivinA for 6 h and 24 h. We found that 122 genes were differentially expressed in ActivinA-treated cells *versus* untreated cells after 6 h of stimulation (FDR<0.05) and that 151 genes were differentially expressed after 24 h of stimulation (FDR<0.05). Gene Ontology (GO) analysis of differentially expressed genes identified enriched GO categories (*Supplementary* Figure S3A) critically linked to carcinogenesis such as “regulation of cell activation”, “positive regulation of antigen receptor-mediated signaling pathway”, “pathways in cancer”, etc.

Interestingly, we also observed that ActivinA was able to influence migration-associated pathways, such as “calcium ion homeostasis and transport into cytosol", “PI3K/AKT activation”, “Ras signaling pathway”, “focal adhesion", suggesting its possible effect on leukemic cell motility. These data are in agreement with the recently recognized role of ActivinA in the regulation of cell migration and invasion in the context of several solid malignancies[12–15]. On the basis of this evidence, we first used qRT-PCR assays to validate the ActivinA-mediated changes in the expression of several genes linked to $Ca^{2+}$ homeostasis (*ATP2B2*, *ATP2B4*), Ras pathway activation (*VAV3*), and cell motility and movement regulation (*ARHGAP25*, *CORO1A*, *DOCK4*, *LCK*, *PTPRC)*. Data obtained

in qRT-PCR on 697 cells were highly concordant with microarray data (*Supplementary* Figure S3B). Raw data are shown in *Supplementary* Figure S4. In addition, qRT-PCR analyses of the above-mentioned genes were performed on 7 primary BCP-ALL patients' samples stimulated or not with ActivinA (*Supplementary* Figure S5). Among them, 3 presented the t(1;19) (grey dots) typical of the 697 cell line. Interestingly, four of the tested genes (*ARHGAP25*, *CORO1A*, *DOCK4* and *PTPRC*) were significantly modulated in at least one stimulation time point (*Supplementary* Figure S5B) by ActivinA in more than 70% of patients, similarly to our observations in 697 cells. It is worth noting that the t(1;19) patients showed a modulation of the *ATP2B4*, *VAV3* and *LCK* genes (*Supplementary* Figure S5B) more similar to 697 cells than the translocation negative ones.

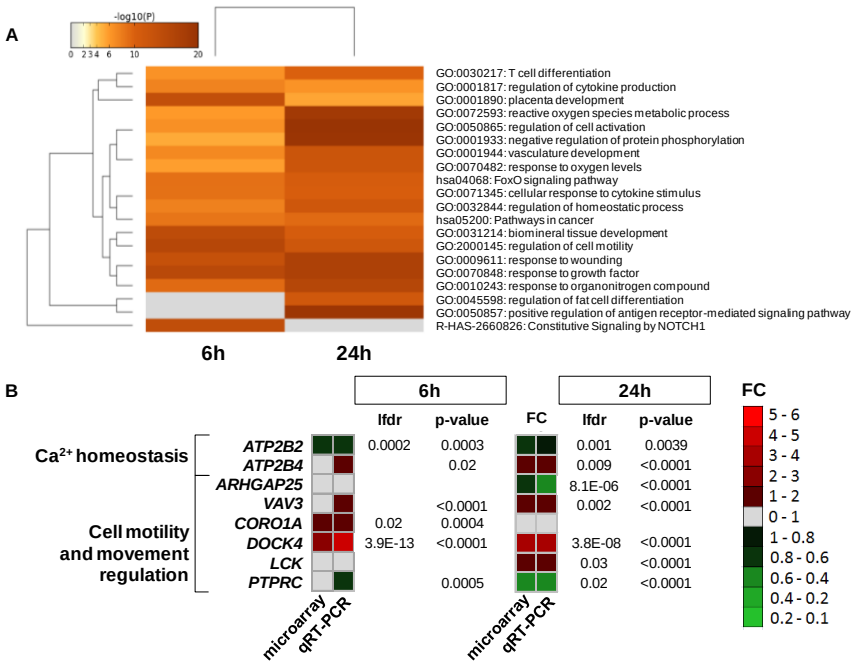


**Supplementary Figure S3. GEP analysis showed that ActivinA positively modulates cell motility in leukemic cells.** **(A)** Gene Ontology (GO) enrichment analysis of cell biological processes, based on differentially expressed genes in the 697 cell line treated or not with ActivinA (50 ng/mL) for 6 hours and 24 hours (n=4 independent experiments). The hierarchical clustering is based on the 20 most significant GO and KEGG terms resulting from Metascape analysis. In the heatmap colored cells were filled according their p-value. Grey cells indicate the lack of enrichment for that term in the corresponding gene list. **(B)** Selected genes significantly modulated in ActivinA treated cells compared to the untreated control were validated by qRT-PCR. Expression levels in qRT-PCR were normalized to GAPDH mRNA levels. Colored squares in the level plot correspond to FC

between treated *vs* untreated cells derived from microarray and qRT-PCR. Lfdr (Shrinkage *t* test) for microarray data and p-value (Mann-Whitney test) for qRT-PCR were respectively shown. FC= Fold Change; lfdr= local false discovery rate.

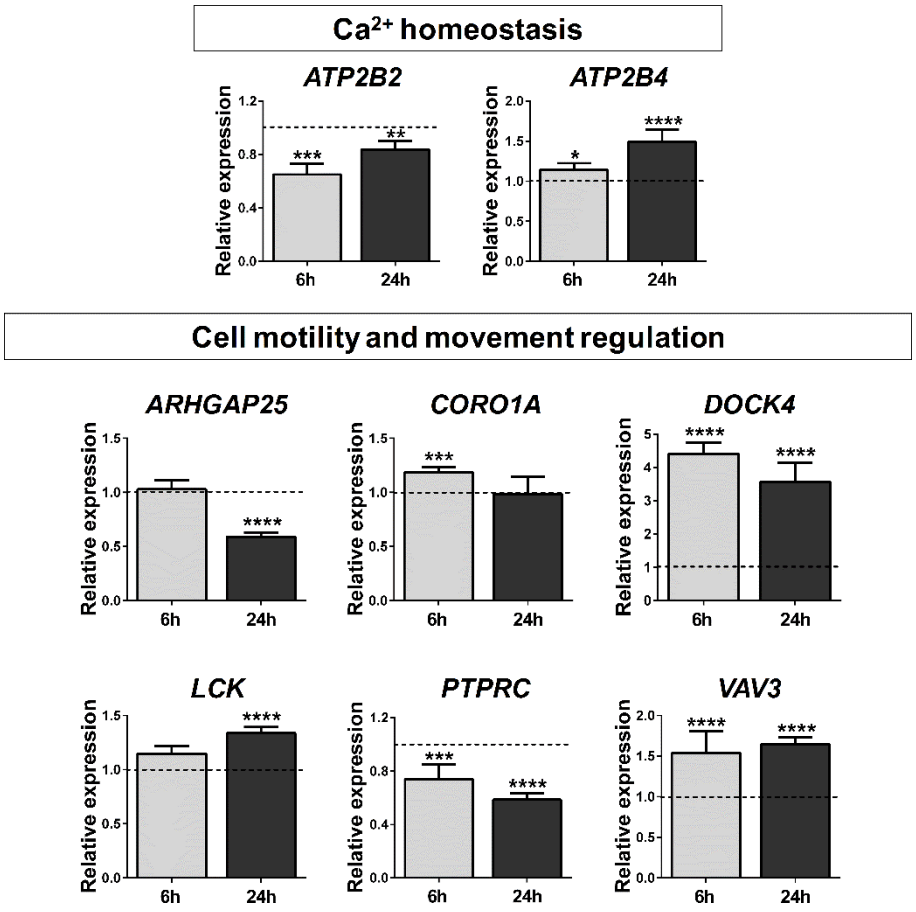


**Supplementary Figure S4. Validation of gene expression analysis data.**

Expression of *ATP2B2, ATP2B4, ARHGAP25, CORO1A, DOCK4, LCK, PTPRC* and *VAV3* was assessed in 697 cells

treated or not with ActivinA (50 ng/mL) for 6 hours or 24 hours. The mean (± SEM, n=3 independent experiments) mRNA fold change calculated for each target gene in the ActivinA-stimulated condition over the unstimulated (dotted line), after normalization to *GAPDH* mRNA (endogenous control), is represented in the graph. **P*<0.05, ***P*<0.01, ****P*<0.001, ****<0.0001: Mann-Whitney test.

**A**

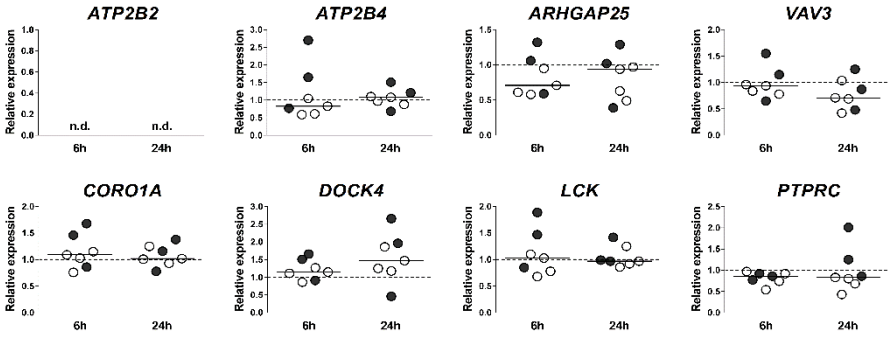


**B**

| | | negative* | | | | t(1;19) | | |
|---|---|---|---|---|---|---|---|---|
| | | UPN6 | UPN13 | UPN14 | UPN15 | UPN2 | UPN3 | UPN12 |
| *ATP2B4* | 6 hrs | 0,83 | 0,59 | 1,05 | 0,61 | ***2,70*** | ***1,65*** | 0,77 |
| | 24 hrs | 1,10 | 0,88 | 0,97 | 1,08 | ***1,21*** | ***1,51*** | 0,68 |
| *ARHGAP25* | 6 hrs | ***0,71*** | ***0,58*** | 0,95 | ***0,61*** | 1,32 | 1,06 | ***0,59*** |
| | 24 hrs | ***0,49*** | 0,94 | ***0,63*** | 0,97 | 1,02 | 1,29 | ***0,39*** |
| *VAV3* | 6 hrs | 0,94 | 0,78 | 0,96 | 0,84 | ***1,55*** | ***1,15*** | 0,65 |
| | 24 hrs | 0,42 | 1,04 | 0,71 | 0,69 | 0,87 | 1,25 | 0,48 |
| *CORO1A* | 6 hrs | 0,76 | ***1,15*** | 1,03 | 1,09 | ***1,68*** | ***1,46*** | 0,86 |
| | 24 hrs | ***1,25*** | 1,02 | 0,93 | 1,01 | 0,78 | ***1,38*** | ***1,16*** |
| *DOCK4* | 6 hrs | ***1,15*** | 0,86 | 1,11 | ***1,27*** | ***1,66*** | ***1,51*** | 0,91 |
| | 24 hrs | 1,25 | ***1,86*** | ***1,47*** | 1,18 | ***2,66*** | ***1,96*** | 0,46 |
| *LCK* | 6 hrs | 0,88 | 0,78 | 1,03 | 1,10 | ***1,89*** | ***1,47*** | 0,85 |
| | 24 hrs | 1,25 | 0,92 | 0,97 | 0,86 | 0,97 | ***1,42*** | 0,99 |
| *PTPRC* | 6 hrs | 0,97 | ***0,54*** | 0,92 | ***0,74*** | 0,92 | ***0,86*** | ***0,77*** |
| | 24 hrs | ***0,43*** | ***0,80*** | ***0,68*** | ***0,83*** | 2,01 | 1,25 | ***0,86*** |

*t(4;11), t(9;22) p190, t(12;21), t(1;19)

**Supplementary Figure S5. Validation of gene expression analysis data on primary BCP-ALL blasts.**

**(A)** Expression of *ATP2B2, ATP2B4, ARHGAP25, CORO1A, DOCK4, LCK, PTPRC* and *VAV3* was assessed in seven primary BCP-ALL patients treated or not with ActivinA (100 ng/mL) for 6 or 24 hours. The mean mRNA fold change calculated for each

target gene in the ActivinA-stimulated condition over the unstimulated (dotted line), after normalization to *GAPDH* mRNA (endogenous control), is represented in the graph. Each dot represents a single patient: white circles indicate patients negative for t(4:11), t(9;22) p190, t(12;21), t(1;19), while grey circles indicate t(1;19) positive patients. Solid lines represent the median values. **(B)** Raw data about mean fold changes are reported in the table. Statistically significant changes ($P<0.05$, Mann-Whitney test) in ActivinA stimulated patients over the unstimulated condition are identified by “italics”.

### 2.4.4. ActivinA increased random motility, chemotaxis and invasion of BCP-ALL cells

To test whether ActivinA was able to modulate BCP-ALL movement, we performed time-lapse microscopy (TLM) analyses and migration assays. TLM studies showed that ActivinA was able to increase random motility both in the 697 cell line ($P<0.0001$) and primary leukemic cells ($P<0.0001$) (Figure 3A, right).

It has been demonstrated that chemokines, and in particular the CXCR4/CXCL12 axis, play a key role in the homing and retention of ALL cells within the BM niche. Therefore, we tested whether ActivinA was able to modulate CXCL12-induced migration of leukemic cells using a Transwell-based migration assay. Notably, we found that ActivinA-pretreated 697 cells showed a significant increase in CXCL12-driven migration ($P<0.05$) (Figure 3B). Importantly, this finding was confirmed in primary leukemic

cells obtained from the BM of 13 BCP-ALL patients collected at diagnosis (Figure 3C). The average percentage of primary unstimulated BCP-ALL blasts migrated in response to CXCL12 (mean:15.6%, range:1.9-43.5%) was significantly increased following ActivinA stimulation (mean:22.9%, range:4.1-61.1%) ($P$<0.001).

To ensure the specificity of the observed effect on CXCL12 mediated migration, we blocked ActivinA/Activin receptor axis by using SB431542, a well-characterized specific inhibitor of transforming growth factor-beta superfamily type I Activin receptor-like kinase (ALK) receptors ALK4, ALK5, and ALK7[16,17]. SB431542 inhibited the migration of ActivinA-pretreated 697, NALM-6 cells (*Supplementary* Figure S6) and primary leukemic blasts (Figure 3D) in response to CXCL12 in a dose-dependent manner. In 3 different patients, we demonstrated that 10 µM SB431542 inhibited ActivinA stimulatory effect on CXCL12-driven migration of 78.8% (range:74.5-84.0%, $P$<0.05).

Interestingly, it has been reported that ActivinA expression is associated with an invasive phenotype in several types of cancer, including ovarian cancer, esophageal adenocarcinoma, breast cancer and oral squamous cell carcinomas[12–15]. Therefore, we tested whether ActivinA was able to modulate leukemic cell invasive capacity using Matrigel-coated Transwells. We found that ActivinA increased the ability of primary BCP-ALL cells to migrate through a complex matrix in presence of CXCL12 (Figure 3E), with a 2-fold increase compared to the untreated condition ($P$<0.05).

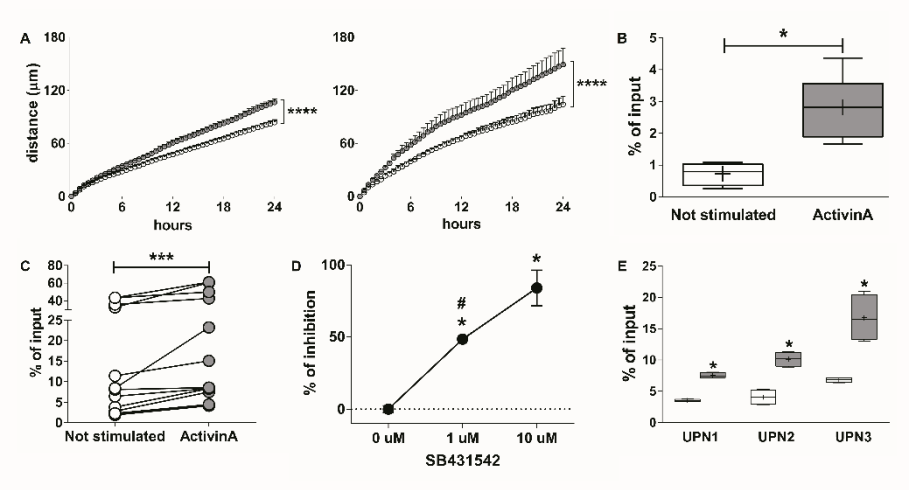


**Figure 3. ActivinA enhanced cell motility, migration and invasion of leukemic cells.**

**(A)** Leukemic cells were treated or not with ActivinA and then tracked for 24 hours (h) by time-lapse microscopy. Dead cells were excluded using PI staining. Data represent the mean ± Standard Error Deviation (SEM) of the migrated distance over time of three independent experiments. The distance migrated after 24 h by all tracked cells was compared between ActivinA-stimulated (grey) and not stimulated (white) cells. (Left) 697 cells treated with 50 ng/mL ActivinA. (Right) B-cell precursor acute lymphoblastic leukemia (BCP-ALL) primary blasts treated with 100 ng/mL ActivinA. **(B)** Chemotaxis assay was performed using 697 cells stimulated with ActivinA for 24 h (50 ng/mL) and allowed to migrate toward CXCL12-containing medium (100 ng/mL) for 4 h (5 µM pore Transwell). Each box plot shows the median and the mean (+) of the percentage of migrated cells and

extends from the lowest to the highest value. The graphs represent the results of six independent experiments. The percentage of migrated cells was determined as described in the *Supplementary Methods*. **(C)** Primary BCP-ALL cells from 13 patients were exposed to ActivinA (100 ng/mL) for 24 h and employed for chemotaxis assays toward CXCL12-containing medium (100 ng/mL). The average percentage of cells migrated after 1 h of culture is shown. **(D)** Chemotaxis assay was performed using BCP-ALL primary cells pretreated for 1 hour with SB431542 or vehicle (DMSO) before the stimulation with or without ActivinA for 24 h (100 ng/mL). Cells were allowed to migrate toward CXCL12-containing medium (100 ng/mL) for 1 h (5 µM pores Transwell). The percentage of migrated cells was determined as described in the *Supplementary Methods*. The average percentage of inhibition ± SEM is represented (one out of three representative experiments). **(E)** Primary BCP-ALL cells pretreated or not with ActivinA for 24 h (100 ng/mL) were allowed to migrate through Transwell inserts (8 µM pores) coated with a Matrigel-barrier (1 mg/mL) for 24 h in the presence of CXCL12 (100 ng/mL) in the lower chamber. Each box plot shows the median and the mean (+) of the percentage of invaded cells and extends from the lowest to the highest value. The graphs represent the results of three different patients. **P*<0.05, ****P*<0.001; ****P<0.0001; Wilcoxon matched-pairs signed rank test (A-C); **P*<0.05: comparison with vehicle (0 µM), Mann-Whitney test; *P<0.05: comparison with 10 µM SB431542, Mann-Whitney test (D); *P<0.05: Mann-Whitney test (E).

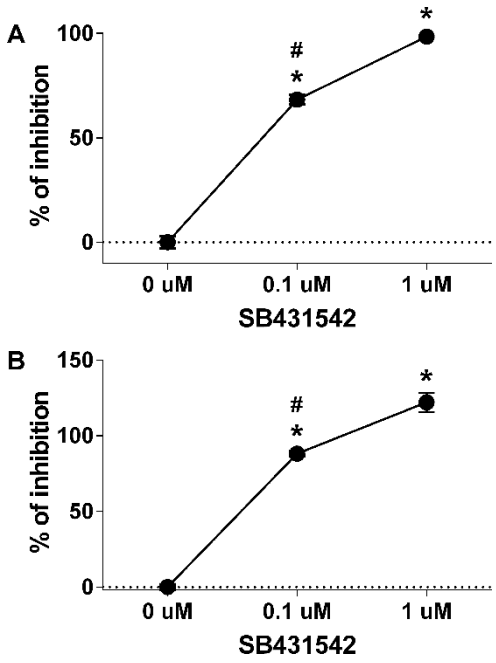


**Supplementary Figure S6. SB431542 specifically inhibits ActivinA stimulatory effect on 697 and NALM-6 cell migration.**

Chemotaxis assays were performed using 697 **(A)** and NALM-6 cells **(B),** pretreated for 1 hour with SB431542 or vehicle (DMSO), before the stimulation with or without ActivinA for 24 hours (50 ng/mL). Cells were allowed to migrate toward CXCL12-containing medium (100 ng/mL) for 4 hours (5 µM pores Transwell). The percentage of migrated cells was determined as described in the *Supplementary Methods*. The average percentage of inhibition ± SEM is represented (one out of three representative experiments).

### 2.4.5. ActivinA enhanced leukemic cells responsiveness to low levels of CXCL12

CXCL12 reduction is one of the microenvironmental alterations occurring in the leukemic BM, as demonstrated both in mice models and leukemic patients[18,19], which is associated to impairment of normal heamatopoiesis[5]. Here, in a large cohort of 70 patients, we confirmed a significant reduction of approximately 6 times the CXCL12 of BM plasma level in BCP-ALL patients (mc:77.7, range:15.7-488.9 pg/mL) compared to HDs (mc:476.8, range:99.1-1763 pg/mL, n=46) ($P$<0.0001) (Figure 4A). To test the potential ability of ActivinA to increase the responsiveness of leukemic cells to suboptimal concentrations of CXCL12, we performed dose-response chemotaxis assays. We demonstrated that ActivinA enhanced 697 cell line migration toward CXCL12 used at a concentration 10- or 100-fold lower than that classically used in *in vitro* migration assays (100 ng/mL). Indeed, ActivinA pretreatment induced a 10-fold increase in the CXCL12-driven chemotaxis toward 10 ng/mL CXCL12 ($P$<0.05) and a 7-fold increase toward 1 ng/mL CXCL12 *(*$P$<0.05), compared to untreated cells, that showed a responsiveness to these low chemokine concentrations comparable to that of empty medium (Figure 4B).

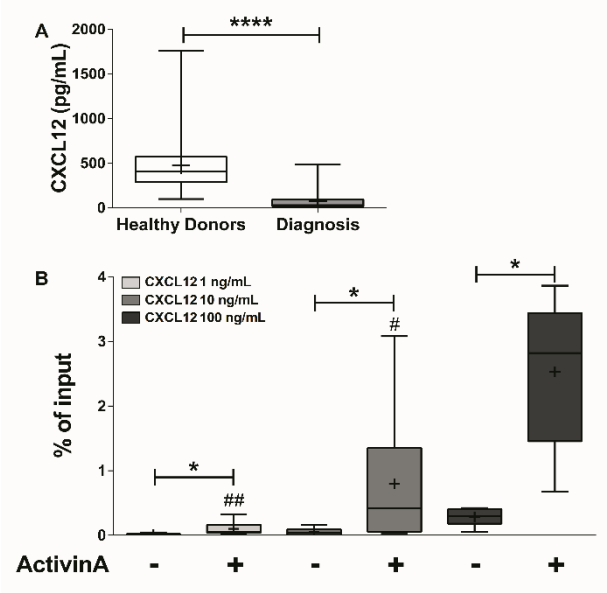


**Figure 4. ActivinA enhanced leukemic cell responsiveness to CXCL12.**

**(A**) CXCL12 bone marrow plasma levels were assessed by ELISA in 46 healthy donors (HDs) and 70 B-cell precursor-acute lymphoblastic leukemia (BCP-ALL) patients at the onset of the disease. Each box plot shows the median and the mean (+) and extends from the lowest to the highest value. ****$P$<0.0001: Mann-Whitney test. **(B)** 697 cells were pretreated with ActivinA (50 ng/mL) for 24 hours and then incubated for 4 h in Transwell chambers toward decreasing concentration of CXCL12 (100-10-1 ng/mL). Each box plot shows the median and the mean (+) of the percentage of migrated cells and extends from the lowest to the highest value. The graphs represent the results of six independent experiments. *$P$<0.01: ActivinA-treated *vs* untreated 697 cells, Wilcoxon matched-pairs signed rank test;

#*P*<0.05, ##*P*<0.01: comparison with 100 ng/mL CXCL12-induced migration, Mann-Whitney test.

### 2.4.6. Intracellular calcium levels and actin polymerization were increased by ActivinA in leukemic cells

To further investigate the enhanced leukemic cell responsiveness to CXCL12, we first evaluated whether ActivinA treatment could affect chemokine receptor expression. Flow cytometry analysis of CXCL12 chemokine receptors on 697 cells showed that the levels of CXCR4 and CXCR7, evaluated both as extracellular receptors and intracellular pool, were not affected by ActivinA (Figure 5A).

We, therefore, performed flow cytometry analysis to determine the effect of ActivinA on the intracellular calcium level of BCP-ALL cells. Our data indicated that both in 697 cells (Figure 5B) and in primary BCP-ALL cells (Figure 5C) the basal intracellular calcium content was increased in ActivinA-pretreated cells as compared to untreated cells (mean range 1, *P*<0.05). Interestingly, on addition of CXCL12, ActivinA-treated cells showed a further significant increase in the concentration of free cytosolic $Ca^{2+}$ compared to the untreated cells (Figure 5B and 5C, peak and mean range 2, *P*<0.05).

Moreover, we evaluated the effect of ActivinA on actin cytoskeleton dynamics. Since the conversion of globular into filamentous actin (F-actin) is a prerequisite for site-directed migration, we analyzed whether the increased chemotactic

response upon ActivinA treatment was associated with enhanced chemokine-induced actin polymerization. Pretreatment of 697 cells with ActivinA for 24 h resulted in a more prominent conversion of globular into F-actin starting from 15 seconds (s) after addition of CXCL12 ($P$<0.05) (Figure 5C). Notably, ActivinA-pretreated cells maintained a higher amount of F-actin compared to untreated condition, even 180 s after CXCL12 stimulation ($P$<0.001). These data strongly support our GEP results highlighting the role of ActivinA as a modulator of several genes involved in cytoskeleton remodeling and regulation of calcium dynamics.

Results on migration, invasion, chemokine receptors and calcium flux were confirmed in the NALM-6 BCP-ALL cell line (*Supplementary* Figure S7).

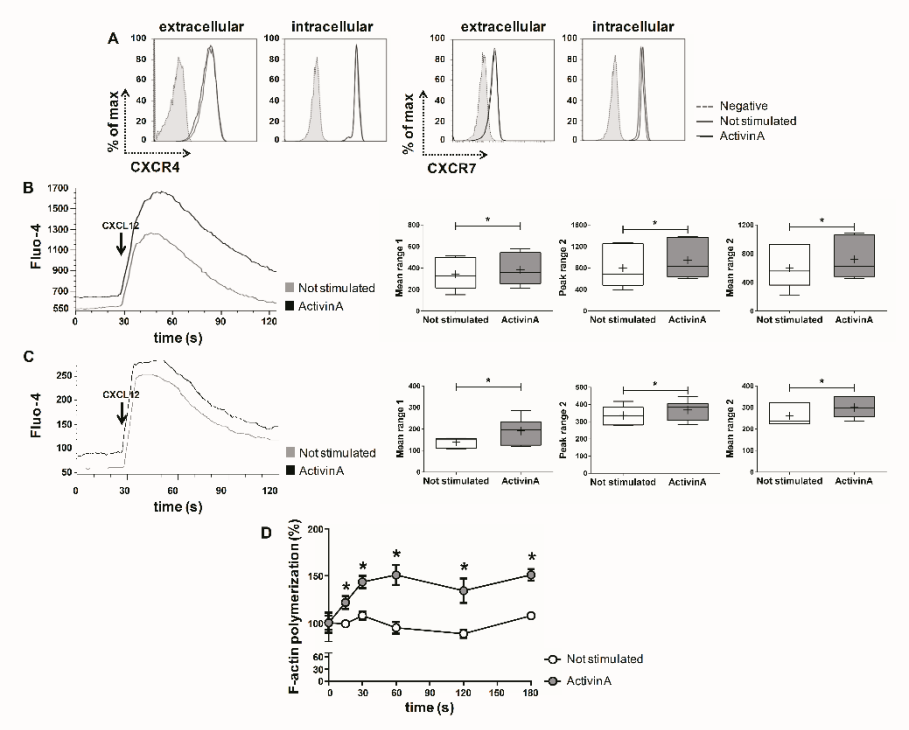


**Figure 5. ActivinA increased CXCL12-induced calcium mobilization and actin polymerization.**

**(A)** The extracellular and intracellular levels of CXCR4 and CXCR7 were analyzed by flow cytometry in 697 cells treated (black line) or not (grey line) with ActivinA for 24 hours (h). Representative data are shown from three independent experiments. 697 cells **(B)** and B-cell precursor-acute lymphoblastic leukemia (BCP-ALL) primary blasts **(C)** were cultured for 24 h either in the presence or in the absence of ActivinA (50 ng/mL or 100 ng/mL, respectively). Cells were loaded with Fluo-4 NW and free cytosolic $Ca^{2+}$ changes were measured by FACS. Background was recorded for 30 seconds (s) and signal upon CXCL12 addition was registered for an

additional 90 seconds. The black line represents data obtained from ActivinA-treated cells-, the grey line represents untreated cells. The arrow indicates CXCL12 addition. The box plots represent the mean fluorescence intensity (MFI) before (mean range 1) and after (mean range 2) the addition of CXCL12 and the maximum peak reached upon CXCL12 addition (peak range 2). Each box plot shows the median and the mean (+) and extends from the lowest to the highest value. The results are representative of one out of six independent experiments. **(D)** 697 cells were starved in low serum medium for 24 h and then stimulated or not with ActivinA (50 ng/mL) for additional 24 h. Cells were then stained with AF647-phalloidin and MFI quantified by flow cytometry. Percentage of MFI change was defined as follows: (MFI after CXCL12 addition/ MFI before CXCL12 addition) x 100. Mean values (± Standard Error of Mean) of one out three independent experiments are represented in the graph. *$P$<0.05: Wilcoxon matched-pairs signed rank test (B and C). *$P$<0.05: Mann-Whitney test (D).

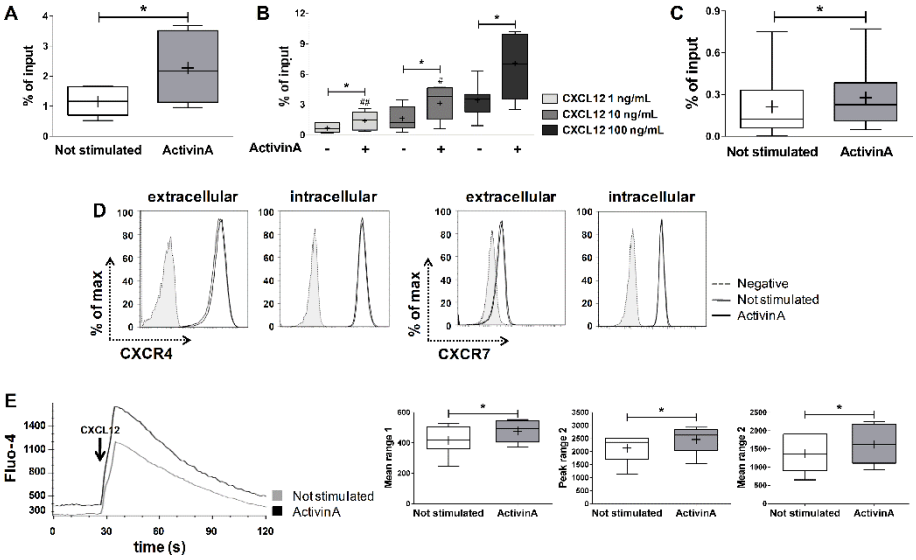


**Supplementary Figure S7. ActivinA increased CXCL12-driven chemotaxis, invasion and calcium content in NALM-6 cells.**

**(A** and **B)** Chemotaxis assay was performed using NALM-6 cells pretreated or not with ActivinA for 24 hours (50 ng/mL) and allowed to migrate toward CXCL12-containing medium for 4 hours. Each box plot shows the median and the mean (+) of the percentage of migrated cells and extends from the lowest to the highest value. The graphs represent the results of six independent experiments. **(C)** Invasion assay was set up using NALM-6 cells either stimulated or not with ActivinA for 24 hours (50 ng/mL) and allowed to migrate through Matrigel-coated (1 mg/mL) Transwell inserts for 24 hours in presence of CXCL12 (100 ng/mL). Each box plot shows the median and the mean (+) of the percentage of invaded cells and extends from the lowest

to the highest value. The graphs represent the results of six independent experiments. **(D)** The extracellular and intracellular CXCR4 and CXCR7 expression in stimulated (black line) or unstimulated cells (grey line) with ActivinA for 24 hours was evaluated by flow cytometry. Data from one out of three independent experiments are shown. **(E)** NALM-6 cells were cultured for 24 hours with or without ActivinA (50 ng/mL). Cells were incubated with Fluo-4 NW dye and cytosolic free $Ca^{2+}$ changes were measured by flow cytometry. The left panel shows a representative calcium flux profile of NALM-6 cells. The black line represents ActivinA-treated cells, while the grey line corresponds to untreated cells. The arrow indicates CXCL12 addition. In the right panels, each box plot shows the median and the mean (+) and extends from the lowest to the highest value. The three plots represent the MFI before (Mean Range 1) and after (Mean Range 2) the addition of CXCL12 and the maximum peak reached upon CXCL12 addition (Peak Range 2). The graphs represent the results of six independent experiments.
*$P$<0.05: Wilcoxon matched-pairs signed rank test (Panels A, B, C and E); #$P$<0.05, ##$P$<0.01: comparison with 100 ng/mL CXCL12-induced migration, Mann-Whitney test (Panel B).

### 2.4.7. ActivinA impaired CXCL12-driven migration of healthy CD34+ cells

We further evaluated whether ActivinA promoted a selective advantage to BCP-ALL cells compared to healthy $CD34^+$ cells. CB- and BM-derived $CD34^+$ cells expressed both type I and type II Activin receptors, thus suggesting that they could both respond to this molecule (Figure 6A).

The effect of ActivinA on CXC12-driven chemotaxis of $CD34^+$ cells was evaluated by Transwell-based migration assays. Surprisingly, we observed the opposite effect to that observed with leukemic cells. ActivinA pretreatment resulted in an average reduction of approximately 55% of CXCL12-driven chemotaxis, compared to untreated CB-$CD34^+$ cells (Figure 6B). Of note, the regulation of cell viability did not account for the reduced chemotaxis (*data not shown*). These data were confirmed in BM-$CD34^+$ cells derived from three HDs, with an average reduction of approximately 25% in CXCL12-driven migration (Figure 6B). This effect on $CD34^+$ cell migration was not due to an ActivinA-mediated regulation of the CXCL12 chemokine receptors, CXCR4 and CXCR7, as demonstrated by flow cytometry analysis of both membrane-bound receptors and intracellular pool (Figure 6C). In addition, ActivinA pretreatment significantly decreased free cytosolic $Ca^{2+}$ of $CD34^+$ cells after the addition of CXCL12 in 2 out of 3 independent experiments (Figure 6D). Overall, these data suggest that leukemic cells could displace healthy haematopoietic stem cells from their niches through an ActivinA-mediated mechanism.

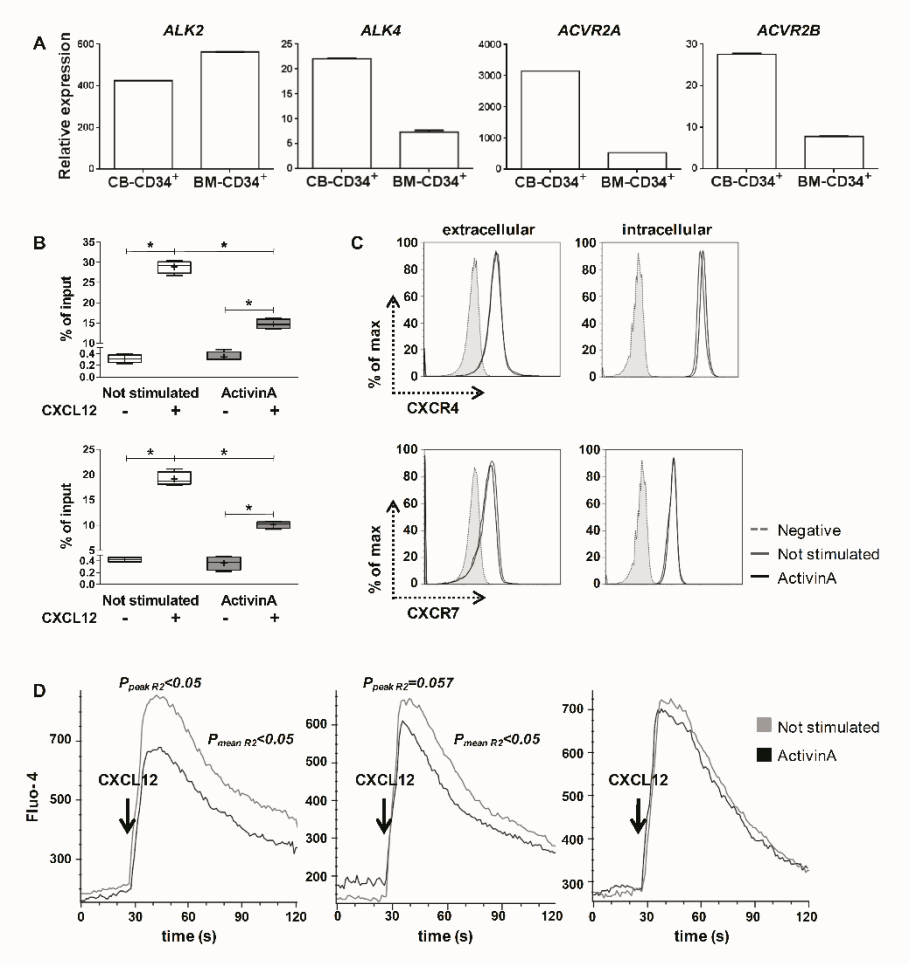


**Figure 6. ActivinA impaired CXCL12-driven migration of healthy CD34$^+$ cells.**

**(A)** Expression of ActivinA receptors *ALK2, ALK4, ACVR2A* and *ACVR2B* was quantified in both cord blood (CB)-CD34+ and bone marrow (BM)-CD34$^+$ cells by qRT-PCR. Data are presented as mRNA fold change of ActivinA receptors normalized to *GAPDH* mRNA (endogenous control). DAUDI cell

line was employed as calibrator because of its low expression of ActivinA receptors (www.proteinatlas.org). **(B)** CB-CD34$^+$ cells (top) and BM-CD34$^+$ (bottom) were pretreated or not with ActivinA (100 ng/mL) for 24 hours (h) and allowed to migrate through 5 µM pores in Transwell chambers toward CXCL12 (100 ng/mL) for 1 h. The graphs represent one representative experiment (CB-CD34$^+$ n=5, BM-CD34$^+$ n=3). Each box plot shows the median and the mean (+) of the percentage of migrated cells and extends from the lowest to the highest value. *$P$<0.05: Mann-Whitney test. **(C)** The extracellular and intracellular levels of CXCR4 and CXCR7 were analyzed in cells either treated (black line) or not (grey line) with ActivinA for 24 h by flow cytometry. Data from one representative experiment out of three are shown. **(D)** CB-CD34$^+$ cells were cultured for 24 h in the presence or absence of ActivinA (100 ng/mL). Cells were loaded with Fluo-4 NW and free cytosolic $Ca^{2+}$ changes were measured by FACS. Background was recorded for 30 seconds (s) and signal upon CXCL12 addition was registered for an additional 90 s. The black line represents results obtained from ActivinA-treated cells, while the grey line represents untreated cells. The results are representative of three independent experiments. *$P$<0.05: Mann-Whitney test ($\boldsymbol{P_{peak\ R2}}$: comparison between MFI peak range 2 in treated *vs.* untreated cells; $\boldsymbol{P_{mean\ R2}}$: comparison between MFI mean range 2 in treated *vs.* untreated cells).

### 2.4.8. ALL-MSCs secrete high amounts of ActivinA

Finally, we focused our attention on the capacity of the BCP-ALL BM microenvironment to influence MSC-derived ActivinA. For this purpose, we isolated BM-MSCs from 15 HDs and 15 BCP-ALL patients at the onset of the disease. ALL-MSCs resulted comparable in terms of immunophenotype and adipogenic/osteogenic differentiation capacity to HD-MSCs (*Supplementary* Figure S8).

After 24 h of culture, ELISA assay showed a significantly higher production of ActivinA ($P<0.05$) by ALL-MSCs (mc:222.2, range:62.5-4855 pg/mL) compared to their normal counterpart (mc:220.7, range:62.5-518 pg/mL) (Figure 7A). Therefore, we hypothesized that BM-MSCs primed by the leukemic microenvironment could account for the high amount of ActivinA in the BM of BCP-ALL patients.

The role of inflammation in the editing of the microenvironment has been defined in several types of cancer, including hematological malignancies. Recent evidence highlighted that the BM of ALL patients is a highly pro-inflammatory environment[20]. These data were confirmed in our cohort of patients. Indeed, higher levels of the pro-inflammatory cytokines IL-1β ($P<0.0001$), IL-6 ($P<0.01$) and TNF-α ($P<0.01$) were detected in the BM plasma of BCP-ALL patients compared to HDs (*Supplementary* Figure S9).

We then investigated whether the pro-inflammatory cytokines IL-1β, IL-6 and TNF-α could regulate ActivinA levels in the BM of BCP-ALL patients, by stimulating both HD-MSCs and ALL-MSCs

with a cocktail of the above-mentioned pro-inflammatory cytokines for 24 h. ELISA assays revealed a significant induction of ActivinA release in BM-MSCs compared to their respective basal condition. Indeed, upon stimulation, ActivinA production by HD-MSCs reached a 28-fold increase compared to the basal condition (mc:5713, range:1446-14221 pg/mL *vs.* basal condition) ($P$<0.0001) (Figure 7A). Interestingly, the molecule was released to a higher extent by ALL-MSCs in pro-inflammatory condition compared to their normal counterpart (mc:10085, range:2904-19776 pg/mL *vs.* inflamed HD-MSCs; $P$<0.01).

Notably, by mimicking an inflamed BM niche through the simultaneous stimulation of HD-MSCs with leukemic blasts and pro-inflammatory cytokines (Figure 7B), we showed a strong increase in the secretion of ActivinA both in the direct (Figure 7 B, bottom, mc:27860, range:13150-92391 pg/mL, n=17) and the indirect (Figure 7B, top, mc:25409, range:9050-65714 pg/mL) co-culture condition. Of note, the combination of both leukemic blasts and pro-inflammatory cytokines (Figure 7B, fourth column) produced a synergistic induction of ActivinA, since the extent of the release was higher compared to the sum of separately used stimuli[21] (Figure 7B, expected additive effect: fifth column=second+third columns; top: $P$<0.001; bottom: $P$<0.0001).

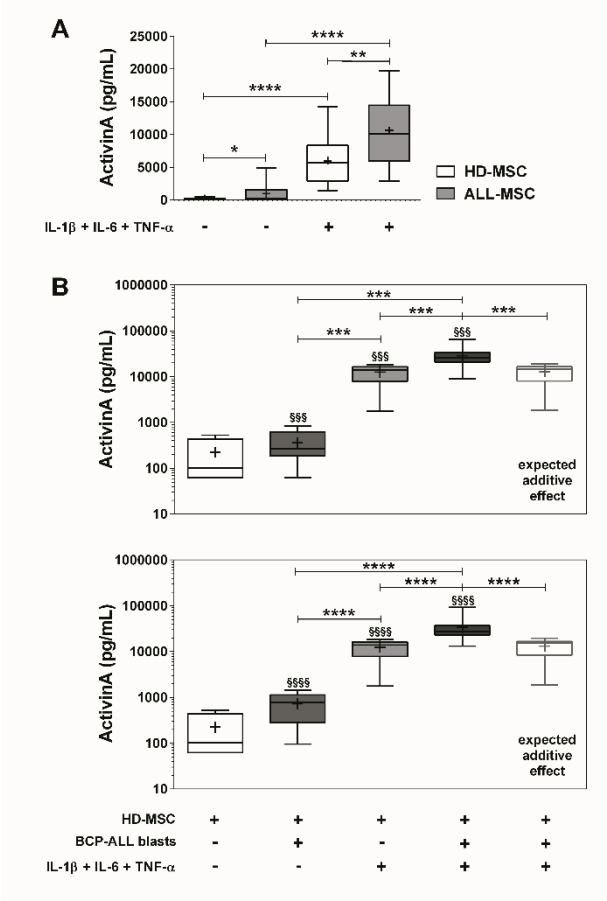


**Figure 7. Inflammation contributed to ActivinA production by bone marrow-mesenchymal stromal cells (BM-MSCs).**

**(A)** ActivinA secretion by BM-MSCs from B-cell precursor-acute lymphoblastic leukemia (BCP-ALL) patients (ALL-MSCs; n=15) and from healthy donors (HDs) (HD-MSCs; n=15) was assessed by ELISA after 24 hours (h) of culture ± IL-1β (50 ng/mL), IL-6 (40 ng/mL) and TNF-α (100 ng/mL). Each box plot shows the median and the mean (+) and extends from the lowest to the highest value. **P*<0.05; ***P*<0.01: Wilcoxon matched-pairs

signed rank test. **(B)** Primary BCP-ALL cells were co-cultured with HD-MSCs directly (bottom) or separated by a Transwell insert (top) in presence of IL-1β, IL-6 and TNF-α for 72 h. ActivinA expression was assessed by ELISA on culture supernatants (n=17 independent co-cultures). The expected additive effect was calculated as the sum of the single effects produced by the two stimulating factors, leukemic cells (second column) and inflammation (third column). Synergism was defined as a "greater-than-the-expected-additive effect". Each box plot shows the median and the mean (+) and extends from the lowest to the highest value. §§§*P*<0.001, §§§§*P*<0.0001: stimulated *versus* unstimulated MSC; ***$P$<0.001, ****$P$<0.0001: measured effect *versus* expected additive effect, indirect contact and direct contact, respectively; Wilcoxon matched-pairs signed rank test.

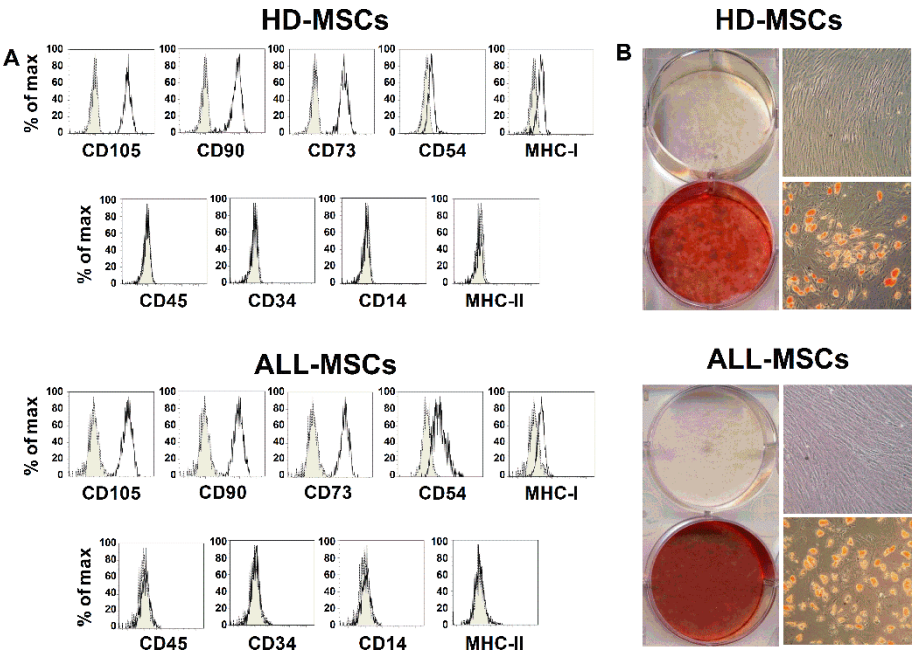


**Supplementary Figure S8. ALL-MSCs were similar to HD-MSCs in terms of phenotype and differentiation capacity.**

**(A)** Immunophenotype of both HD-MSCs and ALL-MSCs was analyzed by flow cytometry. Mesenchymal stromal cells were positive for typical mesenchymal markers including CD105, CD90, CD73, CD54 and MHC-I, while lacked the expression of the markers CD14, CD34, CD45 and MHC-II. **(B)** HD-MSCs and ALL-MSCs were induced to differentiate toward osteogenic (left Panel) and adipogenic lineage (right Panel), as shown by Alizarin Red staining of calcium deposits and Oil Red O lipophilic dye, respectively.

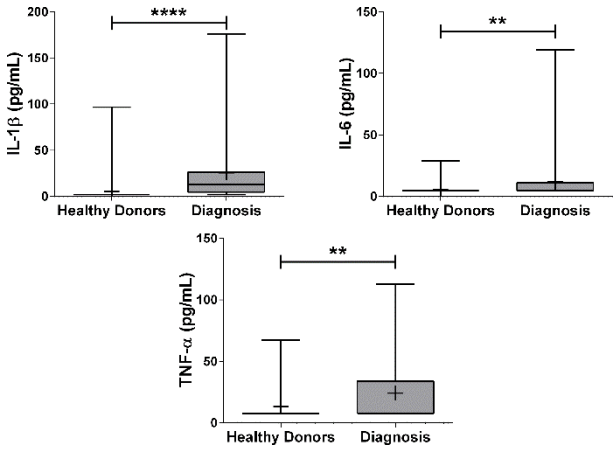


**Supplementary Figure S9. Pro-inflammatory cytokine levels were higher in the leukemic BM microenvironment compared to HDs.**

IL-1β, IL-6 and TNF-α BM plasma levels were assessed by ELISA in HDs and BCP-ALL patients at the onset of the disease. Each box plot shows the median and the mean (+) and extends from the lowest to the highest value. *$P$<0.05, ** $P$<0.01, ****$P$<0.0001: Mann-Whitney test.

### 2.4.9. ActivinA increased the *in vivo* engraftment of BCP-ALL cells to BM and extramedullary sites in a xenograft mouse model

With the aim of testing the efficacy of ActivinA to induce leukemia dissemination *in vivo*, we performed a set of experiments in which 697 or NALM-6 cells *in vitro* pretreated with ActivinA for 24 hours were injected (i.v.) into NSG mice.

Interestingly, on day +7, NSG mice injected with 697 cells (*Supplementary* Figure S10) pretreated with ActivinA showed a

higher leukemic engraftment in the liver (median percentage of leukemic cells=48.4%, range=19.2-54.1% , n=9) compared to untreated cells (median percentage of leukemic cells=27.0% , range=10.9-43.2%, n=9), suggesting a migratory advantage of ActivinA-treated cells. As expected from literature, our data showed a high tropism of 697 cells for the liver[22,23]. On the contrary, the percentages of leukemia engraftment in BM and in other leukemic target organs were modest and were comparable between the two experimental groups.

To test a more physiological environment for leukemia and overcome the low engraftment of 697 in BM, we transplanted mice with NALM-6 cells that are known to have high engraftment levels into the BM[24]. NALM-6 cells, either pretreated or not with ActivinA, were injected (i.v.) at day 0 in NSG mice ($1\times10^6$/mouse) to evaluate their engraftment in different leukemia-target organs (Figure 8A). Mice were subsequently monitored for weight loss over two weeks after transplantation, and leukemia burden was evaluated 11 and 14 days after injection by flow cytometry, determining the percentage of human CD19 and CD10 positive cells in several organs.

First, we evidenced a significant difference in terms of change in body weight between the two experimental groups starting from day 4 after injection ($P<0.05$) with an even greater difference on days 11 and 14 after injection ($P<0.01$), suggesting a different disease progression (Figure 8B).

Moreover, we found that, on injection, both untreated and pretreated cells disseminated through the peripheral blood to

different organs, such as BM, spleen, liver, meninges, and brain. Notably, we found that ActivinA-pretreated cells were able to engraft more rapidly in the BM of recipient mice (median leukemic percentage at day +11: 17.7%, range: 6.1-42.3%) compared to their untreated counterpart (median leukemic percentage at day +11: 10.3%, range: 0-21.4%, n=12). We also observed an increased leukemic percentage in the central nervous system (meninges and brain) of NSG mice following *in vitro* exposure to ActivinA ($P<0.05$) (Figure 8C), indicating that ActivinA stimulation was able to enhance the metastatic potential of leukemic cells *in vivo*.

Therefore, in these two mouse models, we were able to demonstrate that ActivinA stimulation makes leukemic cells more aggressive.

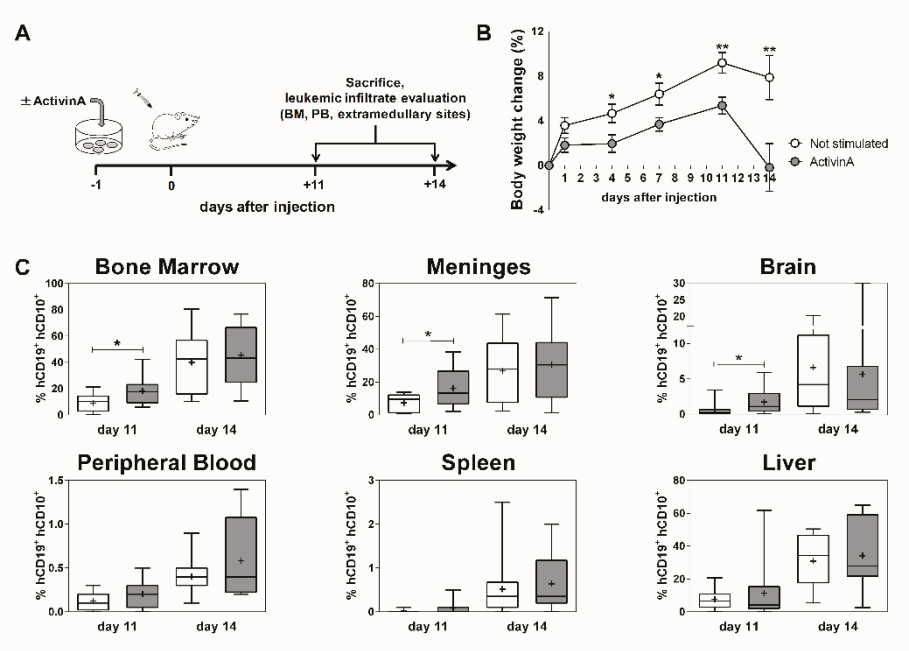


**Figure 8. NALM-6 cells stimulated with ActivinA showed an increased ability to engraft *in vivo* in the bone marrow (BM), meninges and brain of NSG mice.**

**(A)** NSG mice received intravenous (i.v.) transfer of $1\times10^6$ NALM-6 cells, previously cultured for 24 hours (h) in the presence or absence of ActivinA (50 ng/mL). **(B)** Weight loss was periodically monitored over 2 weeks after transplantation. The graph shows mean percentages ± Standard Error of Mean (SEM) of body weight change. Data from 12 mice/group in four independent experiments are shown. **P*<0.05, ***P*<0.01: Mann-Whitney test. **(C)** Mice were sacrificed on days 11 and 14 after transplantation and the percentage of infiltrating $hCD19^+$ $hCD10^+$ leukemic cells was determined by flow cytometry in the BM, peripheral blood, spleen, liver, meninges and brain. Each box

plot shows the median and the mean (+) and extends from the lowest to the highest value (n=12 mice/group, four independent experiments). *$P$<0.05: Mann-Whitney test.

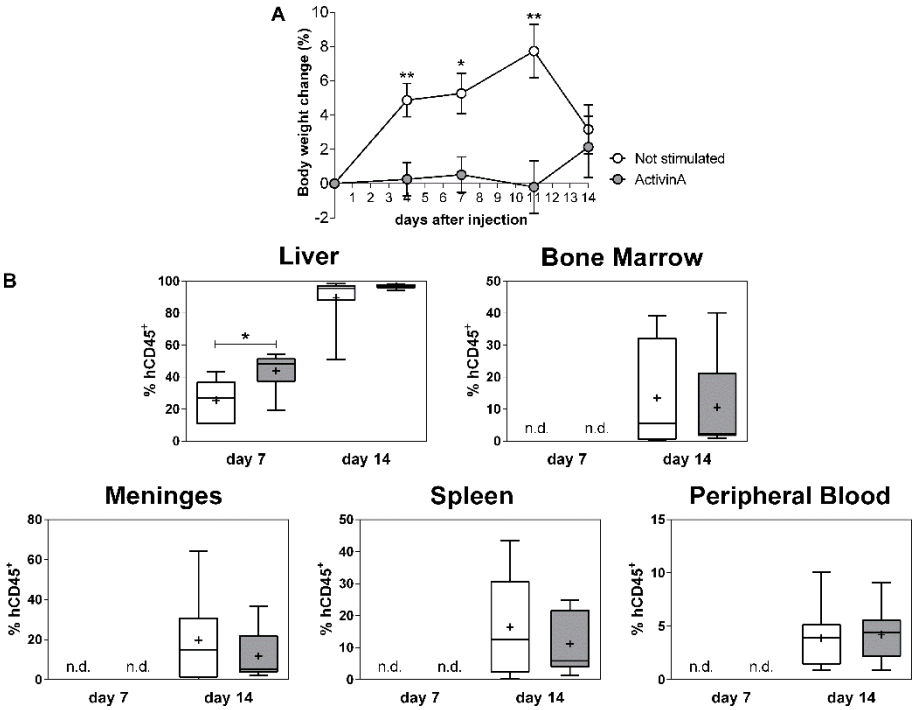


**Supplementary Figure S10. ActivinA enhanced the engraftment of 697 cells to the liver of NSG mice**

**(A)** NSG mice were i.v. injected with $0.5\times10^6$ 697 cells, previously stimulated or not for 24 hours with ActivinA (50 ng/mL). Body weight change was periodically monitored over 2 weeks after transplantation. Mean ± SEM of body weight change (%) from three independent experiments (9 mice/group) is shown. *$P$<0.05, **$P$<0.01: Mann-Whitney test. **(B)** Mice were sacrificed on days 7 and 14 after transplantation and the percentage of infiltrating $hCD45^+$ leukemic cells was determined by flow

cytometry in the liver, bone marrow, meninges, spleen, peripheral blood. Each box plot shows the median and the mean (+) and extends from the lowest to the highest value. *$P$<0.05:

## 2.5. Discussion

There is ample evidence correlating aberrant TGF-β family growth factor activity to carcinogenesis. Despite its prominent role in solid cancer progression[7], the involvement of ActivinA, a member of the TGF-β family, in the pathogenesis of hematological malignancies has never been explored. To the best of our knowledge, here we show for the first time that ActivinA is highly expressed in the BM of BCP-ALL patients at diagnosis compared to HDs. Interestingly, we demonstrated that BM-MSCs are an important source of ActivinA, the production of which is strongly up-regulated following direct contact with leukemic cells or through leukemia-released soluble factors. This finding is in accordance with the recently revised “seed and soil” theory, showing that leukemic cells are able to alter the BM stroma, creating a fertile ground which fuels tumor cell survival and progression[1,25,26]. Of note, we observed that MSCs isolated from the BM of BCP-ALL patients were able to produce higher levels of ActivinA, compared to HD-MSCs, even after several *in vitro* passages. This means that they “remember” the profound alterations that had occurred within the leukemic BM niche.

Nowadays, there is general agreement that inflammation could play a pivotal role in the transformation, survival and proliferation of leukemic cells. In particular, several studies have demonstrated that BM cells in ALL are able to create a pro-inflammatory microenvironment that impairs frequency and function of normal HSCs within the BM[18,20]. In line with this

evidence, we demonstrated that the BM of BCP-ALL patients are characterized by increased levels of the pro-inflammatory cytokines IL-1β, IL-6 and TNF-α, which can synergize with BCP-ALL cells in stimulating ActivinA production and release by BM-MSCs. Accordingly, it has been demonstrated that ActivinA expression was increased in several inflammatory diseases, such as septicemia, inflammatory bowel disease and rheumatoid arthritis[27]. The abundance of ActivinA within the leukemic BM niche and its identification as a new MSC-secreted leukemia-driven molecule, prompted us to investigate its possible effects on BCP-ALL cells.

In accordance with recent literature reporting that ActivinA increases the migration and invasive properties of several solid tumors[12–14,28–33], our GEP analysis of ActivinA-treated leukemic cells showed a crucial effect on different biological processes linked to cell motility. In detail, we used time-lapse microscopy to demonstrate that this molecule was able to increase the spontaneous cell motility of both immortalized and primary BCP-ALL cells.

In addition to increased random motility, ActivinA-treated leukemic cells were more responsive to the CXCL12 chemokine, which plays an essential role in maintaining the quiescent BM HSC pool, thus regulating physiological hematopoiesis[34]. The increase in BCP-ALL migration towards CXCL12 was selectively inhibited by ActivinA/Activin receptor blocking through SB431542[16], ensuring the specific contribution of ActivinA in mediating this advantage.

Importantly, the effect of ActivinA on cell chemotaxis was highly cell-specific. While increasing leukemic cell migration in response to even suboptimal concentrations of CXCL12, ActivinA markedly impaired the ability of healthy $CD34^+$ cells to migrate toward a CXCL12 gradient. This opposite effect could be particularly relevant in the context of the altered BCP-ALL BM niche, where we observed a significantly decreased CXCL12 concentration, in agreement with recent literature[19]. Concerning the molecular mechanisms underlying ActivinA action, a protein-mediated regulation of the CXCL12 receptors, namely CXCR4 and CXCR7, was ruled out. Moreover, in contrast to what Sozzani *et al.* described in dendritic cells[16], ActivinA did not stimulate either leukemic cell chemotaxis itself (*Supplementary* Figure S11) or their secretion of CXCL12 (*data not shown*). On the contrary, our GEP analysis demonstrated that this molecule mainly induces an overall positive regulation of pathways associated with cell motility, such as RAS, PI3K/AKT and calcium homeostasis.

It has been demonstrated that $Ca^{2+}$ co-ordinates structural components of the cell migration machinery and signaling molecules crucial for proper cell motility. Through the activation of actin-interacting molecules such as protein kinase C[35] and calmodulin-dependent kinases[36] and the regulation of Rho GTPases, $Ca^{2+}$ signaling finely tunes actin cytoskeleton dynamics[37]. Interestingly, we demonstrated that ActivinA is able to increase the motility of BCP-ALL cells through an increase in the pool of free cytosolic calcium, resulting in an

increased rate of F-actin polymerization. Strikingly, the increase of intracellular $Ca^{2+}$ was not observed in ActivinA-stimulated $CD34^{+}$ cells, thus explaining the possible molecular mechanism mediating the differential activity of this molecule on the migration of leukemic *versus* healthy hematopoietic cells. Recent literature[28] describing the ability of ActivinA to stimulate the migration of ovarian cancer cells suggests that $Ca^{2+}$ increase could be achieved also in leukemic cells through the activation of non-canonical phospo-AKT, phospho-ERK and Rac1 signaling. In line with this hypothesis, our GEP data demonstrate an ActivinA-dependent increase in DOCK4[38] and CORO1A[39] in the 697 cell line, and primary BCP-ALL cells. This increase positively regulates the CDC42/RAC1 pathway, leading to the generation of phosphatidylinositol-3-phosphate, responsible for calcium release from intracellular stores[40]. In agreement with this, ActivinA-mediated downmodulation of the Rac-GTPase activating protein *ARHGAP25*, that physiologically counterbalance the Rac-activating effect of nucleotide exchange factors[41], could play a prominent role in shaping calcium levels and modulating actin cytoskeleton[42] also in leukemic cells. Moreover, ActivinA could also regulate the extent and duration of calcium responses, through *PTPRC* downregulation. Indeed, in immature B cells, it has been demonstrated that the lack of the *PTPRC* product, CD45, induces enhanced levels of intracellular calcium that can last longer than in CD45 expressing cells, upon BCR engagement[43]. Further studies will be crucial to understand the

possible molecular mechanisms mediating ActivinA differential activity in order to identify potential selective targets to counteract its action.

The ActivinA-mediated migratory advantage observed on BCP-ALL cells was further confirmed in a xenograft mouse model in which we demonstrated that leukemic cells prestimulated with ActivinA were able to engraft in the BM of NSG mice more rapidly than their untreated counterpart. Overall, our *in vivo* data corroborate *in vitro* findings suggesting the effect of the molecule in favoring leukemia. Future studies, testing the efficacy of ActivinA ligand traps on BCP-ALL patients-derived xenografts will be crucial to establish the impact of ActivinA on leukemia propagation.

Recent studies importantly linked ActivinA with the enhancement of cell invasion in several solid cancers (colorectal cancer, prostate cancer, breast cancer, glioblastoma, non-small cell lung cancer)[44–48]. In the context of BCP-ALL, relapses represent the most common cause of treatment failure, mainly occurring in the BM either in an isolated form or in combination with other extramedullary sites[49]. Besides its key role in regulating homing processes in the BM niche, CXCL12 is thought to be involved in the widespread infiltration of other organs, because of its constitutive expression in extramedullary tissues such as liver, spleen, thymus, lung, kidney and brain[50]. Interestingly, our *in vitro* observation demonstrated that ActivinA significantly increased the ability of leukemic cells to pass through an extracellular matrix in response to CXCL12. In addition, *in vivo*

injected ActivinA-stimulated leukemic cells were more able than untreated cells to reach extramedullary disease target organs such as the meninges and the brain, suggesting a possible role for ActivinA in the promotion of leukemic cell invasiveness. Notably, ActivinA was able to up-regulate the expression of its type I receptors in leukemic cells, thus creating a self-reinforcing signaling cascade. Overall, our data suggest the establishment of a positive feedback loop between BCP-ALL cells and MSCs, which, through the key action of MSC-secreted ActivinA, generates a microenvironment favouring leukemia at the expenses of normal hematopoiesis. Indeed, it is conceivable that the abundance of ActivinA, along with the decrease in CXCL12 within the BM niche, could lead to a reduction of the healthy HSC pool in favour of leukemic cells. On the other hand, the leukemic cells could access the BM sanctuaries where they can achieve signals necessary for cell survival and therapy resistance. Indeed, our *in vitro* findings were confirmed by *in vivo* studies and provide the biological rationale for designing therapeutical approaches targeting ActivinA in patients with BCP-ALL. Therefore, the direct targeting of ActivinA or its key downstream mediators could represent a valuable therapeutic option to be combined with conventional chemotherapeutic agents for decreasing the frequency of relapse in BCP-ALL.

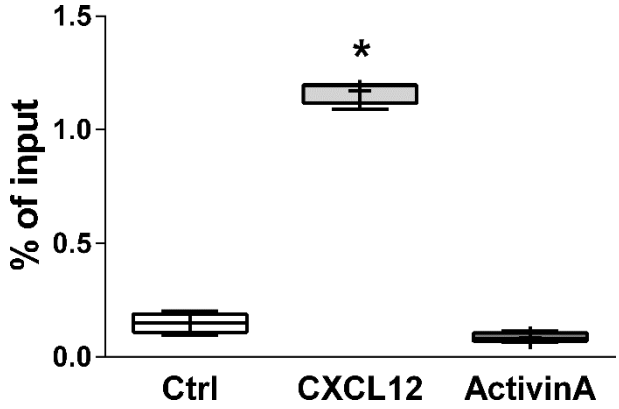


**Supplementary Figure 11. ActivinA did not induce 697 cellular chemotaxis.**

697 cells were allowed to migrate for 4 hours toward empty medium (Ctrl) or toward CXCL12 (100 ng/mL, positive control) or ActivinA (50 ng/mL) added to the lower chamber. The graph represents one experiment in triplicate. Each box plot shows the median and the mean (+) and extends from the lowest to the highest value. *$P$<0.05: Mann-Whitney test *versus* control.

## Supplementary methods

### Patient and healthy donors (HDs) samples

BM plasma samples were collected from 125 BCP-ALL patients (median:4.6; range:1-17 years-old) at disease diagnosis and from 56 healthy donors (HDs) (median:17; range:5-51 years-old). Primary BCP-ALL cells were isolated at disease diagnosis from 22 BM aspirates (>85% blast infiltrate) by Ficoll (GE Healthcare, Uppsala, Sweden) gradient separation and cryopreserved in liquid phase nitrogen until usage.

Informed consent to participate to the study was obtained for all BCP-ALL patients and HDs. All BCP-ALL patients were enrolled in the AIEOP-BFM ALL 2009 protocol (EudraCT-2007-004270-43) and their samples collected at the Pediatric Department of Fondazione MBBM/San Gerardo Hospital (Monza, Italy) or at Bambino Gesù Hospital (Rome, Italy). Enrolled HDs were stem cell donors whose BM was collected at the Pediatric Department of Fondazione MBBM/San Gerardo Hospital (Monza, Italy) for transplant purposes.

### Culture of BCP-ALL cell lines

The leukemic cell lines 697, NALM-6, RS4;11, SUP-B15 and REH (ATCC, Milan, Italy) were cultured in Advanced RPMI 1640 (Thermo Fisher Scientific, Waltham, MA, USA) supplemented with 10% heat-inactivated fetal bovine serum (GE Healthcare), penicillin (100 U/mL), streptomycin (100 µg/mL) and L-glutamine (2 mM) (Euroclone, Milan, Italy). Cell line biological identity was analyzed by cell surface phenotyping (flow

cytometry, FACS Canto II, BD Bioscience, San Jose, CA, USA) and detection of cell-specific translocations.

**Isolation of BM-MSCs**

For BM-MSC isolation, BM-MNCs were seeded in low glucose Dulbecco's Modified Eagle Medium (Lonza, Milan, IT), 10% heat-inactivated FBS, penicillin (100 U/mL), streptomycin (100 µg/mL) and L-glutamine (2 mM). After 48 hours, non-adherent cells were removed from the culture by washing with PBS without calcium and magnesium (Euroclone). When 70-80% confluence was achieved, adherent spindle-shaped cells were harvested using 0.05% trypsin-EDTA (Euroclone) and used for further expansion. After three culture passages, BM-MSCs were analyzed by flow cytometry. All the isolated BM-MSCs lines resulted positive for CD105, CD73, CD90, CD54, MHC-I expression, while they resulted negative for CD45, CD34, CD14 and MHC-II expression (anti-human CD14, CD90 and CD105: eBioscience; anti-human CD45, CD54, CD73, MHC-I and MHC-II: BD Pharmingen; anti-human CD34: BD Biosciences). To evaluate their osteogenic and adipogenic differentiation ability, BM-MSCs were stimulated for 14-21 days with specific differentiation inductive media. Adipogenic inductive medium consisted of DMEM-High glucose (Euroclone) supplemented with 10% FBS, penicillin (100 U/mL), streptomycin (100 µg/mL) and L-glutamine (2 mM), dexamethasone (1 µM), indomethacin (1 µM), 3-isobutyl-1-methylxantine (IBMX) (500 µM) and human recombinant insulin (10 µg/ml) (all from SigmaAldrich, St Louis,

MO, USA). Lipid droplets were stained with Oil Red O (SigmaAldrich). Osteogenic inductive medium consisted of DMEM-Low glucose, 10% FBS, 2-phosphate-ascorbic acid (50 μM), β-glycerol phosphate (10 mM) and dexamethasone (100 nM) (all from SigmaAldrich). The presence of calcium deposits was detected by Alizarin Red staining (SigmaAldrich).

| AGE AT DIAGNOSIS | SEX | DIAGNOSIS | % OF BM INFILTRATE | TRANSLOCATIONS | MRD RISK |
|---|---|---|---|---|---|
| 3 | M | B-II | 90 | NEG* | HR (SER) |
| 3 | M | B-II | 98 | t(12;21) | IR |
| 4 | M | B-II | 90 | NEG* | SR |
| 4 | F | B-II | 77 | NEG* | HR (SER) |
| 4 | M | B-II | 86 | t(12;21) | IR |
| 6 | M | B-II | 80 | NEG* | HR (SER) |
| 6 | F | B-II | 95 | NEG* | IR |
| 7 | M | B-II | 59 | t(12;21) | IR |
| 7 | F | B-II | 98 | t(12;21) | IR |
| 8 | F | B-II | 88 | t(12;21) | SR |
| 9 | F | B-II | 94 | NEG* | HR |
| 9 | M | B-II | 78 | NEG* | HR |
| 10 | M | B-II | N.A. | t(9:22) p210 | HR |
| 15 | M | B-II | 89 | NEG* | IR |
| 18 | M | B-II | 86 | NEG* | IR |

**Supplementary Table 1. Clinical and molecular features of BCP-ALL patients enrolled for BM-MSC isolation.** MRD risk was defined on the basis of residual leukemic cells in the BM at day +15, +33, +78 after treatment beginning (HR: HIGH RISK, IR: INTERMEDIATE RISK, SR: STANDARD RISK, SER: SLOW

EARLY RESPONDER). *NEG: negative for t(4:11), t(9;22) p190, t(12;21), t(1;19).

**CB- and BM-CD34$^+$ cell isolation**

Cord blood (CB) units from healthy neonates were obtained from San Gerardo Hospital, Monza (BM-Niche Protocol, approved by the Host Institution). Human BM samples were obtained from healthy BM donors at the Pediatric Department of Fondazione MBBM/San Gerardo Hospital (Monza, Italy; AIEOP-BFM ALL 2009 Protocol). Mononuclear cells were isolated by Ficoll density gradient centrifugation and CD34$^+$ cells were purified using immunomagnetic CD34 microbeads (CD34 MicroBead Kit, Miltenyi Biotec, Cambridge, MA). The purity was assessed by flow cytometry and was consistently >95%.

**Quantitative RT-PCR**

Total RNA was isolated from the 697 cell line or primary BCP-ALL cells treated or not with ActivinA for 6 hours and 24 hours using TRIzol reagent (Invitrogen, Carlsbad, CA, USA) and used for cDNA preparation (Superscript reverse transcriptase, Invitrogen). qRT-PCR was performed using LightCycler® 480 (Roche, Basel, Switzerland). Primers and probes, synthesized with Universal Probe Library (UPL, Roche) software, are listed in Supplementary Table 2. Gene expression levels of target genes were normalized on GAPDH levels.

| TARGET | PRIMER | SEQUENCE |
|---|---|---|
| **ALK2** | Forward | acactccccacgggaaac |
| | Reverse | aaagaagagaagcacaggcaat |
| **ALK4** | Forward | gaagtgcagcccctctca |
| | Reverse | cgtctccactggcagtctc |
| **ACVR2A** | Forward | aaagcccagttgcttaacga |
| | Reverse | tgccatgactgtttgtcctg |
| **ACVR2B** | Forward | gcataagctgggttttctcct |
| | Reverse | cctgagcaactcatgcaaag |
| **ATP2B2** | Forward | tgcaggattggtggtgatt |
| | Reverse | tccctggaactggcatctac |
| **ATP2B4** | Forward | ccttgtctttgcgggtga |
| | Reverse | ggctgggtggtgaatgtaga |
| **ARHGAP25** | Forward | tggcccgaagctctgtag |
| | Reverse | tggttgtatcagagtcgcttgt |
| **CORO1A** | Forward | agtttgtggccctgatctgt |
| | Reverse | cattcttgtccacacgtcca |
| **DOCK4** | Forward | agcccgatgagaccatctt |
| | Reverse | gctctctggaatgggagtca |
| **GAPDH** | Forward | agccacatcgctcagacac |
| | Reverse | gcccaatacgaccaaatcc |
| **LCK** | Forward | agtcagatgtgtggtcttttgg |
| | Reverse | cctccgggttggtcatc |
| **PTPRC** | Forward | ttcatgcagctagcaagtgg |
| | Reverse | gccgtgtccctaagaaacag |
| **VAV3** | Forward | ccttagatacaactctgcagtttcc |
| | Reverse | gcccagcacttttggactta |

**Supplementary Table 2. Primer sequences for quantitative real-time PCR.**

**Gene expression profile (GEP) analysis**

RNA from four independent experiments was extracted using TRIzol reagent (Invitrogen) and quality and purity were assessed on the Agilent Bioanalyzer 2100 (Agilent Technologies, Waldbronn, Germany). RNA concentration was determined using NanoDrop ND-2000 Spectrophotometer (Thermo Scientific, Waltham, USA). *In vitro* transcription, hybridization and biotin labeling were performed according to 3'IVT Plus Reagent Kit (Affymetrix, Santa Clara, CA, USA). All data analyses were performed in R (http://www.R-project.org/ version 3.0.2) using Bioconductor and R packages. Probe level signals were converted to expression values using the robust multi-array averaging (RMA) algorithm[51].

Supervised analyses were performed using shrinkage test[52] and multiplicity corrections were used to control FDR (false discovery rate); probes with local FDR lower than 0.05 were considered significant. Gene ontology (GO) and KEGG pathway analyses were performed using Metascape (http://metascape.org)[53] on selected Affymetrix IDs. Enriched terms, hypergeometric p-value and enrichment factors were calculated and used for filtering from the Software. Remaining significant terms were then hierarchically clustered in a tree based on kappa-statistical similarities among their gene membership. Then 0.3 kappa score was applied as the threshold to cast the tree into the term clusters. In the dendogram the 20 best p-value were used in the representation. Heatmap cells were colored according to their p-

value. Grey cells indicate the lack of enrichment for that term in the corresponding gene list.

**Time-lapse microscopy**

Leukemic cells were seeded ($3\times10^3$ cells per well) in Advanced RPMI 1640 1% FBS in a 8-well chamber slide (Ibidi, Martinsried, Germany), previously coated with a 1% Gelatin B solution in PBS (SigmaAldrich). After overnight incubation to promote adherence, cells were stained with Propidium Iodide (PI) to discrimate live cells and stimulated or not with ActivinA. For cell tack recording, chamber slides were mounted on a heated stage within a temperature-controlled chamber maintained at 37°C and constant $CO_2$ concentrations (5%). Images were acquired over 24 hours. Frame-by-frame displacements and velocities of randomly selected leukemic cell movements were calculated by tracking individual cells using ImageJ software (NIH) on manual tracking mode.

**Chemotaxis assays**

After ActivinA pretreatment, leukemic and healthy $CD34^+$ cells were resuspended in Advanced RPMI 1640 1% FBS and allowed to migrate through Transwell inserts (5 μm pore size, PC membrane) for 4 hours (BCP-ALL cell lines) or 1 hour (BCP-ALL primary blasts and healthy $CD34^+$ cells). Advanced RPMI 1640 1% FBS containing or not CXCL12 (100 ng/mL, if not otherwise specified) (Peprotech, Rocky Hill, NJ) was added to the lower chambers.

For ActivinA receptors blockade experiments, BCP-ALL cell lines (697 and NALM-6) and primary blasts were pretreated for 1 hour with either SB431542 (SigmaAldrich) or vehicle (DMSO, SigmaAldrich) before the addition, or not, of ActivinA (50 or 100 ng/mL, respectively). After 24 hours cells were collected, washed and resuspended at a concentration of $0.5\times10^6$/100uL in Advanced RPMI 1640 1% FBS added of SB431542 or DMSO. After 1 hour, ActivinA was added or not and cells were allowed to migrate through Transwell inserts (5 μm pore size, PC membrane) for 4 hours (BCP-ALL cell lines) or 1 hour (BCP-ALL primary blasts). Advanced RPMI 1640 1% FBS containing or not CXCL12 (100 ng/mL) (Peptrotech) was added to the lower chambers. The percentage of migrated cells in response to CXCL12 was calculated over input cells for the following experimental conditions: ActivinA-treated cells + DMSO (A); ActivinA-treated cells + SB431542 (B); unstimulated cells + DMSO (C). The percentage of inhibition was calculated as (A-B)/(A-C)*100.

Migrated cells were counted by flow cytometer on a FACS Canto II cytometer (BD Biosciences) after adding a known number of fluorescent reference beads (BD Trucount tubes, BD Bioscience). Technical duplicates were performed for each condition. Input cells and cells harvested from each well were counted twice, for 60 seconds. The percentage of migrated cells was determined by dividing the number of cells in the lower chamber by the total input of cells added to the upper chamber.

**Invasion assays**

Membrane filters (Costar Transwell® Permable Supports, Corning Inc., pore size 8 µm) were coated with 50 µL of Matrigel (1mg/mL) (Corning) that was allowed to form a gel layer for 1 hour at 37 °C. BCP-ALL cell lines and primary blasts treated or not with ActivinA (50 or 100 ng/mL, respectively) were loaded on the upper chamber ($5\times10^5$ cells/well in 100 µL Advanced RPMI 1640 1% FBS). The medium containing or not CXCL12 (100 ng/mL) was added to the lower chamber. The percentage of cells migrated after 24 hours through the Matrigel barrier into the lower chamber was quantified as described for chemotaxis assay.

**Activin Receptor analyses**

The expression of Activin Receptors ALK4, ACVR2A and ACVR2B was evaluated by flow cytometry, using the following anti-human antibodies: anti-Activin RIB/ALK-4 Alexa Fluor® 488-conjugated mAb (R&D Systems); anti-human Activin RIIA APC-conjugated mAb (R&D Systems); primary anti-human Activin Receptor Type IIB mAb used in combination with secondary goat anti-mouse IgG H&L DyLight® 488-conjugated mAb (Abcam, Cambridge, UK). To ensure the specificity of the staining, Fc Receptor Binding Inhibitor Polyclonal Antibody (eBioscience, CA, USA) was used. Mouse IgG APC-conjugated antibody (R&D Systems), mouse IgG FITC-conjugated antibody (BD Biosciences) were used as isotype controls for directly stained antibodies. Concerning ACVR2B indirect staining, the secondary antibody mouse IgG H&L DyLight® 488-conjugated mAb

(Abcam) was used alone as negative control. Cells were analyzed with a FACS Canto II cytometer (BD Biosciences) and data analyzed by FlowJo software (Tree Star, Inc. Ashland, OR, USA).

ALK2 expression was evaluated by Western Blot analyses on BCP-ALL cell extracts. For this purpose, cells were washed with ice cold PBS and lysed for 30 minutes on ice. Cell extracts were prepared in lysis buffer containing 1% NP-40 (SigmaAldrich), 0.5% Na-Deoxyxholate (SigmaAldrich), 350 mM NaCl (SigmaAldrich), 0.1% SDS (SigmaAldrich), 1% Protease Inhibitor (SigmaAldrich) and 0.25 mM PMSF (SigmaAldrich) in PBS. Cell debris were removed by centrifugation at 21'000 × g at 4 °C for 5 minutes and protein concentration measured using Pierce BCA Protein Assay Kit (Thermo Scientific). Samples were then separated on Any kD™ Mini-PROTEAN® TGX™ Precast Protein Gels (Bio-Rad, CA, USA). Gels were blotted onto Immun-Blot® PVDF Membranes (Bio-Rad), blocked with 10% dried milk in Tris-buffered saline with 0.1% Tween 20 (SigmaAldrich) (TBS-T) and incubated with primary antibodies. Primary antibodies used were rabbit monoclonal anti-human Activin Receptor Type IA antibody (Abcam) and mouse monoclonal anti-β-Actin antibody (SigmaAldrich). Blots were washed in TBS-T before incubation with horseradish peroxidase conjugated secondary antibodies, goat anti-rabbit IgG (Invitrogen) and rabbit anti-mouse IgG (SigmaAldrich). The blots were washed thoroughly with TBS-T before bands detection using LiteAblot Extend (Euroclone) as luminescence substrate. Image detection was

performed with Alliance LD2-77WL system (Uvitec, Cambridge) and image quantification with ImageJ software (NIH, USA). In detail, the ALK2 57 kDa band was quantified by densitometric analysis and normalized to the constitutive protein β-actin.

Concerning $CD34^+$ cells, Activin receptor expression was evaluayed by qRT-PCR. In addition, Activin receptor modulation was evaluated on 697 cells pretreated or not with ActivinA (50 ng/mL) for 6, 24 or 48 hours by qRT-PCR. Primers for qRT-PCR are listed in Supplementary Table 2.

**CXCR4 and CXCR7 staining**

PE-conjugated anti-human CXCR4 mAb (BioLegend, San Diego, CA) or PE-conjugated anti-human CXCR7 mAb (BioLegend) were used. For intracellular detection, the cells were firstly permeabilized with Cytofix/Cytoperm (BD Biosciences) and then incubated with the above-mentioned antibodies. Cells were analyzed with a FACS Canto II cytometer (BD Biosciences) and data analyzed by FlowJo software (Tree Star, Inc. Ashland, OR, USA).

**Filamentous (F)-actin polymerization assay**

697 cells were starved overnight in RPMI 1640 1% FBS and pretreated or not with ActivinA (50 ng/mL) for additional 24 hours. Cells were then harvested and resuspended in culture medium at 37 °C with or without CXCL12 (100 ng/mL) for 15, 30, 60, 120, 180 seconds. To block stimulation, cells were rapidly put on ice and washed with ice-cold PBS. Cells were then

permeabilized using Cytofix/Cytoperm and stained with AlexaFluor 647-labeled phalloidin (Invitrogen) following manifacturer's instructions. Cells were analyzed with a FACS Canto II cytometer and MFI was determined for each sample. MFI percentage change was calculated for each time point over the basal value (unstimulated cells).

**Calcium mobilization**

To evaluate intracellular calcium mobilization 697 cells, NALM-6 cells, BCP-ALL primary blasts and CB-$CD34^+$ cells were plated in 96-well plates in Advanced RPMI 1% FBS for 24 hours with or without ActivinA (50 or 100 ng/mL). Cells were then loaded with the cell-permeant Fluo-4NW dye, according to manifacturer's instructions. Analyses were performed by flow cytometry on a FACS Canto II cytometer. After a 30-second baseline recording, sample aspiration was briefly paused and CXCL12 (100 ng/mL) was quickly added. The $Ca^{2+}$ response was measured as MFI of the cells as a function of time. Data analysis was performed using FlowJo "kinetics" tool.

**B-cell acute lymphoblastic leukemia xenograft model**

7- to 9-week-old NOD-SCID-γchain$^{-/-}$ (NSG) female mice were obtained from Charles River Laboratories-Italy (Calco, Italy) and housed in dedicated rooms with pathogen-free, individually ventilated cages (IVC, Tecniplast spa, Varese, Italy) in the animal facility of the University of Milano-Bicocca (Monza, Italy). All the procedures involving animals handling and care were in

accordance with protocols approved by Milano-Bicocca University, in compliance with national and international law and policies. This study was approved by the Italian Ministry of Health (approval n.64/2014, issued on the 4$^{th}$ December 2016).

NALM-6 and 697 cells were stimulated or not with ActivinA (50 ng/mL) 24 hours before transplantation. Animals received i.v. $10^6$ NALM-6 cells or $0.5\times10^6$ cells in 0.1 mL sterile PBS. Mice were sacrificed at two different timepoints (day +7 and +14 after 697 cell injection and day +11 and +14 after NALM-6 injection), and bone marrow, peripheral blood, liver, spleen, meninges and brain were analyzed for the presence of leukemic cells by flow cytometry. Engraftment was detected using anti-human CD19 APC-conjugated mAb (BD Pharmingen, CA, USA) and anti-human CD10 PE-Cy™7-conjugated mAb (BD Pharmingen) in the case of NALM-6 cells and anti-human CD45 PerCP-conjugated mAb (BD Pharmingen). PE-conjugated monoclonal antibody reacting with murine CD45 (eBioscience) was used to exclude murine hematopoietic cells. To ensure the specificity of the staining, Fc Receptor Binding Inhibitor Polyclonal Antibody (eBioscience) was used. Cells were analyzed with a FACS Canto II cytometer (BD Biosciences) and data analyzed by FlowJo software.

## References


1. Chiarini F, Lonetti A, Evangelisti C, et al. Advances in understanding the acute lymphoblastic leukemia bone marrow microenvironment: From biology to therapeutic targeting. Biochimica et Biophysica Acta - Molecular Cell Research 2016;1863(3):449–463.
2. Pui C, Robison L, Look A. Acute lymphoblastic leukaemia. The Lancet 2008;371(9617):605–615.
3. O'Brien MM, Seif AE, Hunger SP. Acute lymphoblastic leukemia in children. In: Wintrobe's Clinical Hematology: Fourteenth Edition. Wolters Kluwer Health Pharma Solutions (Europe) Ltd; 2018. p4939–5015.
4. Ayala F, Dewar R, Kieran M, Kalluri R. Contribution of bone microenvironment to leukemogenesis and leukemia progression. *Leukemia* 2009;23(12):2233–2241.
5. Colmone A, Amorim M, Pontier AL, Wang S, Jablonski E, Sipkins DA. Leukemic Cells Create Bone Marrow Niches That Disrupt the Behavior of Normal Hematopoietic Progenitor Cells. Science 2008;322(5909):1861–1865.
6. Hanahan D, Weinberg RA. Hallmarks of Cancer: The Next Generation. Cell 2011;144(5):646–674.
7. Loomans H, Andl C. Intertwining of Activin A and TGFβ Signaling: Dual Roles in Cancer Progression and Cancer Cell Invasion. Cancers 2014;7(1):70–91.
8. Pangas SA, Woodruff TK. Activin Signal Transduction Pathways. Trends in Endocrinology & Metabolism 2000;11(8):309–314.
9. Abdulkadyrov KM, Salogub GN, Khuazheva NK, et al. Sotatercept in patients with osteolytic lesions of multiple myeloma. British Journal of Haematology 2014;165(6):814–823.
10. Conter V, Bartram CR, Valsecchi MG, et al. Molecular response to treatment redefines all prognostic factors in children and adolescents with B-cell precursor acute lymphoblastic leukemia: results in 3184 patients of the AIEOP-BFM ALL 2000 study. Blood 2010;115(16):3206–3214.
11. Vallet S, Mukherjee S, Vaghela N, et al. Activin A promotes multiple myeloma-induced osteolysis and is a promising target for myeloma bone disease. Proceedings of the National Academy of Sciences 2010;107(11):5124–5129.
12. Bashir M, Damineni S, Mukherjee G, Kondaiah P. Activin-a signaling promotes epithelial–mesenchymal transition, invasion, and metastatic growth of breast cancer. npj Breast Cancer;1.
13. Taylor C, Loomans HA, le Bras GF, et al. Activin a signaling regulates cell invasion and proliferation in esophageal adenocarcinoma. Oncotarget 2015;6(33):34228–34244.
14. Bufalino A, Cervigne NK, de Oliveira CE, et al. Low miR-143/miR-145 Cluster Levels Induce Activin A Overexpression in Oral Squamous Cell Carcinomas, Which Contributes to Poor Prognosis. PLOS ONE 2015;10(8):e0136599.
15. Steller MD, Shaw TJ, Vanderhyden BC, Ethier J-F. Inhibin resistance is associated with aggressive tumorigenicity of ovarian cancer cells . Mol Cancer Res [Epub ahead of print].
16. Salogni L, Musso T, Bosisio D, et al. Activin A induces dendritic cell migration through the polarized release of CXC chemokine ligands 12 and 14. Blood 2009;113(23):5848–5856.

17. Watabe T, Nishihara A, Mishima K, et al. TGF-β receptor kinase inhibitor enhances growth and integrity of embryonic stem cell–derived endothelial cells. Journal of Cell Biology 2003;163(6):1303–1311.
18. Balandrán JC, Purizaca J, Enciso J, et al. Pro-inflammatory-Related Loss of CXCL12 Niche Promotes Acute Lymphoblastic Leukemic Progression at the Expense of Normal Lymphopoiesis. Frontiers in Immunology;7.
19. van den Berk LCJ, van der Veer A, Willemse ME, et al. Disturbed CXCR4/CXCL12 axis in paediatric precursor B-cell acute lymphoblastic leukaemia. British Journal of Haematology 2014;166(2):240–249.
20. Vilchis-Ordoñez A, Contreras-Quiroz A, Vadillo E, et al. Bone Marrow Cells in Acute Lymphoblastic Leukemia Create a Proinflammatory Microenvironment Influencing Normal Hematopoietic Differentiation Fates. BioMed Research International 2015;20151–14.
21. Roell KR, Reif DM, Motsinger-Reif AA. An Introduction to Terminology and Methodology of Chemical Synergy—Perspectives from Across Disciplines. Frontiers in Pharmacology;8.
22. Yuan N, Song L, Zhang S, et al. Bafilomycin A1 targets both autophagy and apoptosis pathways in pediatric B-cell acute lymphoblastic leukemia. Haematologica 2015;100(3):345–356.
23. Pillozzi S, Masselli M, de Lorenzo E, et al. Chemotherapy resistance in acute lymphoblastic leukemia requires hERG1 channels and is overcome by hERG1 blockers. Blood 2011;117(3):902–914.
24. Barrett DM, Seif AE, Carpenito C, et al. Noninvasive bioluminescent imaging of primary patient acute lymphoblastic leukemia: a strategy for preclinical modeling. Blood 2011;118(15):e112–e117.
25. Raaijmakers MHGP, Mukherjee S, Guo S, et al. Bone progenitor dysfunction induces myelodysplasia and secondary leukaemia. Nature 2010;464(7290):852–857.
26. Sison EAR, Brown P. The bone marrow microenvironment and leukemia: biology and therapeutic targeting. Expert Review of Hematology 2011;4(3):271–283.
27. Sozzani S, Musso T. The yin and yang of Activin A. Blood 2011;117(19):5013–5015.
28. Dean M, Davis DA, Burdette JE. Activin A stimulates migration of the fallopian tube epithelium, an origin of high-grade serous ovarian cancer, through non-canonical signaling. Cancer Letters 2017;391114–124.
29. ZHU J, LIU F, WU Q, LIU X. Activin A regulates proliferation, invasion and migration in osteosarcoma cells. Molecular Medicine Reports 2015;11(6):4501–4507.
30. Kang H-Y, Huang H-Y, Hsieh C-Y, et al. Activin A Enhances Prostate Cancer Cell Migration Through Activation of Androgen Receptor and Is Overexpressed in Metastatic Prostate Cancer. Journal of Bone and Mineral Research 2009;24(7):1180–1193.
31. Yoshinaga K, Yamashita K, Mimori K, Tanaka F, Inoue H, Mori M. Activin A Causes Cancer Cell Aggressiveness in Esophageal Squamous Cell Carcinoma Cells. Annals of Surgical Oncology 2008;15(1):96–103.
32. Chang W-M, Lin Y-F, Su C-Y, et al. Dysregulation of RUNX2/Activin-A Axis upon miR-376c Downregulation Promotes Lymph Node Metastasis in Head

and Neck Squamous Cell Carcinoma. Cancer Research 2016;76(24):7140–7150.
33. Tamminen JA, Yin M, Rönty M, et al. Overexpression of activin-A and -B in malignant mesothelioma – Attenuated Smad3 signaling responses and ERK activation promote cell migration and invasive growth. Experimental Cell Research 2015;332(1):102–115.
34. Sugiyama T, Kohara H, Noda M, Nagasawa T. Maintenance of the Hematopoietic Stem Cell Pool by CXCL12-CXCR4 Chemokine Signaling in Bone Marrow Stromal Cell Niches. Immunity 2006;25(6):977–988.
35. Lipp P, Reither G. Protein Kinase C: The “Masters” of Calcium and Lipid. Cold Spring Harbor Perspectives in Biology 2011;3(7):a004556–a004556.
36. Swulius MT, Waxham MN. Ca2+/Calmodulin-dependent Protein Kinases. Cellular and Molecular Life Sciences 2008;65(17):2637–2657.
37. Parsons JT, Horwitz AR, Schwartz MA. Cell adhesion: integrating cytoskeletal dynamics and cellular tension. Nature Reviews Molecular Cell Biology 2010;11(9):633–643.
38. Kobayashi M, Harada K, Negishi M, Katoh H. Dock4 forms a complex with SH3YL1 and regulates cancer cell migration. Cellular Signalling 2014;26(5):1082–1088.
39. Pick R, Begandt D, Stocker TJ, et al. Coronin 1A, a novel player in integrin biology, controls neutrophil trafficking in innate immunity. Blood 2017;130(7):847–858.
40. Downward J. Targeting RAS signalling pathways in cancer therapy. Nature Reviews Cancer 2003;3(1):11–22.
41. Csépányi-Kömi R, Wisniewski É, Bartos B, et al. Rac GTPase Activating Protein ARHGAP25 Regulates Leukocyte Transendothelial Migration in Mice. The Journal of Immunology 2016;197(7):2807–2815.
42. Csépányi-Kömi R, Sirokmány G, Geiszt M, Ligeti E. ARHGAP25, a novel Rac GTPase-activating protein, regulates phagocytosis in human neutrophilic granulocytes. Blood 2012;119(2):573–582.
43. Ogimoto M, Katagirl T, Mashima K, Hasegawa K, Mizuno K, Yakura H. Negative regulation of apoptotic death in immature B cells by CD45. International Immunology 1994;6(4):647–654.
44. Li M, Zhang S, Wu N, Wu L, Wang C, Lin Y. Overexpression of miR-499-5p inhibits non-small cell lung cancer proliferation and metastasis by targeting VAV3. Scientific Reports 2016;6(1):23100.
45. Salhia B, Tran NL, Chan A, et al. The Guanine Nucleotide Exchange Factors Trio, Ect2, and Vav3 Mediate the Invasive Behavior of Glioblastoma. The American Journal of Pathology 2008;173(6):1828–1838.
46. Jiang K, Lu Q, Li Q, Ji Y, Chen W, Xue X. Astragaloside IV inhibits breast cancer cell invasion by suppressing Vav3 mediated Rac1/MAPK signaling. International Immunopharmacology 2017;42195–202.
47. Lin K-T, Gong J, Li C-F, et al. Vav3-Rac1 Signaling Regulates Prostate Cancer Metastasis with Elevated Vav3 Expression Correlating with Prostate Cancer Progression and Posttreatment Recurrence. Cancer Research 2012;72(12):3000–3009.
48. Uen Y-H, Fang C-L, Hseu Y-C, et al. VAV3 Oncogene Expression in Colorectal Cancer: Clinical Aspects and Functional Characterization. Scientific Reports 2015;5(1):9360.

49. Locatelli F, Schrappe M, Bernardo ME, Rutella S. How I treat relapsed childhood acute lymphoblastic leukemia. Blood 2012;120(14):2807–2816.
50. Crazzolara R, Kreczy A, Mann G, et al. High expression of the chemokine receptor CXCR4 predicts extramedullary organ infiltration in childhood acute lymphoblastic leukaemia. British Journal of Haematology 2001;115(3):545–553.
51. Irizarry RA. Exploration, normalization, and summaries of high density oligonucleotide array probe level data. Biostatistics 2003;4(2):249–264.
52. Opgen-Rhein R, Strimmer K. Accurate Ranking of Differentially Expressed Genes by a Distribution-Free Shrinkage Approach. Statistical Applications in Genetics and Molecular Biology;6(1):.
53. Tripathi S, Pohl MO, Zhou Y, et al. Meta- and Orthogonal Integration of Influenza “OMICs” Data Defines a Role for UBR4 in Virus Budding. Cell Host & Microbe 2015;18(6):723–735.

# 3. ActivinA modifies leukemic B cell vesiculation providing distinct cross-talk interactions within the niche

Cricrì G.[1], Pergoli L.[2], Dioni L.[2], Fallati A.[1], Portale F.[1], Di Marzo N.[1], Bollati V.[2], Biondi A.[1,3], Dander E.[1]* and D'Amico G.[1]*
*These authors shared co-last authorship

***Ready for Submission***

[1]Centro Ricerca Tettamanti, Pediatric Dep, University of Milano-Bicocca, Fondazione MBBM, Monza, Italy

[2]EPIGET – Epidemiology, Epigenetics and Toxicology Lab, Department of Clinical Sciences and Community Health, University of Milan, Milano, Italy

[3]Clinica Pediatrica Ospedale S. Gerardo, Fondazione MBBM, University of Milano-Bicocca, Monza, Italy

## 3.1. Abstract

B-Cell Precursor Acute Lymphoblastic Leukemia (BCP-ALL) cells harbor the t(1;19) chromosomal translocation which in turn generates the E2A-Pbx1 fusion gene capable of leukemogenesis and relapse development. Previously, we identified ActivinA as a new crucial factor exploited by BCP-ALL cells to create a self-reinforcing niche. Here, we reported that leukemic cells release high numbers of extracellular vesicles (EVs) in response to ActivinA. We demonstrated that these EVs contained genetic material, as we detected the t(1;19) oncogene in the EV-RNA thus reflecting the status of the parental cells. Moreover, we observed that ActivinA-stimulated BCP-ALL cells acquired a chemoresistant phenotype which was then reverted by blocking ActivinA signaling. Interestingly, we found that EVs secreted by ActivinA-stimulated cells participate to leukemic cell chemoprotection from Asparaginase-induced apoptosis. To explore the possible mechanisms underlying this biological effect, we evaluated the miRNA cargo of EVs derived from BCP-ALL cells stimulated or not with ActivinA. Notably, we observed that ActivinA is able to modulate the miRNA contents of EVs released by BCP-ALL cells. Interestingly one of these miRNAs, the miR-491-5p, has been previously linked to BCP-ALL cell chemoresistance. These data provide information of a new role of ActivinA in promoting chemoprotection through the release of EVs that are considered the new frontier of cell-to-cell communication. Overall, studying the role of leukemia-derived EVs would be of fundamental importance for the development of

combination therapies that potentiate the effects of conventional drugs targeting leukemic cells.

## 3.2. Introduction

B-Cell Precursor-Acute Lymphoblastic Leukemia (BCP-ALL) is a clonal hematopoietic stem cell disorder characterized by the malignant transformation and proliferation of lymphoid progenitor cells in the bone marrow (BM), blood and extramedullary sites[1]. BCP-ALL commonly occurs in children, primarily affecting patients aged 3-5 years[2]. The majority of childhood BCP-ALL cases harbors recurring genetic alterations including a series of chromosomal translocations. Among these, the t(1;19) translocation, occurring in approximately 23% of pediatric patients, results in the formation of the chimeric E2A-PBX1 oncoprotein with a constitutive differentiation blocking activity[3]. Progressive improvements in the efficacy of multiagent chemotherapy regimens have increased the survival rate over 85%[4]. Perturbations in the complex BM microenvironment in which leukemic cells reside are thought to contribute to BCP-ALL relapse and cancer-related mortality[5]. The BM microenvironment comprises different cells including Mesenchymal Stromal Cells (MSCs) which activate multiple signaling pathways in BCP-ALL cells by the secretion of growth factors and cytokines necessary for hematopoiesis which make it a sanctuary for leukemic cell homing, survival and chemoresistance[6]. In turn, BCP-ALL cells can also affect the BM microenvironment during the maintenance and evolution of leukemia by constantly remodeling its composition and altering biological properties to create protective niches that favour BCP-ALL cell survival and confer protection and resistance to conventional chemotherapy[2]. Thus, to develop

more effective therapeutic approaches and improve clinical outcome, it is critical to understand the contribution of cellular and molecular components with a key role in the BM leukemic niche. In the context of BCP-ALL, we recently identified ActivinA as a new factor exploited by leukemic cells to create a self-reinforcing microenvironment[7]. Interestingly, we demonstrated that ActivinA can influence the biological properties of leukemic cells, such as their migratory and invasive ability through a calcium- and actin polymerization-mediated mechanism. In view of the peculiar processes modulated by ActivinA on BCP-ALL cells, we investigated the effect of this molecule on cell vesiculation. The role of extracellular vesicles (EVs) stands out as a biologically unique, poorly understood and important emerging topic. For many years, they were considered inert cellular debris because of cell damage or dynamic plasma-membrane turnover[8]. Only recent studies have assigned a defined function to these EVs which are designed as the new frontier of intercellular communication[9]. Indeed, EVs can be involved in conveying messages to maintain healthy cells and to mediate disease progression depending on the relevant functional molecules they enclose. The most studied class of EV-enclosed molecules is the class of microRNAs (miRNAs) which, following their release in the extracellular milieu, function in repressing their target mRNAs in recipient cells[10]. Relatively few papers have investigated the role of EVs in the context of hematological malignancies and so far, the role of EVs in BCP-ALL awaits to be thoroughly elucidated. In the current study, we investigated modifications

induced by ActivinA in EVs from BCP-ALL cells determining their impact on cell survival and chemoresistance.

## 3.3. Experimental procedures

### 3.3.1. Culture of BCP-ALL cell lines

The BCP-ALL cell line 697 (ATCC, Milan, Italy) was grown in RPMI 1640 medium (Roswell Park Memorial Institute) supplemented with 10% heat-inactivated Fetal Bovine Serum (FBS) (GE Healthcare), penicillin (100 U/mL), streptomycin (100 µg/mL) and L-glutamine (2 mM) (Euroclone, Milan, Italy). Cell line biological identity was analysed by cell surface phenotyping (flow cytometry, FACS Canto II, BD Bioscience, San Jose, CA, USA) ($CD3^-$ $CD34^-$ $CD10^+$ $CD19^+$ $CD38^+$ $MHC\text{-}II^+$) (anti-human CD3, CD34, CD10, CD19: BD Biosciences; anti-human CD38: eBioscience, San Diego, CA, USA; anti-human MHC-II: BD Pharmingen, San Diego, CA, USA) and detection of t(1;19) cell-specific translocation by gel electrophoresis and RT-qPCR. Flow cytometry data were analysed by using FlowJo Software (Tree Star, Inc. Ashland, OR, USA).

### 3.3.2. BCP-ALL cell stimulation for EV production

697 cell line was maintained in RPMI 1640 complete medium supplemented with 10% FBS (GE Healthcare), washed 2 times in saline solution, switched to serum-free medium to avoid contaminations by FBS-derived vesicles and treated or not with ActivinA (50 ng/mL) for 24 hours and 48 hours.

### 3.3.3. Cell proliferation and viability assay

To analyse proliferation, 697 cells ($0.5*10^6$/mL) were seeded in 48-multiwell plates by using both medium deprived and supplemented with FBS. Cultures were maintained at 37°C in a 5% $CO_2$ humidified atmosphere for four days, without replacing culture medium. Cell growth was assessed each day by trypan blue exclusion cell count (Gibco-Life Technologies, Thermo Fisher Scientific). The number of population doublings was calculated using the formula: log10(N)/log10(2) where N=cells seeded and results are expressed as cumulative population doublings[11]. To assess cell viability, 697 cell line ($10^6$), cultured in serum-free conditions for 24 hours and 48 hours, was stained with Apoptosis/Necrosis detection kit (Enzo Life Sciences) for 15 min at room temperature in the dark. Apoptosis was evaluated by flow cytometry after double labeling with Annexin-V/7-aminoactinomycin D (7AAD) which recognizes respectively early apoptotic cells and late apoptotic or necrotic cells, performed according to the manufacturer's instructions. Flow cytometry data were analysed by using FACSDiva Software (BD).

### 3.3.4. Isolation, quantification and flow cytometry characterization of EVs from 697 cells treated or not with ActivinA

Cell culture supernatant was centrifuged at 1000, 2000, and 3000 x g for 15 min at 4 °C (*Supplemental* method S1). Numbers and dimensions of EVs contained in cell culture supernatant were assessed by NanoParticle tracking analysis (NTA), using a

NanoSight NS300 System. Five 30 s recordings were made for each sample. Collected data were analyzed with NTA software and based on their size, EVs were categorized into exosomes (30-150 nm) and microvesicles (151-700 nm).

EVs were characterized by flow cytometry (MACSQuant, Miltenyi Biotec). To analyze EVs integrity, 60 µl aliquots of ultracentrifuged samples were stained with 0.02 µM CFSE (5(6)-carboxyfluorescein diacetate N-succinimidyl ester). Each aliquot of CFSE-stained EVs was incubated with CD19-APC, CD9-APC and CD63-APC antibodies (Miltenyi Biotec). Gating strategy is illustrated in *Supplemental* method S2. Before use, each antibody was centrifuged at 17.000 x g for 30 min at 4°C to eliminate aggregates. A stained PBS control sample was used background normalization.

### 3.3.5. Total RNA extraction from 697and their EVs and quantitative PCR

Total RNA was extracted from cells by using TRIzol reagent (Invitrogen, Carlsbad, CA, USA) according to the manufacturer's instructions. EV-associated mRNA was purified using the RNeasy Mini Kit (Qiagen, Hilden, Germany) guidelines. RNA quantity and quality were evaluated by NanoDrop ND-2000 spectrophotometer (Thermo Scientific, Waltham, USA). Briefly, mRNA from both cells and EVs was reverse transcribed into complementary DNA (cDNA) using Superscript RT kit (Invitrogen) and then amplified for specific targets using primers

and probes synthesized with Universal Probe Library (UPL, Roche) software on a LightCycler® 480 apparatus (Roche, Basel, Switzerland) as follows: 50 cycles at RT for 5 min, 40 °C for 45 min, 99 °C for 5 min and 4 °C for 5 min. Data were analyzed using the LightCycler® 480 software (Roche).

For detection of miRNA expression in cells, cellular miRNA profile was firstly verified using Agilent 2100 Bioanalyzer RNA 6000 Nano assay kit. Briefly, cDNA was synthesized from 2 µg of total RNA using the TaqMan miRNA reverse transcription kit accordingly to the Creating Custom RT pool protocol (Applied Biosystems, Foster City, CA, USA) with minor modifications. Then, each sample was amplified for specific targets using TaqMan assays on a ViiA 7 Real-Time PCR System (Applied Biosystems) as follows: 40 cycles at 95 °C for 15 s and 60 °C for 1 min. Data were analyzed using the ViiA 7 software (Applied Biosystems).

Quantitative PCR reactions were performed in triplicates for each data point. Raw data were extracted and relative changes in expression between control and treated samples were determined with the ΔΔCrt method. Expression levels of the target mRNA or miRNA transcript were normalized to the endogenous control GAPDH or RNU6, constantly expressed in all samples (ΔCrt). For ΔΔCrt values, additional subtractions were made between treated samples and control ΔCrt values. Final values were expressed as fold of induction.

### 3.3.6. Detection of t(1;19) translocation by RT-PCR

For detection of t(1;19) translocation-associated fusion gene in 697-derived EVs, RT-PCR was carried out using the following primers: E2A-forward: CACCAGCCTCATGCACAAC; PBX-reverse: TCGCAGGAGATTCATCACG; amplification product: 19 bp. ABL gene was further amplified as housekeeping control. cDNA from 697 cells was used as positive control for the presence of the fusion transcript.

### 3.3.7. Drugs

Asparaginase Erwinia chrysanthemi (ERWINAZE, Jazz Pharmaceuticals, Dublin, Ireland) was reconstituted in 2 mL of free sterile sodium chloride (0.9%) to obtain a 5000 International Units/mL stock solution and stored at -20 °C.

SB-431542 (SigmaAldrich, St Louis, MO, USA) was solubilized at a stock concentration of 26 mM in DMSO and stored at -20 °C. Working dilution of 1 µM was prepared in medium.

### 3.3.8. Chemosensitivity assay

To test the ability of ActivinA to influence Asparaginase-induced cytotoxicity against the BCP-ALL 697 cell line, $0.5\times10^6$ cells/mL were pre-stimulated for 24 hours with 10% FBS RPMI 1640 medium alone or containing 50 ng/mL of ActivinA. Cells were then counted, washed, resuspended in complete growth medium, re-stimulated or not with ActivinA (50 ng/mL) and seeded in 24-well plates at $0.5\times10^6$ cells/mL. Asparaginase (ASNase) at the dose of 1 U/mL was added to selected wells.

In selected experiments, cells were pretreated for 1 hour at 37 °C with 1 µM of the ActivinA blocker SB-431542 or DMSO (control vehicle) before ActivinA (50 ng/mL) stimulation. After 72 hours of culture, cells viability was analyzed by Apoptosis/Necrosis detection kit (Enzo Life Sciences).

Furthermore, EVs isolated from 697 cells stimulated or not with ActivinA for 24 hours as previously described, were used in selected chemosensitivity assays instead of rhActivinA itself. Briefly, EV pellet isolated from $10x10^6$ 697 cells treated or not with ActivinA was resuspended in 100 µl of PBS. 697 cells ($0.5x10^6$ cells/mL) were cultured alone or in presence of 20 µl of EVs (from 697 cells stimulated or not with ActivinA) for 24 hours. The following day, cells were counted, washed and re-seeded at $0.5x10^6$ cells/mL. 697-derived EVs were re-added and 697 cells were cultured for 72 hours in presence or not of 1U/mL ASNase. Apoptosis was evaluated as previously described.

### 3.3.9. Isolation of EV-associated miRNAs

MiRNAs were isolated from frozen EV pellets by using the miRNeasy Kit and Rneasy CleanUp Kit (Qiagen), according to the manufacturer's instructions. Isolation of EV-miRNAs from cell supernatant was performed as described in the *Supplemental* method S4.

### 3.3.10. Screening of miRNA expression

MiRNAs were prepared by standard reverse transcription (RT) and preamplification procedures, followed by RT-qPCR analysis with the QuantStudio 12 K Flex OpenArray Platform (QS12KFlex). RT was performed by using Megaplex™ RT Primers, Pool A v2.1 and Pool B v3.0, with the TaqMan® Micro RNA Reverse Transcriptase Kit (Life Technologies, Foster City, CA). Two distinct reactions were performed, to cover RT of 754 target miRNAs (16 replicates of three internal controls: RNU48, RNU44, and U6). Detailed protocol of each reaction is reported in the *Supplemental* method S5.

*Expression Suite Software* was used to process miRNA expression data from the miRNA panel. In addition, a Volcano Plot comparing the fold change (biological significance) to the statistical significance (*p*-value) was built.

### 3.3.11. miRNA normalization and screening data analysis

We obtained 758 Crt (Cycle Threshold of a reaction) values for each subject (n=12), which included 754 unique miRNAs and three internal controls (RNU48, RNU44 and U6). For each amplification curve, we obtained an AmpScore value, a quality measurement that indicates the low signal in the amplification curve linear phase. MiRNAs with Crt value < 28 or AmpScore > 1.24 were considered amplified, resulting in 251 miRNAs being included in the analysis.

The expression data were normalized using the average Crt of RNU48, RNU44 and U6. miRNA expression was determined using the relative quantification $2^{-\Delta Crt}$.

### 3.3.12. Validation of miRNA expression

The top-10 miRNAs, normalized with endogenous control RNU48, RNU44, U6, were validated in Custom miRNA OpenArray® Plates in triplicate. RT was performed by using the Custom Primers Pool and TaqMan® Micro RNA Reverse Transcriptase Kit (Life Technologies). Preamplification, loading, and analysing conditions were the same of the screening phase, with minor modifications (*Supplemental* Method S6).

miRNA expression was determined using the relative quantification $2^{-\Delta Crt}$. The expression data were normalized to the average Crt of three endogenous controls (RNU48, RNU44 and U6). Relative quantification of each miRNA was calculated using the RQ= $2^{(-\Delta crt)}$ formula, with -Δcrt= measured crt-medium_normalization crt.

### 3.3.13. Statistical analysis

Differences between subgroups were compared with the Mann-Whitney test. Data were analyzed and graphics were constructed using GraphPad Prism 5.0 (GraphPad Software, San Diego, CA, USA).

In the screening phase, after normalization, the differentially expressed miRNAs were identified with fold-change filtering and *p*-value <0.05. In the validation phase, for each miRNA, we

applied linear regression models with repeated measurements to verify the association between ActivinA exposure and miRNA expression. MiRNA expression values were log2-transformed to achieve a normal distribution. Geometric means and 95% Confidence Interval (CI) of relative quantification were calculated and compared, their ratio (ActivinA exposure/control group) was used to obtain the Fold Change (FC). The statistical analysis was performed using SAS software (version 9.4, SAS Institute, Milan, Italy). A two-sided *p*-value of less than 0.05 was considered statistically significant.

## 3.4. Results

### 3.4.1. The BCP-ALL cell line 697 generates EVs *in vitro* and their production is induced by ActivinA stimulation

To study EV production by BCP-ALL cells, we cultured the leukemic cells 697 for their kinetic evaluation. To avoid contaminating aggregates interfering with the analysis, we cultured 697 cells in serum-free medium. Therefore, we firstly investigated the effect of serum deprivation on 697 proliferation and viability. Even if the growth of 697 cells in serum-free conditions resulted significantly decreased compared to plain medium (10% FBS) (Figure 1A, n=6), cell viability resulted comparable between cells cultured either in presence or in absence of FBS (*data not shown*).

Given that cell viability was not significantly influenced by serum absence, we evaluated EV production by 697 cells, cultured in serum-free RPMI, by NTA.

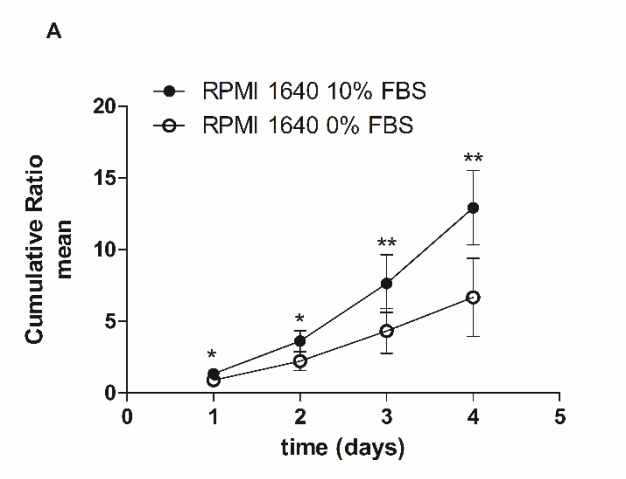


**Figure 1. Serum-deprivation effect on BCP-ALL B-cell proliferation.**

Proliferation of cells cultured in serum-deprived medium was evaluated by using the dead cell permeant dye trypan blue. The data are expressed as the mean ± SD (n=6). *p<0.05 and **p<0.01, compared with complete medium.

NTA analysis showed that 697 cells were able to produce both exosomes (size range: 30-150 nm) and microvesicles (size range: 151-700 nm) (Figure 1B). After 24 hours of culture, 697 cells showed a mean exosome production of 4.13E+08 particle/mL (range: 2.35E+08-6.36E+08) (Figure 1C) and a mean MV production of 3.61E+08 particle/mL (range: 1.40E+08-6.12E+08) (Figure 1D). The production of both EV subgroups resulted further increased after 48 hours of culture (mean

exosome: 7.95E+08 particle/mL, range: 5.39E+08-1.36E+09 and mean MV: 5.19E+08 particle/mL, range: 2.16E+08-7.57E+08).

We next investigated the impact of ActivinA on EV production at both time-points. Interestingly, after 24 hours of treatment, ActivinA significantly increased the production of exosomes of 61% (mean concentration: 6.66E+08 particle/mL, range: 4.78E+08-1.13E+09, n=8, Figure 1C) ($p<0.008$). Furthermore, exosome production by ActivinA-treated cells increased of 28% (mean concentration of exosomes: 1.02E+09 particle/mL, range: 5.86E+08-1.49E+09, $p<0.016$) compared to their untreated counterparts, also at 48 hours. The average percentage of 697-derived microvesicles released in response to ActivinA (mean concentration of microvesicles: 4.50E+08 particle/mL, range: 3.31E+08-5.76E+08) was slightly increased of about 25% following 24 hours of ActivinA stimulation compared to the basal condition ($p<0.0547$) and this difference became statistically significant after 48 hours with an increase of 30% (mean concentration of microvesicles: 6.74E+08 particle/mL, range 3.98E+08-1.02E+09) compared to untreated cells ($p<0.016$) (Figure 1D). These results indicate a clear effect of ActivinA on BCP-ALL cell vesiculation.

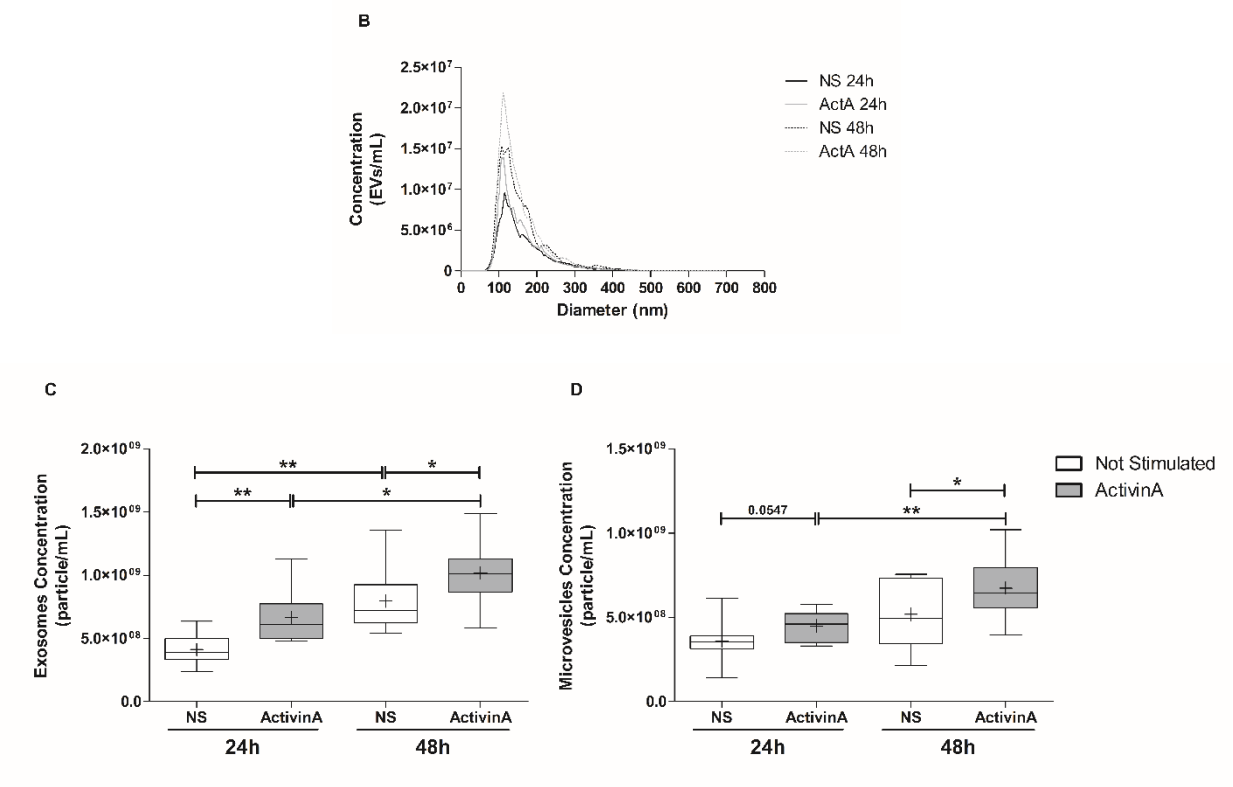


**Figure 1. ActivinA modulates EV release from BCP-ALL cells**

**(B)** Size distribution (nm) (mean ± s.d.; *n*=5 acquisitions of one sample per condition), calculated by NTA, of BCP-ALL EVs that were isolated from medium conditioned by ActivinA-stimulated and not stimulated 697 cells (n=8).

**(C, D)** Concentration, determined by NTA, of exosomes and microvesicles (mean ± SEM; *n*=8 independent EV preparation per condition) released by 697 cells pretreated or not with ActivinA for 24 hours and 48 hours.

### 3.4.2. Immunophenotypical characterization of BCP-ALL-derived EVs

To investigate MV identity, we performed an immunophenotypical analysis of 697-derived EVs. Immunophenotyping revealed the expression of CD19, which is a typical B cell-marker, expressed on the membrane of 697 cells, thus indicating microvesicle identity. The percentage of CD19+ MVs resulted comparable between untreated and ActivinA-stimulated 697 supernatants at 24 hours (NS: 4.24%-#, ActA: 4.7%-#) (Figure 2A). After 48 hours of culture, CD19+ MVs remained comparable between the two stimulation groups (NS: 4.5%-#, ActA: 5.3%-#) (Figure 2B). Moreover, the exosome markers CD9 and CD63 resulted highly expressed on both EVs from ActivinA pre-stimulated and unstimulated 697 cell culture supernatants. Interestingly, CD9+ exosomes resulted the most represented vesicle population in all conditions tested.

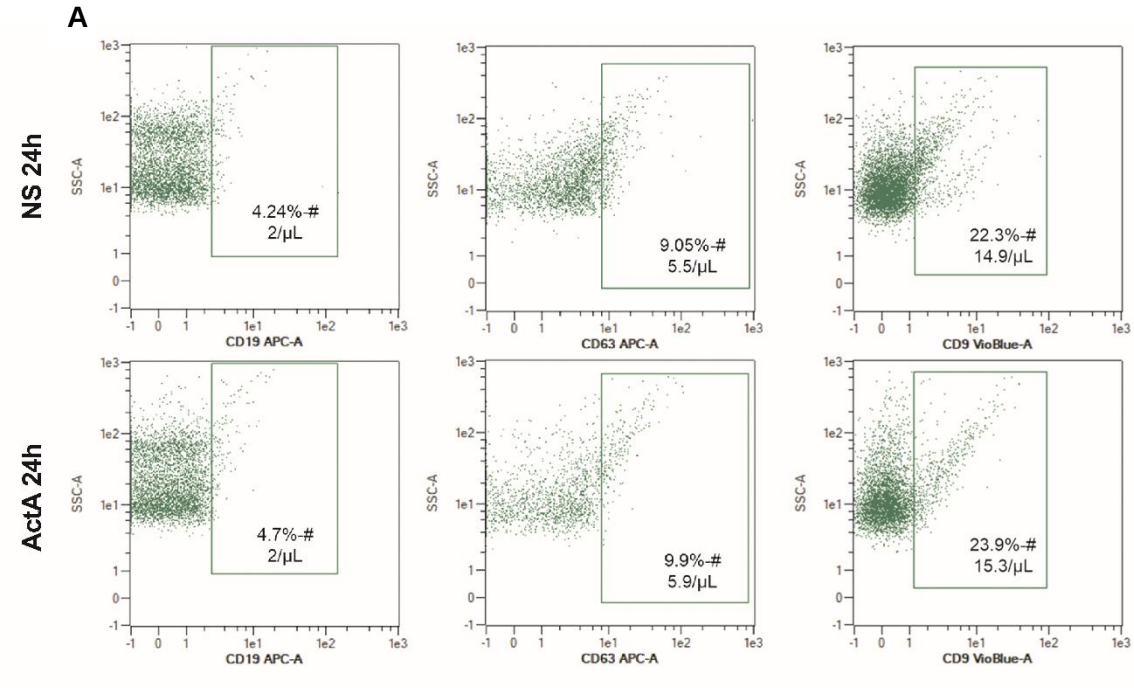
A
NS 24h
ActA 24h
SSC-A
CD19 APC-A
CD63 APC-A
CD9 VioBlue-A
4.24%-#
2/µL
9.05%-#
5.5/µL
22.3%-#
14.9/µL
4.7%-#
2/µL
9.9%-#
5.9/µL
23.9%-#
15.3/µL

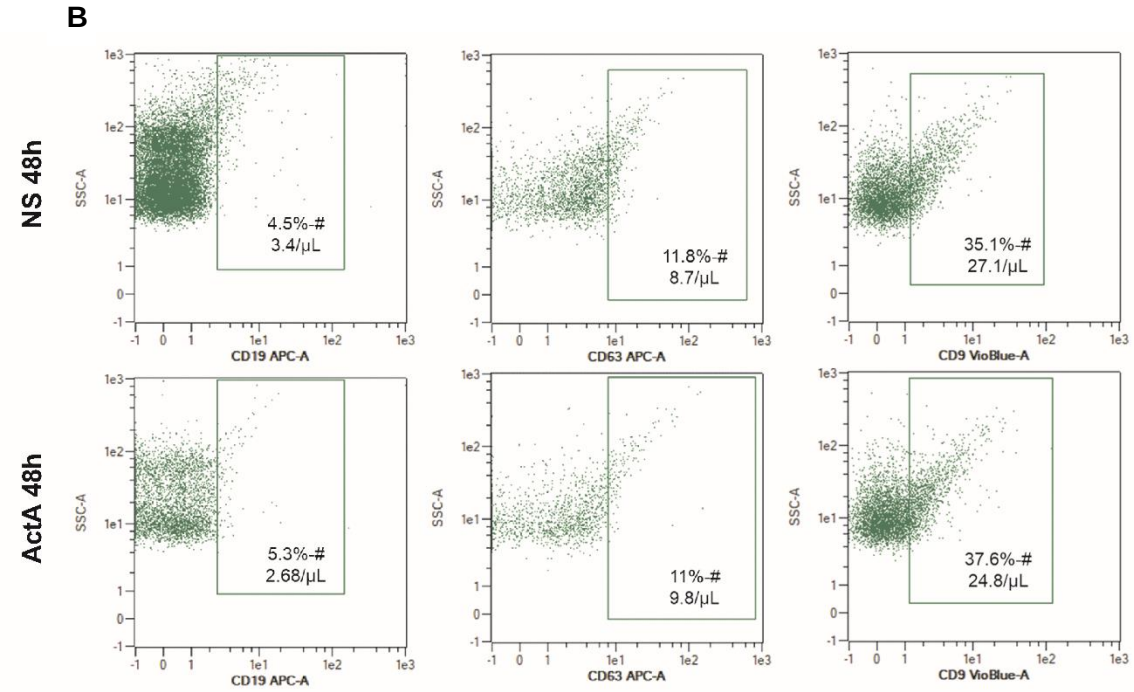
B
NS 48h
ActA 48h
SSC-A
CD19 APC-A
CD63 APC-A
CD9 VioBlue-A
4.5%-#
3.4/µL
11.8%-#
8.7/µL
35.1%-#
27.1/µL
5.3%-#
2.68/µL
11%-#
9.8/µL
37.6%-#
24.8/µL

**Figure 2. Characterization of 697-derived EVs.**

**(A-B)** Phenotyping of BCP-ALL EVs was performed by flow cytometry. Plot representative of three independent experiments. %-# indicates percent gated/percent parent.

697 cells, pre-stimulated or not with ActivinA for 24 hours and 48 hours, released EVs showing the expression profile of specific exosome markers (CD9, CD63) and B-cell markers (CD19) without any difference between the two conditions.

### 3.4.3. The BCP-ALL E2A-PBX1 fusion transcript is secreted by 697 cells by EVs

Recent studies showed fusion transcripts enrichment in EVs from several tumours[12,13]. The E2A-PBX1 oncoprotein that results from the t(1;19) chromosomal translocation is typically expressed in the 697 BCP-ALL cell line. Therefore, we analyzed the presence of the E2A-PBX1 fusion transcript in 697-derived EVs. Interestingly, by RT-PCR analysis (n=3) we were able to identify E2A-PBX1 mRNA as part of 697-derived EV cargo (Figure 3A). Quality of the retro-transcribed RNA was evaluated by testing the *housekeeping* gene Abelson (see *Supplemental* method S3).

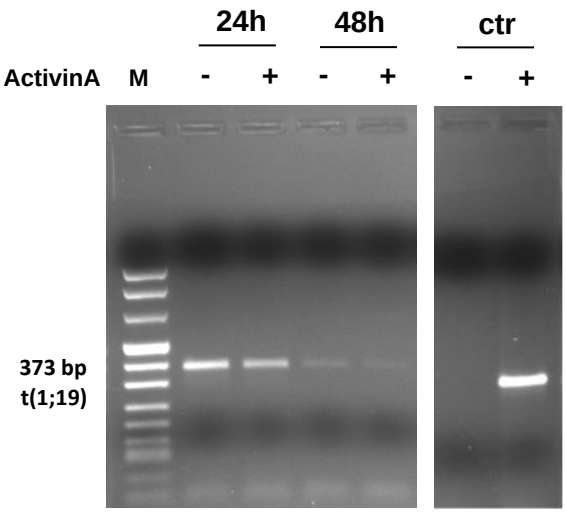


**Figure 3. t(1;19) fusion transcript is detected in 697-derived EVs**

**(A)** Agarose gel electrophoresis of RT-PCR products obtained by the amplification of the E2A-PBX1 fusion transcript (373 bp). M is a size marker. Lanes 1 to 4 indicate cDNA of EVs derived from 697 cultured, respectively, in the absence or presence of ActivinA for 24 hours and 48 hours. Lane 13, negative control; lane 14, 697 positive control. Plot representative of three independent experiments.

### 3.4.4. ActivinA confers Asparaginase resistance to BCP-ALL cells

In several studies, ActivinA was described to contribute to the regulation of drug response of cancer cells[14]. To understand if this could be the case also in the context of BCP-ALL, we firstly evaluated whether ActivinA could modulate chemoresistance to Asparaginase (ASNase), which is one of the most used anti-leukemic drugs. For this purpose, 697 cells were cultured in the presence or absence of ActivinA for 24 hours and then treated for 72 hours with ASNase before evaluating their viability. The results revealed that BCP-ALL cells cultured in the presence of ActivinA showed a significant increase in their number compared to 697 cells cultured alone (Figure 4A). The higher number of ActivinA-stimulated cells after treatment could be explained by their increased resistance to the action of ASNase. Indeed, we demonstrated that the addition of ActivinA in BCP-ALL 697 culture increased cell viability of 44% after 72 hours of treatment with ASNase at the dose of 1U/mL (mean: 67.47%, range: 53 - 77.50, n=11) compared to control (mean: 47.00%, range: 36.05 - 58.45, n=11) (*p* value: 0.0005) (Figure 4B). Consequently, we found that ActivinA-stimulated cells significantly decreased the number of apoptotic 697 cells (mean: 32.52%, range: 22.45 - 47.00) after 72 hours with a fold-decrease of 39% compared to controls (mean: 53.00, range: 41.65 - 63.95) (Figure 4C). Hence, we demonstrated that the rate of ASNase-induced apoptosis was lower in BCP-ALL cells stimulated with ActivinA compared with

not stimulated cells suggesting that culture with ActivinA decreased chemosensitivity of BCP-ALL cells.

To ensure the specificity of the observed effect on ActivinA mediated protection, we blocked ActivinA receptor ALK4 by using SB-431542 and repeated the chemoresistance assay. We observed that 1 hour of 697 pre-treatment with 1 µM SB-431542, followed by stimulation with ActivinA (50 ng/mL) for 24 hours, was sufficient to inhibit the anti-apoptotic effect mediated by ActivinA in response to ASNase. Indeed, the average percentage of viable 697 cells was 45.08% (range: 25.40 - 66.20, n=6) in presence of SB-431542, compared to 66.11% (range: 53 - 77.50, n=6) (*p* value: 0.0260) in the absence of the inhibitor (Figure 4D). Consequently, the fold-increase of apoptotic cells treated with ASNase following ALK4 blocker treatment resulted of 62% (mean: 54.94, range: 33.80 - 74.65) compared to ActivinA-stimulated cells alone (mean: 33.87, range: 22.45 - 47.00) (*p* value: 0.0260). Of note, the percentage of ActivinA-stimulated 697 cells undergoing apoptosis after treatment with SB-431542 and ASNase was similar to the percentage of apoptotic cells treated only with the drug (mean: 53.79, range: 45.45 - 61.60) (Figure 4E). Overall, we demonstrated that ActivinA specifically inhibits cell apoptosis and induces chemoresistance also in the context of BCP-ALL.

We next evaluated whether EVs could play a role in the observed chemoprotection. Results from one preliminary experiment showed that 697 cells pretreated with ActivinA-induced 697 EVs

(EV ActA) were more resistant to ASNase than unstimulated 697 cells or 697 cells pretreated with EVs from unstimulated cells (EV NS). Interestingly, Figure 4F shows that EV Act A increased the number of alive BCP-ALL cells of about 14% after 72 hours of ASNase treatment, compared to EV NS. These results indicated that a non-negligible part of the chemoprotective effect mediated by ActivinA is also mediated through EVs.

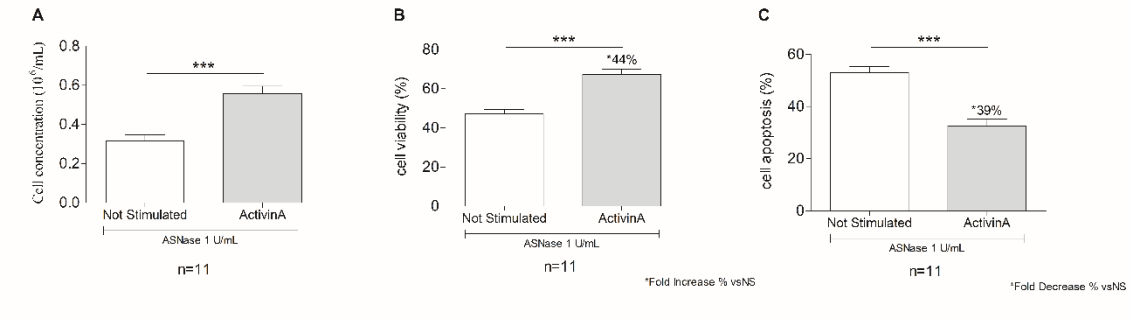


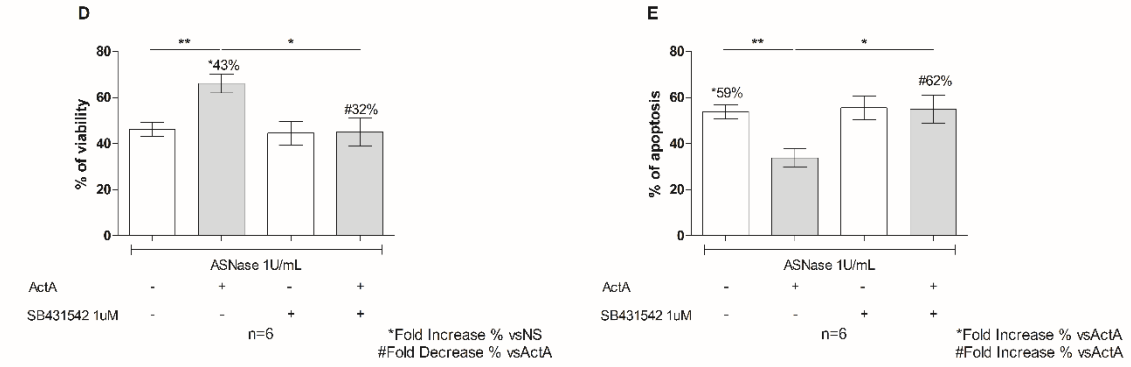

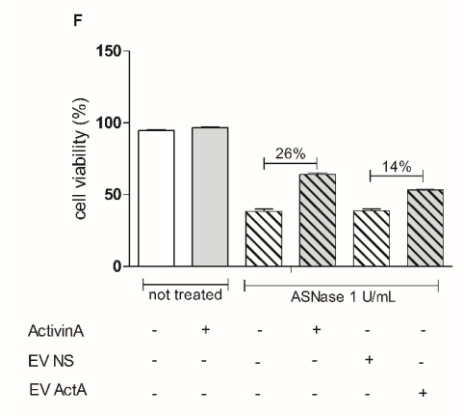


**Figure 4. ActivinA protects BCP-ALL 697 cells from the chemotherapeutic agent ASNase through an EV-mediated mechanism**

BCP-ALL 697 cells were pre-stimulated or not for 24 hours with ActivinA and then incubated with ASNase in presence or not of ActivinA for 72 hours.

**(A)** Cell growth was established 72 hours after ASNase treatment by trypan blue exclusion (n=11). ***$p$ < 0.001: comparison with not stimulated BCP-ALL cells, Mann-Whitney test.

**(B-C)** Cell viability was analyzed by annexin-V/7AAD staining. Viable cells were calculated as annexin-/7AAD- cells, while annexin+7AAD- and annexin+7AAD+ cells were considered as apoptotic cells (early and late apoptotic cells, respectively). The data are expressed as the mean ± SEM (n=11). ***$p$ < 0.001: comparison with not stimulated BCP-ALL cells, Mann-Whitney test.

**(D-E)** Chemoresistance assay was performed using BCP-ALL 697 cells pretreated for 1 hour with SB431542 or vehicle (DMSO) before the stimulation with or without ActivinA for 24 hours (50 ng/mL). Alive population of cells stained with Annexin-V/7AAD were assessed after 72 hours of 1 U/mL of ASNase treatment. The graphs represent the results of 6 different experiments. *p<0.05: comparison with 1 µM SB-431542; **p<0.01: comparison with ActivinA-stimulated or not stimulated 697 cells, Mann-Whitney test.

**(F)** ASNase cytotoxicity was studied after 72 hours of incubation on 697 cells cultured alone (as a negative control) or pre-treated with EVs for 24 hours. The addition of ActivinA 697-EVs in BCP-ALL cell culture protected them from drug-induced apoptosis. We observed a decrease in number of apoptotic cells in the presence of ASNase. The results were compared with apoptosis of cells without drug and EVs. ActivinA condition was added as a positive control.

### 3.4.5. ActivinA-stimulated BCP-ALL 697 cells secrete EVs enriched in distinctive miRNA species

To understand the potential mechanisms by which BCP-ALL cell-derived EVs may mediate drug resistance, we deeply investigated the miRNA cargo of EVs derived from 697 cells stimulated or not with ActivinA. OpenArray technology was used to screen EV-miRNA expression among 12 samples. After data cleaning (AmpScore>1.24), we identified 10 miRNAs that were significantly altered in response to ActivinA stimulation when levels were normalized by three endogenous control genes RNU44, RNU48 and U6 (Figure 5A-B).

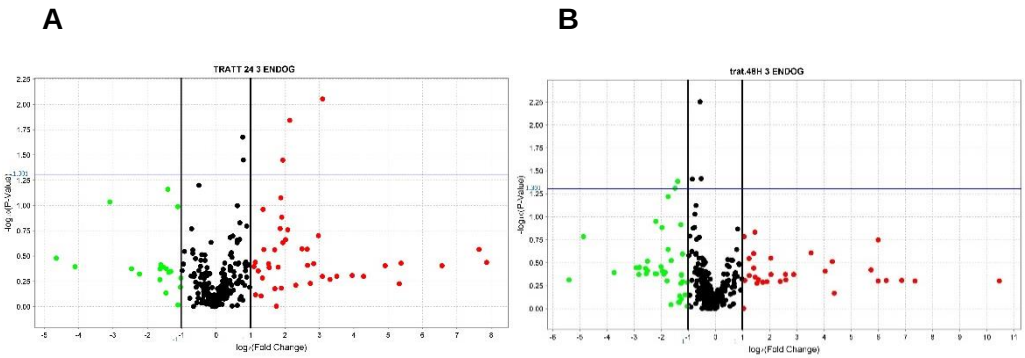


**Figure 5. miRNA species are highly enriched in ActivinA-mediated EVs**

Volcano plot of EV-associated miRNAs isolated from ActivinA-stimulated and not stimulated 697 cells. The $\log_2$ of miRNA levels in ActivinA-derived samples in comparison to control samples (fold-change) is plotted against the $-\log_{10}$ of the *p*

value. Different coloured dots show the differential regulation of miRNAs: red, up-regulated and green, down-regulated.

**(A, B)** Stimulation of cells with ActivinA for 24 hours and 48 hours increased and reduced, respectively, the expression values of five miRNAs, normalized to endogenous control miRNAs and presented in Table 1.

*Table 1. EV-associated miRNAs derived from 697 cells, stimulated with ActivinA for 24 hours and 48 hours, that are significantly different based on RNU44, RNU48, U6 and the unadjusted fold-change ($p<0.05$)*

| MicroRNA (24 hours) | Expression level | Fold change in BCP-ALL-derived 697 EVs vs control |
|---|---|---|
| **Let-7i-3p** | **Upregulated** | **8.535-fold change, $p = 0.009$** |
| **miR-639** | **Upregulated** | **4.405.-fold change, $p = 0.014$** |
| **miR-135b-3p** | **Upregulated** | **1.707-fold change, $p = 0.021$** |
| **miR-491-5p** | **Upregulated** | **1.730-fold change, $p = 0.035$** |
| **miR-139-5p** | **Upregulated** | **3.841-fold change, $p = 0.036$** |
| **MicroRNA (48 hours)** | **Expression level** | **Fold change in BCP-ALL-derived 697 EVs vs control** |
| **miR-15b-3p** | **Downregulated** | **0.355-fold change, $p = 0.049$** |
| **miR-18a-3p** | **Downregulated** | **0.672-fold change, $p = 0.006$** |
| **Let-7e-5p** | **Downregulated** | **0.692-fold change, $p = 0.038$** |
| **miR-1236-3p** | **Downregulated** | **0.553-fold change, $p = 0.039$** |
| **miR-23b-3p** | **Downregulated** | **0.380-fold change, $p = 0.041$** |

To validate the expression of the top 10 candidate miRNA species obtained at 24 hours and 48 hours after analysis based on endogenous control genes, we analysed 20 validation samples, using an OpenArray custom panel. Validation analysis confirmed the difference in terms of expression levels of two different miRNAs: one at 24 hours and one at 48 hours. In particular, miR-491-5p resulted significantly up-regulated in EVs derived from ActivinA-stimulated 697 cells compared to controls (RQ=2.919, *p* value<0.0001) (Table 2). On the contrary, 48 hour-ActivinA stimulation significantly decreased the expression level of leukemia-derived EV-associated miR-1236-3p (RQ=0.139, *p* value= 0.0461) (Table 2). Compared to expression difference of miRNAs in the screening phase, several deregulated miRNAs had not consistent expression patterns in the validation phase. Among of the other small RNA species, only let-7i-3p and miR-18a-3p maintain the same expression level of the screening phase. However, their difference in expression was not statistically significant. On the contrary, although deregulated miRNAs such as miR-139-5p and let-7e-5p were significantly modulated, but they showed opposing deregulated expression patterns.

*Table 2. Among the differentially expressed miRNAs, miR-491-5p and miR-1236-3p were validated by RT-qPCR assay. The results are presented as geometric mean and 95% CI of expression of miRNA in ActivinA-derived 697 EVs relative to controls (n=8).*

| miRNA | Treatment | RQ Mean | 95% CI | | *P* value | Fold change |
|---|---|---|---|---|---|---|
| let-7i-3p* | control | 0.000004 | 0.000000 | 0.000077 | 0.8158 | 1.276 |
| | ActivinA exposure | 0.000004 | 0.000000 | 0.000043 | | |
| miR-639* | control | 0.000022 | 0.000007 | 0.000072 | 0.0891 | 0.289 |
| | ActivinA exposure | 0.000006 | 0.000001 | 0.000041 | | |
| mir-135b-3p* | control | 0.000000075 | 0.000000018 | 0.000000317 | 0.2079 | 0.431 |
| | ActivinA exposure | 0.000000032 | 0.000000017 | 0.000000061 | | |
| **miR-491-5p*** | **control** | **0.000087** | **0.000047** | **0.000160** | | |
| | **ActivinA exposure** | **0.000253** | **0.000161** | **0.000397** | **<0.0001** | **2.919** |
| miR-139-5p* | control | 0.000042 | 0.000028 | 0.000065 | 0.0174 | 0.177 |
| | ActivinA exposure | 0.000008 | 0.000002 | 0.000033 | | |
| | | | ***24h*** | | | |
| miR-15b-3p* | control | 0.00563 | 0.00239 | 0.01328 | 0.4672 | 1.599 |
| | ActivinA exposure | 0.00900 | 0.00342 | 0.02367 | | |
| miR-18a-3p* | control | 0.00142 | 0.00025 | 0.00809 | 0.6661 | 0.607 |
| | ActivinA exposure | 0.00086 | 0.00005 | 0.01565 | | |
| let-7e-5p* | control | 0.978 | 0.668 | 1.287 | 0.0089 | 2.335 |
| | ActivinA exposure | 2.283 | 1.276 | 3.290 | | |
| **miR-1236-3p*** | **control** | **0.0000113** | **0.0000009** | **0.0000003** | | |
| | **ActivinA exposure** | **0.0000016** | **0.0001376** | **0.0000076** | **0.0461** | **0.139** |
| miR-23b-3p* | control | 0.00165 | 0.00010 | 0.02740 | 0.8322 | 1.276 |
| | ActivinA exposure | 0.00216 | 0.00005 | 0.09331 | | |
| | | | ***48h*** | | | |

*geometric mean

On the overall, our data suggest that ActivinA could influence EV miRNA cargo of BCP-ALL cells. In view of the extensive regulatory capacity of miRNAs, the finding that specific EV-associated miRNAs can be shuttled between leukemic cells and other target cells, suggests a novel mechanism of cell-to-cell communication potentially modulating the activity of recipient cells.

## 3.5. Discussion

Recently, Extracellular Vesicles (EVs) which are composed of both exosomes and microvesicles (MVs) have received considerable attention as important mediators of cell-to-cell communication. Once released with a process based on calcium influx and cytoskeleton reorganization[15], they come into contact with target cells and influence their biological properties, depending on the identity of their parental cells and processes of EV biogenesis[16]. Previously, we demonstrated that stromal cells produce the soluble molecule ActivinA which controls the migration of BCP-ALL cells over healthy hematopoiesis through a calcium- and actin polymerization-mediated mechanism[7]. As EV role in BCP-ALL disease is largely unexplored and in view of the peculiar processes modulated by ActivinA on leukemic cells, we investigated the effect of this molecule on leukemic B cell vesiculation. Particularly, we aimed to characterize both EV populations secreted by BCP-ALL cells, explore their miRNA cargo and study their potential effect on chemoresistance.

To obtain EVs from BCP-ALL-cell-conditioned culture medium, serum deprivation was applied. Our data provide a quantitative and qualitative analysis of EVs derived from supernatants of cultured BCP-ALL cells. Using NTA technology, we showed that the total population of EVs, released by leukemic cells, was very heterogenous in size and consisted of a mixture of different vesicle types (30-700 nm). Interestingly, ActivinA differentially regulated the release of these distinct EV subpopulations compared to unstimulated cells, by strongly increasing the

production of both exosomes (30-150 nm) and MVs (151-700 nm). Phenotypical characterization confirmed their identity as exosomes, as evaluated by the expression of the typical exosomal markers CD9 and CD63 and MV, as evaluated by the expression of BCP-ALL membrane-derived CD19.

Recent works showed that vesicular cargo comprises genetic material such as fusion transcripts of cancer cells[12,13]. BCP-ALL 697 cells, from which we obtained EVs, are characterized by the t(1;19) chromosomal translocation which results in the formation of the E2A-Pbx1 fusion transcript promoting leukemogenesis. Therefore, we explored the molecular cargo of EVs by attempting to detect the t(1;19) oncogene. Interestingly, we found the presence of EV-associated t(1;19) fusion transcript, thus indicating that EVs can carry RNA transcripts with prognostic relevance also in BCP-ALL and potentially deliver it to target cells. To find evidence of the biological effects mediated by EVs released from leukemic cells stimulated with ActivinA, we studied their potential role in promotion of chemoresistance. In this study, we firstly demonstrated that ActivinA confers resistance to ASNase-induced apoptosis which results in increasing of survival in BCP-ALL cells. To precisely define the specificity of ActivinA-mediated protection in response to ASNase in BCP-ALL cells, we used the small-molecule SB-431542, which acts as a potent and specific inhibitor of ALK4. Specific inhibition of ActivinA sensitized BCP-ALL cells to ASNase, thus suggesting that ALK4/ActivinA signaling mediates protection against chemotherapy in leukemic cells. Notably, we observed that 24

hours ActivinA-induced 697 EVs were able to confer resistance to ASNase to untreated 697 cells. This result suggests that ActivinA could exert its protective effect on leukemic cells directly, or in a paracrine circuit in an EV-dependent manner.

To understand the mechanisms behind chemoresistance, we explored the miRNA cargo of leukemic EVs. miRNA dysregulation plays a causal role in multiple steps of cancer pathogenesis. Based on their ability to modulate oncogenic or tumor-suppressive gene networks[17], miRNAs can be considered tumor suppressors or oncogenes, respectively. Gene regulatory networks in both solid tumors and hematological malignancies may be influenced by miRNA-containing EVs which can act as autocrine, paracrine and endocrine factors[18]. In our study, profiling of miRNAs in EVs from ActivinA-stimulated 697 cells compared to not stimulated cells allowed us to identify important miRNAs, already reported to be of relevance in disease biology. Among these, two microRNAs were highlighted for their high differential expression in ActivinA-induced 697 EVs: miR-491-5p and miR-1236-3p. Concerning their potential biological function, we based on literature data available in the context of other malignancies. miR-1236-3p, which significantly decreased following 48 hours of ActivinA stimulation, resulted in several studies on solid tumours associated, through its down-regulation, with promotion of cell migration, invasion and metastasis thus contributing to tumour progression. On the contrary, miR-491-5p that was significantly increased in 697 EVs induced by ActivinA stimulation after 24 hours, resulted overexpressed in drug-

resistant paediatric ALL cells, closely associated with the apoptosis suppression and Asparaginase (ASNase) resistance. Moreover, by using the online bioinformatic software mirPath v.3[19], we found that these two miRNAs directly target the “adherence junction” pathway which was previously reported to contribute to drug resistance via the HIPPO signalling[20]. In addition, KEGG analysis identified TCF7 between the genes involved in the above-mentioned pathway. TCF7 is a transcription factor implicated in the promotion of Wnt signalling activation. Recently, Hinze et al. found that, in acute leukemias, Wnt signaling induces asparaginase sensitivity by limiting Asparagine availability[21]. Overall, these data suggest that miR-491-5p could be implicated in the observed chemoresistance process. Future studies will provide whether EV chemoprotection could occur through these pathways.

In conclusion, we report for the first time that ActivinA can be considered a key regulator of leukemic B cell vesiculation, can rescue leukemic cells from drug-induced apoptosis and EVs participate to chemoprotection process.

## Supplementary Methods

### Supplemental method S1: Isolation of EVs

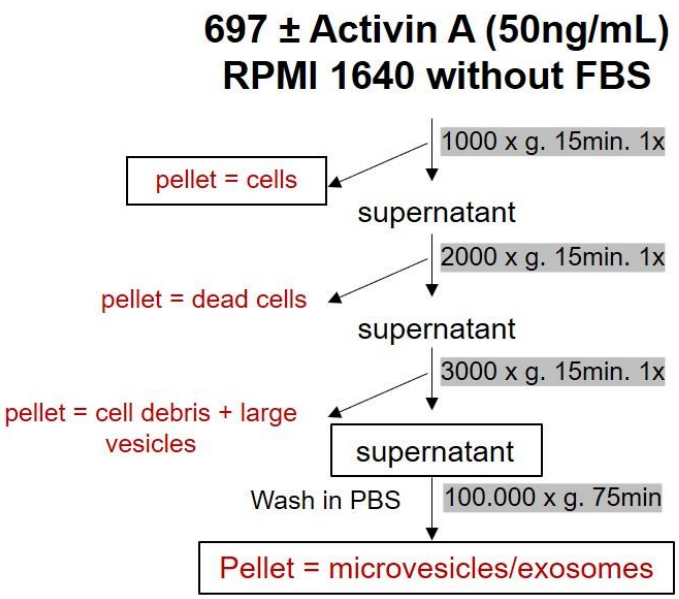


To isolate EVs, 5 mL of fresh supernatant was transferred to a 13.5 mL ultracentrifuge tube, which was filled with PBS. PBS was filtered through a 0.10 µm pore-size polyethersulfone filter to minimize the background contribution of interfering particles. The supernatant was ultracentrifuged at 110.000 x g for 75 min at 4°C (Optima$^{TM}$ Max-TL Ultracentrifuge, Beckman Coulter), to obtain an EV-rich pellet.

## Supplemental method S2: Characterization of EVs

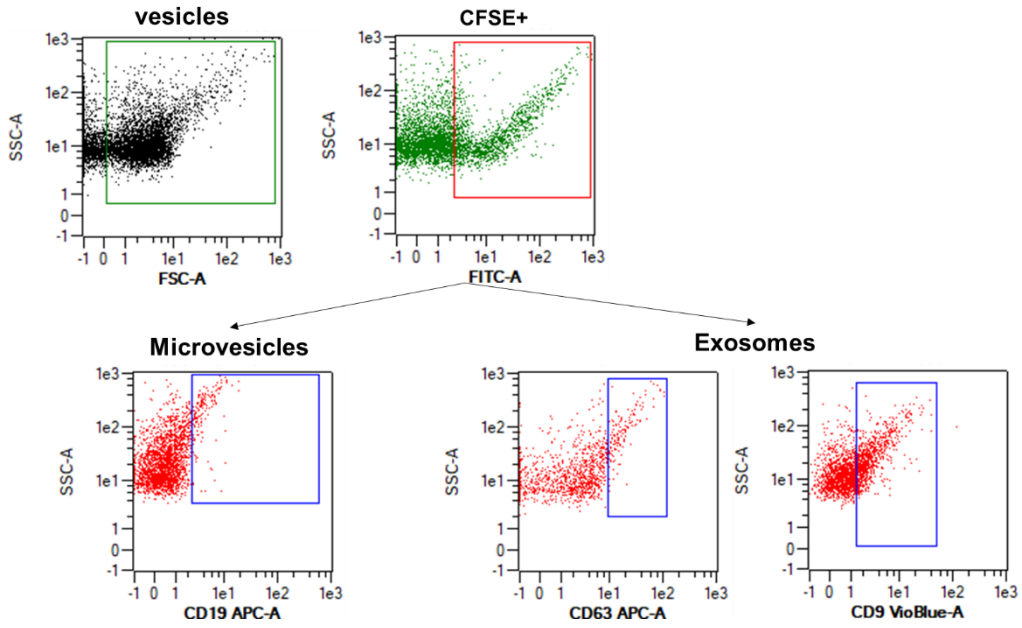


**Characterization of Extracellular Vesicles (EVs) by flow cytometry.** Microvesicles and exosomes purified from 697 culture supernatant were visualized, by flow cytometry, as CFSE-positive CD19+ (MVs) and CD63+ or CD9+ (exosomes) events.

**Supplemental method S3: quality of EVs-cDNA**

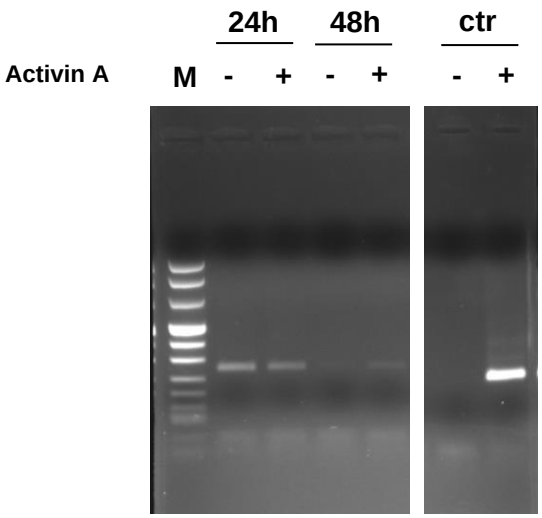


**Quality of the retro-transcribed EV-RNA was evaluated by testing the housekeeping gene Abelson.**

M is a size marker. Lanes 1 to 4 indicate cDNA of EVs derived from 697 cultured, respectively, in the absence or presence of Activin A for 24 hours and 48 hours. Lane 13, negative control; lane 14, 697 positive control. Plot representative of three independent experiments.

**Supplemental method S4: Isolation of EV-miRNAs**

The EV pellet of each ultracentrifuge tube was mixed with 700 µl of QIAzol Lysis Reagent and left at room temperature for 5 min. The non-human spike-in *Arabidopsis thaliana* (ath)-miR-159a (5 µl) was added in order to correct for possible differences in efficiency of the RNA extraction and cDNA generation. After addition of 140 µl chloroform, the lysate was separated into aqueous and organic phases by centrifugation at 12.000 x g for 15 min at 8°C. The aqueous phase containing total RNA was collected in a new tube with 350 µl of 70% ethanol. 700 µl of the sample was then applied to the RNeasy spin column and centrifuged at ≥10.200 rpm for 15 s at room temperature. The flow-through (which contains miRNA) was mixed with 450 µl 100% ethanol and then 700 µl of the sample was transferred in a RNeasy MinElute spin column (stored at 4°C) which was centrifuged at ≥10.200 rpm for 15 s at room temperature. The spin column was placed in a new collection tube and the remainder of the sample was transferred in the RNeasy MinElute spin column to repeat the centrifuge. Furthermore, 500 µl of RPE Buffer was added in the RNeasy MinElute spin column which was centrifuged at ≥10.200 rpm for 15 s. After the transfer of the spin column in a new collection tube, 500 µl of 80% ethanol was added and centrifuged at ≥10.200 rpm for 2min to dry the spin column membrane. The RNeasy MinElute spin column placed into a new collection tube was centrifuged with open lid at ≥10.200 rpm for 5min. Finally, the RNeasy MinElute spin column was placed into a 1.5 ml collection tube and 20 µl of RNase-free

water were added onto the spin column membrane. The spin column was centrifuged at ≥10.200 rpm for 1min to elute the miRNA-enriched fraction. To assess quality of miRNAs purification and quantify them, samples were analyzed by 2100 Bioanalyzer (Agilent Technologies, Santa Clara, CA) using Agilent RNA 6000 Pico Kit. Isolated miRNAs were stored at -80°C until further use.

**Supplemental method S5: Screening of miRNA expression**

Each reaction included: 0.75 µl of Megaplex RT Primers Pool A or Pool B, 0.15 µl of dNTPs (100 mM), 0.75 µl of 10x RT Buffer, 0.90 µl of MgCl2 (25 mM), 0.1 µl of RNase Inhibitor (20 U/µl), 1.5 µl of MultiScribe™ Reverse Transcriptase (50 U/µl), and 3.4 µl of miRNAs (40ng). After incubation on ice for 5 min, the mixture was subjected to the following thermal protocol in a C1000 Thermal Cycler (Biorad, Hercules, CA): 40 cycles at 16 °C for 2 min, 42 °C for 1 min, and 50 °C for 1 s, plus one cycle at 85 °C for 5 min. The cDNA samples were stored at -20 °C until use.

Each cDNA requiring preamplification was loaded onto a 96-well plate in accordance with the protocol provided by the manufacturer (Application Note 2011, Life Technologies). 2.5 µl of each reverse-transcribed miRNA was combined with the following reaction mix: 12.5 µl of TaqMan® PreAmp Master Mix (2x), 7.5 µl of nuclease-free water, and 2.5 µl of Megaplex™ PreAmp Primers Pool A or B (10x). Thermal conditions for the preamplification reaction were as follows: 95 °C for 10 min, 55 °C for 2 min, 72 °C for 2 min, 14 cycles of 95 °C for 15 s, 60 °C for 4 min, and 99.9 °C for 10 min to inactivate polymerases and final stage at 4°C. Preamplified samples were stored at 4°C until expression analysis with the OpenArray® System.

Each preamplified cDNA was diluted 1:20 with nuclease-free water. TaqMan Open Array® Real Time PCR Master Mix (2x) was added in a 1:1 volume ratio. Then, 6 µl of the reaction RT-PCR mix was aliquoted with the MicroLab STAR Let instrument

(Hamilton Robotics, Birmingham, UK) into eight wells of a 384-well OpenArray® plate. The reaction mix was loaded from the 384-well plate into a TaqMan™ OpenArray® Human miRNA Panel, with QuantStudio™ AccuFill System Robot (Life Technologies, Foster City, CA). The mixture was analyzed with the QuantStudio™ 12K Flex Real-Time PCR System with the OpenArray® Platform (QS12KFlex), according to the manufacturer's instructions.

**Supplemental method S6: Validation of miRNA expression**

Each reaction included: 6 µl of RT Primers Pool, 0.3 µl of dNTPs (100 mM Total), 1.5 µl 10× RT Buffer, 0.19 µl of RNases Inhibitor (20 U/µl), 3 µl of MultiScribe™ Reverse Transcriptase (50 U/µl), and 50 ng of miRNA. After incubation on ice for 5 min, the mixture was subjected to the following thermal protocol in a C1000 Thermal Cycler (Biorad): 16 °C for 30 min, 42 °C for 30 min, and 85 °C for 5 min. The cDNA samples were stored at -20 °C until further use.

Each cDNA was pre-amplified in a 96-well plate, in a reaction mix that included: 12.5 µl of TaqMan® PreAmp Master Mix (2x), 2 µl of nuclease-free water, 2.5 µl of PreAmp Custom Primers Pool, and 8 µl of reverse-transcribed miRNA. Preamplification reaction was performed using the same cycle of the screening phase. Each preamp product was first diluted with nuclease-free water to a ratio of 1:8 and then amplified using 5 µl of the TaqMan® Universal Master Mix II No AmpErase® UNG (Life Technologies, Carlsbad, CA, USA) and 0.5 µl of the appropriate 20x TaqMan® MicroRNA Assays. In detail, 6 µl reaction RT-PCR mix and 4 µl of cDNA were aliquoted with robot MicroLab STAR Let (Hamilton Robotics, Birmingham, UK) into three wells of a 384-well OpenArray® plate and then loaded on QuantStudio™ 12K Flex Real-Time PCR System with the following thermal cycling parameters: 95 °C for 10 min, 40 cycles of 95°C for 15 s and 60°C for 60 s.

# References


1. Chiarini F, Lonetti A, Evangelisti C, et al. Advances in understanding the acute lymphoblastic leukemia bone marrow microenvironment: From biology to therapeutic targeting. Biochimica et Biophysica Acta - Molecular Cell Research 2016;1863(3):449–463.
2. Bhojwani D, Yang JJ, Pui CH. Biology of childhood acute lymphoblastic leukemia. *Pediatric Clinics of North America* 2015;62(1):47–60.
3. Alvarnas JC, Co-Chair /, Hopkins J, et al. Acute Lymphoblastic Leukemia NCCN Guidelines ® NCCN Acute Lymphoblastic Leukemia Panel Members. 2015. 1258 p.
4. Preston DL, Kusumi S, Tomonaga M, et al. Supplement: Cancer Incidence in Atomic Bomb Survivors. Radiation Effects Research Foundation, Hiroshima and Nagasaki. 68–97 p.
5. O'Connor D, Bate J, Wade R, et al. Infection-related mortality in children with acute lymphoblastic leukemia: An analysis of infectious deaths on UKALL2003. Blood 2014;124(7):1056–1061.
6. Roberts KG, Mullighan CG. Genomics in acute lymphoblastic leukaemia: insights and treatment implications. Nature Reviews Clinical Oncology 2015;12(6):344–357.
7. Hong D, Gupta R, Ancliff P, et al. Initiating and Cancer-Propagating Cells in TEL-AML1-Associated Childhood Leukemia. Source: Science, New Series 2008;319(5861):336–339.
8. Ren R. Mechanisms of BCR-ABL in the pathogenesis of chronic myelogenous leukaemia. *Nature Reviews Cancer* 2005;5(3):172–183.
9. Kamps MP. E2A-Pbxl Induces Growth, Blocks Differentiation, and Interacts with Other Homeodomain Proteins Regulating Normal Differentiation.
10. Vrooman LM, Silverman LB. Treatment of Childhood Acute Lymphoblastic Leukemia: Prognostic Factors and Clinical Advances. *Current Hematologic Malignancy Reports* 2016;11(5):385–394.
11. Holmfeldt L, Wei L, Diaz-Flores E, et al. The genomic landscape of hypodiploid acute lymphoblastic leukemia. Nature Genetics 2013;45(3):242–252.
12. Mullighan CG, Goorha S, Radtke I, et al. Genome-wide analysis of genetic alterations in acute lymphoblastic leukaemia. Nature 2007;446(7137):758–764.
13. Roberts KG, Morin RD, Zhang J, et al. Genetic Alterations Activating Kinase and Cytokine Receptor Signaling in High-Risk Acute Lymphoblastic Leukemia. Cancer Cell 2012;22(2):153–166.
14. Cooper SL, Brown PA. Treatment of pediatric acute lymphoblastic leukemia. *Pediatric Clinics of North America* 2015;62(1):61–73.
15. Heikamp EB, Pui CH. Next-Generation Evaluation and Treatment of Pediatric Acute Lymphoblastic Leukemia. Journal of Pediatrics 2018;20314-24.e2.
16. R Shofield. The relationship between the spleen colony-forming cell and the haemopoietic stem cell. Blood Cells [Epub ahead of print].

17. Bakker ST, Passegué E. Resilient and resourceful: Genome maintenance strategies in hematopoietic stem cells. *Experimental Hematology* 2013;41(11):915–923.
18. Pietras EM, Warr MR, Passegué E. Cell cycle regulation in hematopoietic stem cells. Journal of Cell Biology 2011;195(5):709–720.
19. Perry JM, Li L. Disrupting the Stem Cell Niche: Good Seeds in Bad Soil. *Cell* 2007;129(6):1045–1047.
20. Kiel MJ, Yilmaz ÖH, Iwashita T, Yilmaz OH, Terhorst C, Morrison SJ. SLAM family receptors distinguish hematopoietic stem and progenitor cells and reveal endothelial niches for stem cells. Cell 2005;121(7):1109–1121.
21. Winkler IG, Barbier V, Nowlan B, et al. Vascular niche E-selectin regulates hematopoietic stem cell dormancy, self renewal and chemoresistance. Nature Medicine 2012;18(11):1651–1657.
22. Poulos MG, Guo P, Kofler NM, et al. Endothelial Jagged-1 Is necessary for homeostatic and regenerative hematopoiesis. Cell Reports 2013;4(5):1022–1034.
23. Yamazaki S, Ema H, Karlsson G, et al. Nonmyelinating schwann cells maintain hematopoietic stem cell hibernation in the bone marrow niche. Cell 2011;147(5):1146–1158.
24. Yamazaki S, Iwama A, Takayanagi S, Eto K, Ema H, Nakauchi H. TGF-β as a candidate bone marrow niche signal to induce hematopoietic stem cell hibernation. Blood 2009;113(6):1250–1256.
25. Bruns I, Lucas D, Pinho S, et al. Megakaryocytes regulate hematopoietic stem cell quiescence through CXCL4 secretion. Nature Medicine 2014;20(11):1315–1320.
26. Zhao M, Perry JM, Marshall H, et al. Megakaryocytes maintain homeostatic quiescence and promote post-injury regeneration of hematopoietic stem cells. Nature Medicine 2014;20(11):1321–1326.
27. Kiel MJ, Morrison SJ. Uncertainty in the niches that maintain haematopoietic stem cells. *Nature Reviews Immunology* 2008;8(4):290–301.
28. Frisch BJ, Porter RL, Calvi LM. Hematopoietic niche and bone meet.
29. Tie2/Angiopoietin-1 Signaling Regulates Hematopoietic Stem Cell Quiescence in the Bone Marrow Niche.
30. Tzeng YS, Li H, Kang YL, Chen WG, Cheng W, Lai DM. Loss of Cxcl12/Sdf-1 in adult mice decreases the quiescent state of hematopoietic stem/progenitor cells and alters the pattern of hematopoietic regeneration after myelosuppression. Blood 2011;117(2):429–439.
31. Zhang J, Niu C, Ye L, et al. Identification of the haematopoietic stem cell niche and control of the niche size. Nature 2003;425(6960):836–841.
32. Calvi LM, Adams GB, Weibrecht KW, et al. Osteoblastic cells regulate the haematopoietic stem cell niche. Nature 2003;425(6960):841–846.
33. Weber JM, Calvi LM. Notch signaling and the bone marrow hematopoietic stem cell niche. *Bone* 2010;46(2):281–285.

34. Stier S, Ko Y, Forkert R, et al. Osteopontin is a hematopoietic stem cell niche component that negatively regulates stem cell pool size. Journal of Experimental Medicine 2005;201(11):1781–1791.
35. Fox N, Priestley G, Papayannopoulou T, Kaushansky K. Thrombopoietin expands hematopoietic stem cells after transplantation. Journal of Clinical Investigation 2002;110(3):389–394.
36. Kollet O, Dar A, Shivtiel S, et al. Osteoclasts degrade endosteal components and promote mobilization of hematopoietic progenitor cells. Nature Medicine 2006;12(6):657–664.
37. Adams GB, Chabner KT, Alley IR, et al. Stem cell engraftment at the endosteal niche is specified by the calcium-sensing receptor. Nature 2006;439(7076):599–603.
38. Naveiras O, Nardi V, Wenzel PL, Hauschka P v., Fahey F, Daley GQ. Bone-marrow adipocytes as negative regulators of the haematopoietic microenvironment. Nature 2009;460(7252):259–263.
39. Zhou BO, Yu H, Yue R, et al. Bone marrow adipocytes promote the regeneration of stem cells and haematopoiesis by secreting SCF. Nature Cell Biology 2017;19(8):891–903.
40. Claycombe K, King LE, Fraker PJ. A role for leptin in sustaining lymphopoiesis and myelopoiesis.
41. Mercier FE, Ragu C, Scadden DT. The bone marrow at the crossroads of blood and immunity. *Nature Reviews Immunology* 2012;12(1):49–60.
42. Degliantoni G, Murphy M, Kobayashi M, Francis MK, Perussia B, Trinchieri G. NATURAL KILLER (NK) CELL-DERIVED HEMATOPOIETIC COLONY-INHIBITING ACTIVITY AND NK CYTOTOXIC FACTOR Relationship with Tumor Necrosis Factor and Synergism with Immune Interferon.
43. Sharara LI, Andersson Å, Guy-Grand D, Fischer A, Disanto JP. Deregulated TCRαβ T cell population provokes extramedullary hematopoiesis in mice deficient in the common γ chain. European Journal of Immunology 1997;27(4):990–998.
44. Urbieta M, Barao I, Jones M, et al. Hematopoietic progenitor cell regulation by CD4+CD25+ T cells. Blood 2010;115(23):4934–4943.
45. Fujisaki J, Wu J, Carlson AL, et al. In vivo imaging of T reg cells providing immune privilege to the haematopoietic stem-cell niche. Nature 2011;474(7350):216–220.
46. Chow A, Lucas D, Hidalgo A, et al. Bone marrow CD169+ macrophages promote the retention of hematopoietic stem and progenitor cells in the mesenchymal stem cell niche. Journal of Experimental Medicine 2011;208(2):761–771.
47. Albiero M, Poncina N, Ciciliot S, et al. Bone marrow macrophages contribute to diabetic stem cell mobilopathy by producing oncostatin M. Diabetes 2015;64(8):2957–2968.
48. Ludin A, Itkin T, Gur-Cohen S, et al. Monocytes-macrophages that express α-smooth muscle actin preserve primitive hematopoietic cells in the bone marrow. Nature Immunology 2012;13(11):1072–1082.

49. Hoggatt J, Singh P, Sampath J, Pelus LM. Prostaglandin E2 enhances hematopoietic stem cell homing, survival, and proliferation. Blood 2009;113(22):5444–5455.
50. Kawano Y, Fukui C, Shinohara M, et al. G-CSF-induced sympathetic tone provokes fever and primes antimobilizing functions of neutrophils via PGE 2 Key Points • G-CSF-induced sympathetic tone provokes fever and modulates microenvironment via PGE 2 production by bone marrow Gr-1 high neutrophils [Epub ahead of print].
51. Frisch BJ, Porter RL, Gigliotti BJ, et al. In vivo prostaglandin E2 treatment alters the bone marrow microenvironment and preferentially expands short-term hematopoietic stem cells. Blood 2009;114(19):4054–4063.
52. Casanova-Acebes M, Pitaval C, Weiss LA, et al. XRhythmic modulation of the hematopoietic niche through neutrophil clearance. Cell 2013;153(5):1025.
53. Mesenchymal progenitor cells localize within hematopoietic sites throughout ontogeny [Epub ahead of print].
54. Friedenstein A, Petrakova K, Kurolesova A, Frolova G. Heterotopic of bone marrow. Analysis of precursor cells for osteogenic and hematopoietic tissues. Transplantation [Epub ahead of print].
55. Greenbaum A, Hsu YMS, Day RB, et al. CXCL12 in early mesenchymal progenitors is required for haematopoietic stem-cell maintenance. Nature 2013;495(7440):227–230.
56. Méndez-Ferrer S, Michurina T v., Ferraro F, et al. Mesenchymal and haematopoietic stem cells form a unique bone marrow niche. Nature 2010;466(7308):829–834.
57. Meisel R, Zibert A, Laryea M, Göbel U, Däubener W, Dilloo D. Human bone marrow stromal cells inhibit allogeneic T-cell responses by indoleamine 2,3-dioxygenase–mediated tryptophan degradation. Blood 2004;103(12):4619–4621.
58. Aggarwal S, Pittenger MF. Human mesenchymal stem cells modulate allogeneic immune cell responses [Epub ahead of print].
59. Waterman RS, Tomchuck SL, Henkle SL, Betancourt AM. A new mesenchymal stem cell (MSC) paradigm: Polarization into a pro-inflammatory MSC1 or an immunosuppressive MSC2 phenotype. PLoS ONE;5(4):.
60. Kreso A, Dick JE. Evolution of the cancer stem cell model. *Cell Stem Cell* 2014;14(3):275–291.
61. Schepers K, Campbell TB, Passegué E. Normal and leukemic stem cell niches: Insights and therapeutic opportunities. *Cell Stem Cell* 2015;16(3):254–267.
62. Hanoun M, Zhang D, Mizoguchi T, et al. Acute myelogenous leukemia-induced sympathetic neuropathy promotes malignancy in an altered hematopoietic stem cell Niche. Cell Stem Cell 2014;15(3):365–375.
63. Arranz L, Sánchez-Aguilera A, Martín-Pérez D, et al. Neuropathy of haematopoietic stem cell niche is essential for myeloproliferative neoplasms. Nature 2014;512(1):78–81.

64. Schepers K, Pietras EM, Reynaud D, et al. Myeloproliferative neoplasia remodels the endosteal bone marrow niche into a self-reinforcing leukemic niche. Cell Stem Cell 2013;13(3):285–299.
65. Jacamo R, Chen Y, Wang Z, et al. Reciprocal leukemia-stroma VCAM-1/VLA-4-dependent activation of NF-κB mediates chemoresistance. Blood 2014;123(17):2691–2702.
66. Døsen-Dahl G, Munthe E, Nygren MK, Stubberud H, Hystad ME, Rian E. Bone marrow stroma cells regulate TIEG1 expression in acute lymphoblastic leukemia cells: Role of TGFβ/BMP-6 and TIEG1 in chemotherapy escape. International Journal of Cancer 2008;123(12):2759–2766.
67. Juarez J, Baraz R, Gaundar S, Bradstock K, Bendall L. Interaction of interleukin-7 and interleukin-3 with the CXCL12-induced proliferation of B-cell progenitor acute lymphoblastic leukemia. Haematologica 2007;92(4):450–459.
68. Frolova O, Samudio I, Benito J, et al. Regulation of HIF-1α signaling and chemoresistance in acute lymphocytic leukemia under hypoxic conditions of the bone marrow microenvironment. Cancer Biology and Therapy 2012;13(10):858–870.
69. Iwamoto S, Mihara K, Downing JR, Pui CH, Campana D. Mesenchymal cells regulate the response of acute lymphoblastic leukemia cells to asparaginase. Journal of Clinical Investigation 2007;117(4):1049–1057.
70. Colmone A, Amorim M, Pontier AL, Wang S, Jablonski E, Sipkins DA. Leukemic Cells Create Bone Marrow Niches That Disrupt the Behavior of Normal Hematopoietic Progenitor Cells. Science 2008;322(5909):1861–1865.
71. Duan C-W, Shi J, Chen J, et al. Leukemia Propagating Cells Rebuild an Evolving Niche in Response to Therapy. Cancer Cell 2014;25(6):778–793.
72. de Rooij B, Polak R, van den Berk LCJ, Stalpers F, Pieters R, den Boer ML. Acute lymphoblastic leukemia cells create a leukemic niche without affecting the CXCR4/CXCL12 axis. *Haematologica* 2017;102(10):e389–e393.
73. Zhang B, Ho YW, Huang Q, et al. Altered Microenvironmental Regulation of Leukemic and Normal Stem Cells in Chronic Myelogenous Leukemia. Cancer Cell 2012;21(4):577–592.
74. Li Z-W, Dalton WS. Tumor microenvironment and drug resistance in hematologic malignancies. Blood Reviews 2006;20(6):333–342.
75. Kim J-A, Shim J-S, Lee G-Y, et al. Microenvironmental Remodeling as a Parameter and Prognostic Factor of Heterogeneous Leukemogenesis in Acute Myelogenous Leukemia. Cancer Research 2015;75(11):2222–2231.
76. Manabe A, Coustan-Smith E, Behm F, Raimondi S, Campana D. Bone marrow-derived stromal cells prevent apoptotic cell death in B-lineage acute lymphoblastic leukemia. Blood [Epub ahead of print].
77. Vilchis-Ordoñez A, Contreras-Quiroz A, Vadillo E, et al. Bone Marrow Cells in Acute Lymphoblastic Leukemia Create a Proinflammatory

Microenvironment Influencing Normal Hematopoietic Differentiation Fates. BioMed Research International 2015;20151–14.
78. Enciso J, Mayani H, Mendoza L, Pelayo R. Modeling the pro-inflammatory tumor microenvironment in acute lymphoblastic leukemia predicts a breakdown of hematopoietic-mesenchymal communication networks. Frontiers in Physiology;7(AUG):
79. Tabe Y, Konopleva M. Role of Microenvironment in Resistance to Therapy in AML. Current Hematologic Malignancy Reports 2015;10(2):96–103.
80. Doepfner KT, Spertini O, Arcaro A. Autocrine insulin-like growth factor-I signaling promotes growth and survival of human acute myeloid leukemia cells via the phosphoinositide 3-kinase/Akt pathway. Leukemia 2007;21(9):1921–1930.
81. Huan J, Hornick NI, Goloviznina NA, et al. Coordinate regulation of residual bone marrow function by paracrine trafficking of AML exosomes. Leukemia 2015;29(12):2285–2295.
82. Huan J, Hornick NI, Shurtleff MJ, et al. RNA Trafficking by Acute Myelogenous Leukemia Exosomes. Cancer Research 2013;73(2):918–929.
83. Chen W, ten Dijke P. Immunoregulation by members of the TGFβ superfamily. Nature Reviews Immunology 2016;16(12):723–740.
84. Harrison CA, Gray PC, Vale WW, Robertson DM. Antagonists of activin signaling: Mechanisms and potential biological applications. *Trends in Endocrinology and Metabolism* 2005;16(2):73–78.
85. Antsiferova M, Werner S. The bright and the dark sides of activin in wound healing and cancer. *Journal of Cell Science* 2012;125(17):3929–3937.
86. Robson NC, Phillips DJ, Mcalpine T, et al. Activin-A: a novel dendritic cell-derived cytokine that potently attenuates CD40 ligand-specific cytokine and chemokine production [Epub ahead of print].
87. Ogawa K, Funaba M, Chen Y, Tsujimoto M. Activin A Functions as a Th2 Cytokine in the Promotion of the Alternative Activation of Macrophages. The Journal of Immunology 2006;177(10):6787–6794.
88. Mantovani A, Sozzani S, Locati M, Allavena P, Sica A. Macrophage polarization: tumor-associated macrophages as a paradigm for polarized M2 mononuclear phagocytes.
89. Robson NC, Wei H, McAlpine T, Kirkpatrick N, Cebon J, Maraskovsky E. Activin-A attenuates several human natural killer cell functions. Blood 2009;113(14):3218–3225.
90. Shiozaki M, Sakai R, Tabuchi M, Eto Y, Kosaka M, Shibai H. Invivo treatment with erythroid differentiation factor (EDF / activin a) increases erythroid precursors (CFU-E and BFU-E) in mice. Biochemical and Biophysical Research Communications 1989;165(3):1155–1161.
91. Shav‐Tal Y, Zipori D. The Role of Activin A in Regulation of Hemopoiesis. Stem Cells 2002;20(6):493–500.
92. SHOHAM T, PARAMESWARAN R, SHAV-TAL Y, BARDA-SAAD M, ZIPORI D. The Mesenchymal Stroma Negatively Regulates B Cell

Lymphopoiesis through the Expression of Activin A. Annals of the New York Academy of Sciences 2003;996(1):245–260.
93. Burdette JE, Jeruss JS, Kurley SJ, Lee EJ, Woodruff TK. Activin A mediates growth inhibition and cell cycle arrest through Smads in human breast cancer cells. Cancer Research 2005;65(17):7968–7975.
94. Hempen PM, Zhang L, Bansal RK, et al. Evidence of Selection for Clones Having Genetic Inactivation of the Activin A Type II Receptor (ACVR2) Gene in Gastrointestinal Cancers 1. 994–999 p.
95. Grusch M, Drucker C, Peter-Vörösmarty B, et al. Deregulation of the activin/follistatin system in hepatocarcinogenesis. Journal of Hepatology 2006;45(5):673–680.
96. Bufalino A, Cervigne NK, de Oliveira CE, et al. Low miR-143/miR-145 Cluster Levels Induce Activin A Overexpression in Oral Squamous Cell Carcinomas, Which Contributes to Poor Prognosis. PLOS ONE 2015;10(8):e0136599.
97. Taylor C, Loomans HA, le Bras GF, et al. Activin a signaling regulates cell invasion and proliferation in esophageal adenocarcinoma. Oncotarget 2015;6(33):34228–34244.
98. Loumaye A, de Barsy M, Nachit M, et al. Circulating Activin A predicts survival in cancer patients. Journal of Cachexia, Sarcopenia and Muscle 2017;8(5):768–777.
99. Hoda MA, Rozsas A, Lang E, et al. High circulating activin A level is associated with tumor progression and predicts poor prognosis in lung adenocarcinoma. Oncotarget 2016;7(12):13388–13399.
100. Bashir M, Damineni S, Mukherjee G, Kondaiah P. Activin-a signaling promotes epithelial–mesenchymal transition, invasion, and metastatic growth of breast cancer. npj Breast Cancer;1.
101. Ramirez MI, Amorim MG, Gadelha C, et al. Technical challenges of working with extracellular vesicles. *Nanoscale* 2018;10(3):881–906.
102. Pan B-T, Johnstone RM. Fate of the transferrin receptor during maturation of sheep reticulocytes in vitro: Selective externalization of the receptor. Cell 1983;33(3):967–978.
103. Harding C, Heuser J, Stahl P. Receptor-mediated endocytosis of transferrin and recycling of the transferrin receptor in rat reticulocytes. Journal of Cell Biology 1983;97(2):329–339.
104. Mathivanan S, Ji H, Simpson RJ. Exosomes: Extracellular organelles important in intercellular communication. *Journal of Proteomics* 2010;73(10):1907–1920.
105. Cocucci E, Meldolesi J. Ectosomes and exosomes: Shedding the confusion between extracellular vesicles. *Trends in Cell Biology* 2015;25(6):364–372.
106. Mathivanan S, Ji H, Simpson RJ. Exosomes: Extracellular organelles important in intercellular communication. *Journal of Proteomics* 2010;73(10):1907–1920.
107. Soler N, Marguet E, Verbavatz J-M, Forterre P. Virus-like vesicles and extracellular DNA produced by hyperthermophilic archaea of the order Thermococcales. Research in Microbiology 2008;159(5):390–399.

108. Knox KW, Vesk M, Work E. Relation Between Excreted Lipopolysaccharide Complexes and Surface Structures of a Lysine-Limited Culture of Escherichia coli. Journal of Bacteriology 1966;92(4):1206–1217.
109. Lee E-Y, Choi D-Y, Kim D-K, et al. Gram-positive bacteria produce membrane vesicles: Proteomics-based characterization of Staphylococcus aureus-derived membrane vesicles. PROTEOMICS 2009;9(24):5425–5436.
110. Tatischeff I, Bomsel M, de Paillerets C, et al. Dictyostelium discoideum cells shed vesicles with associated DNA and vital stain Hoechst 33342. Cellular and Molecular Life Sciences (CMLS) 1998;54(5):476–487.
111. Albuquerque PC, Nakayasu ES, Rodrigues ML, et al. Vesicular transport in *Histoplasma capsulatum* : an effective mechanism for trans-cell wall transfer of proteins and lipids in ascomycetes. Cellular Microbiology 2008;10(8):1695–1710.
112. Rodrigues ML, Nimrichter L, Oliveira DL, et al. Vesicular Polysaccharide Export in Cryptococcus neoformans Is a Eukaryotic Solution to the Problem of Fungal Trans-Cell Wall Transport. Eukaryotic Cell 2007;6(1):48–59.
113. Regente M, Corti-Monzón G, Maldonado AM, Pinedo M, Jorrín J, de la Canal L. Vesicular fractions of sunflower apoplastic fluids are associated with potential exosome marker proteins. FEBS Letters 2009;583(20):3363–3366.
114. Wolf P. The Nature and Significance of Platelet Products in Human Plasma. British Journal of Haematology 1967;13(3):269–288.
115. Gangoda L, Boukouris S, Liem M, Kalra H, Mathivanan S. Extracellular vesicles including exosomes are mediators of signal transduction: Are they protective or pathogenic? *Proteomics* 2015;15(2–3):260–271.
116. Raposo G, Stoorvogel W. Extracellular vesicles: Exosomes, microvesicles, and friends. *Journal of Cell Biology* 2013;200(4):373–383.
117. Keerthikumar S, Gangoda L, Liem M, et al. Proteogenomic analysis reveals exosomes are more oncogenic than ectosomes.
118. Balaj L, Lessard R, Dai L, et al. Tumour microvesicles contain retrotransposon elements and amplified oncogene sequences. Nature Communications 2011;2(1):180.
119. Thakur BK, Zhang H, Becker A, et al. Double-stranded DNA in exosomes: A novel biomarker in cancer detection. *Cell Research* 2014;24(6):766–769.
120. Guescini M, Genedani S, Stocchi V, Agnati LF. Astrocytes and Glioblastoma cells release exosomes carrying mtDNA. Journal of Neural Transmission 2010;117(1):1–4.
121. Ratajczak J, Wysoczynski M, Hayek F, Janowska-Wieczorek A, Ratajczak MZ. Membrane-derived microvesicles: Important and underappreciated mediators of cell-to-cell communication. *Leukemia* 2006;20(9):1487–1495.

122. Kunz F, Kontopoulou E, Reinhardt K, et al. Detection of AML-specific mutations in pediatric patient plasma using extracellular vesicle–derived RNA. Annals of Hematology 2019;98(3):595–603.
123. Reclusa P, Laes JF, Malapelle U, et al. EML4-ALK translocation identification in RNA exosomal cargo (ExoALK) in NSCLC patients: A novel role for liquid biopsy. *Translational Cancer Research* 2019;8S76–S78.
124. Nolte'T Hoen ENM, Buermans HPJ, Waasdorp M, Stoorvogel W, Wauben MHM, 'T Hoen PAC. Deep sequencing of RNA from immune cell-derived vesicles uncovers the selective incorporation of small non-coding RNA biotypes with potential regulatory functions. Nucleic Acids Research 2012;40(18):9272–9285.
125. Yang Q, Diamond MP, Al-Hendy A. The emerging role of extracellular vesicle-derived miRNAs: implication in cancer progression and stem cell related diseases.
126. Zhang B, Pan X, Cobb GP, Anderson TA. microRNAs as oncogenes and tumor suppressors. Developmental Biology 2007;302(1):1–12.
127. Fong MY, Zhou W, Liu L, et al. Breast-cancer-secreted miR-122 reprograms glucose metabolism in premetastatic niche to promote metastasis. Nature Cell Biology 2015;17(2):183–194.
128. Lunavat TR, Cheng L, Einarsdottir BO, et al. BRAFV600 inhibition alters the microRNA cargo in the vesicular secretome of malignant melanoma cells. Proceedings of the National Academy of Sciences of the United States of America 2017;114(29):E5930–E5939.
129. Liu Y, Luo F, Wang B, et al. STAT3-regulated exosomal miR-21 promotes angiogenesis and is involved in neoplastic processes of transformed human bronchial epithelial cells. Cancer Letters 2016;370(1):125–135.
130. Liao J, Liu R, Shi YJ, Yin LH, Pu YP. Exosome-shuttling microRNA-21 promotes cell migration and invasion-targeting PDCD4 in esophageal cancer. International Journal of Oncology 2016;48(6):2567–2579.
131. Qin X, Yu S, Zhou L, et al. Cisplatin-resistant lung cancer cell–derived exosomes increase cisplatin resistance of recipient cells in exosomal miR-100–5p-dependent manner. International Journal of Nanomedicine 2017;123721–3733.
132. Yeh Y-Y, Ozer HG, Lehman AM, et al. Characterization of CLL exosomes reveals a distinct microRNA signature and enhanced secretion by activation of BCR signaling [Epub ahead of print].
133. Paggetti J, Haderk F, Seiffert M, et al. Exosomes released by chronic lymphocytic leukemia cells induce the transition of stromal cells into cancer-associated fibroblasts. Blood 2015;126(9):1106–1117.
134. Bouvy C, Wannez A, Laloy J, Chatelain C, Dogné JM. Transfer of multidrug resistance among acute myeloid leukemia cells via extracellular vesicles and their microRNA cargo. Leukemia Research 2017;6270–76.
135. Mirzaei H, Sahebkar A, Jaafari MR, Goodarzi M, Mirzaei HR. Diagnostic and Therapeutic Potential of Exosomes in Cancer: The

Beginning of a New Tale? *Journal of Cellular Physiology* 2017;232(12):3251–3260.

136. Pant S, Hilton H, Burczynski ME. The multifaceted exosome: Biogenesis, role in normal and aberrant cellular function, and frontiers for pharmacological and biomarker opportunities. *Biochemical Pharmacology* 2012;83(11):1484–1494.

# 4. Summary, Conclusions and future perspectives

BCP-ALL is the most common pediatric malignancy and is newly diagnosed in approximately 3-4 cases per 100,000 annually, with a peak incidence at 2-5 years of age[1]. Despite in the past BCP-ALL was considered to be an intractable disease, nowadays it has achieved an overall survival probability of 85%. The main contributors to this dramatic improvement are the availability of better supportive care, more precise risk stratification, the biological features of leukemic cells and optimization of treatment regimens. However, relapse remains a significant cause of treatment failure and treatment-related morbidity[2]. Extensive research has demonstrated that BM microenvironment plays an active role in leukemogenesis as well as its leukemia-induced remodeling may selectively support leukemic cells over normal hematopoiesis[3]. Accordingly, identification of the crucial factors involved in the reciprocal leukemia-stroma crosstalk may offer a new important therapeutic strategy. The first part of the presented study identifies ActivinA, a TGF-β family member, as a novel key player in the interaction between BCP-ALL cells and their BM niche.

We firstly evaluated ActivinA levels in the BM plasma of both leukemic patients at diagnosis and HDs and found an overexpression of the molecule in patients compared to controls. Several cells of the tumor microenvironment like fibroblasts, endothelial cells and immune cells including T/B lymphocytes,

neutrophils, macrophages, dendritic cells, natural killer cells were shown to be capable of producing and responding to ActivinA[4]. Here, we demonstrated that BM-MSCs are an important source of ActivinA, whose production is strongly upregulated following co-culture with leukemic cells. Notably, we showed a significantly higher production of ActivinA by BCP-ALL MSCs compared to their normal counterpart, thus hypothesizing that BM-MSCs primed by the leukemic microenvironment could be accountable for the high amount of ActivinA in the BM of BCP-ALL patients. These results suggested a role for ActivinA in the remodeling of the BM niche, in accordance with the “seed and soil” theory stating that leukemic cells alter the BM stroma to create a leukemia-supporting microenvironment that favors disease progression[1]. Chronic inflammation is considered to be one of the hallmarks of malignancy. In line with recent literature[5,6], we found higher levels of the pro-inflammatory cytokines IL-1β, IL-6 and TNF-α in the BM plasma of BCP-ALL patients compared to HDs, suggesting that also in BCP-ALL an inflammatory microenvironment could promote tumor development. By mimicking an inflamed BM niche through the simultaneous stimulation of HD-MSCs with leukemic blasts and pro-inflammatory mediators, we showed a strong increase in the secretion of ActivinA. The abundance of ActivinA within the leukemic BM niche and its identification as a new MSC-secreted leukemia-driven molecule prompted us to investigate its possible effects on BCP-ALL cells. A gene expression profile analysis, performed on 697 cell line, revealed that ActivinA modulates

several gene categories critically linked to carcinogenesis. According to the recognized role of ActivinA in the regulation of cell migration and invasion in solid tumors[7], we focused our attention on several motility-associated pathways. We observed that ActivinA was able to positively regulate the expression of VAV3 and DOCK4 (guanine nucleotide exchange factors for Rho family GTPases) whereas it negatively regulated ARHGAP25 (negative regulator of Rho GTPases). Moreover, ActivinA was able to contribute to cellular calcium (Ca2+) homeostasis by regulating CORO1A, ATP2B2, ATP2B4. In particular, CORO1A promotes the formation of the second messenger InsP3, responsible of Ca2+ release from intracellular stores. ATP2B2 and ATP2B4 are plasma membrane Ca2+ ATPases implicated in Ca2+ extrusion from the cytosol into the extracellular space. Since they resulted downregulated and upregulated, respectively, by ActivinA, we could hypothesize that, according to their specific localization in the plasma membrane, they could establish a back-to-front Ca2+ gradient which promotes the reorganization of actin cytoskeleton and the formation of lamellipodia and filopodia during cell migration. In accordance with GEP data, we demonstrated that ActivinA was able to enhance both the spontaneous motility and CXCL12-mediated chemotaxis of BCP-ALL cells. By investigating the molecular mechanisms underlying the promotion of leukemic cell motility mediated by ActivinA, we observed that this molecule increased the intracellular calcium content and, upon CXCL12 addition, induced a higher calcium peak in ActivinA stimulated compared

to untreated leukemic cells. Moreover, we highlighted that ActivinA pretreatment of leukemic cells resulted in a more prominent conversion of globular into filamentous-actin which is an important process in site-directed migration. The known association between increasing Ca2+ levels and induction of F-actin polymerization allowed us to hypothesize the existence of a calcium-mediated mechanism involved in the ActivinA-induced pro-migratory phenotype. Several works revealed that CXCL12 reduction is one of the microenvironmental alterations occurring in the leukemic BM[8]. Here, we confirmed, in our cohort of patients, a significant reduction of CXCL12 BM plasma level in BCP-ALL patients. Of note, another work recently published by our research group[9] showed that CXCL12 reduction can be, at least partially, explained by a direct effect of ActivinA on MSC chemokine secretion. Moreover, we demonstrated that ActivinA was able to increase the migration of leukemic cells also towards suboptimal CXCL12 concentrations. Thus, we hypothesized that the increased responsiveness of leukemic cells even to very low levels of CXCL12 induced by ActivinA might promote a selective advantage to BCP-ALL cells compared to healthy CD34+ cells. Indeed, we observed in ActivinA-stimulated CD34+ cells, an opposite effect compared to leukemic cells: a reduction of free cytosolic Ca2+ and a consequent reduction of migration in response to CXCL12. Hence, these data suggest that leukemic cells could displace healthy HSCs from their niches through an ActivinA-mediated mechanism.

The migratory advantage conferred to leukemic cells by ActivinA was confirmed also *in vivo*. In fact, we showed, by using a xenograft mouse model of human BCP-ALL, the ability of Activin A to enhance both BM engraftment and metastatic potential into extra-medullary sites of leukemic cells such as the liver, spleen, meninges and brain. Interestingly, an increased leukemic burden was observed in the CNS of mice receiving ActivinA-treated cells.

Overall, our results showed that the leukemic BM, at the onset of BCP-ALL, is characterized by high levels of ActivinA, which is strongly induced in stromal cells after direct contact with leukemic cells or through leukemia-released soluble factors. Interestingly, we demonstrated that ActivinA selectively influences the biological properties of leukemic cells, by enhancing their migratory and invasive ability. Moreover, ActivinA could affect both HSC and MSC behaviors: on the one side, it was able to impair CXCL12-driven migration of HSCs and on the other side to inhibit CXCL12 release by MSCs. These two effects may represent a key mechanism in the displacement of healthy hematopoietic cells from the BM niche in favor of leukemic cells. Therefore, the discovery of ActivinA-mediated crosstalk between BCP-ALL cells and MSCs adds significant insights into the mechanisms of communication in the leukemic niche. Hence, our data provide a new concept to develop alternative therapeutic strategies targeting the leukemia-stroma interplay. Future studies will focus on the study of ActivinA ability to promote the localization of leukemic cells in extramedullary sites and in

particular in the Central Nervous System (CNS), which represents a relapse site clinically difficult to treat.

Moreover, in order to eradicate BCP-ALL, we will target the leukemic stromal microenvironment through inhibition of ActivinA pathway or its receptors by using the previously mentioned SB-431542 or the ActivinA trap RAP-011, already clinically used in multiple myeloma and anemia hematologic disorders. This anti-microenvironmental therapy could be combined with therapies actually used to directly target BCP-ALL disease.

In the second part of the project, we focused on BCP-ALL released extracellular vesicles (EVs). Interestingly, EVs are released through a mechanism dependent on calcium influx and cytoskeleton reorganization. For this reason, in view of the peculiar calcium pathways modulated by ActivinA on BCP-ALL cells, we investigated the effect of this molecule on cell vesiculation. EVs have received considerable attention in recent years, both as mediators of intercellular communication that lead to tumor progression, and as potential sources for discovery of novel cancer biomarkers. They can be categorized depending upon where in the cell they originate; in particular, vesicles that are derived from multivesicular bodies are referred to as exosomes and those from the plasma membrane as microvesicles[10]. Interestingly, we found that 697 cells alone were able to produce both EV populations, but the addition of ActivinA significantly increased vesicle release. As other groups reported enrichment of fusion transcripts within EVs derived from tumor

cells[11], we evaluated the presence of eventual fusion transcript also in EVs deriving from BCP-ALL cells. BCP-ALL 697 cell line is characterized by the presence of the chromosomal translocation t(1;19) which is one of the most common translocations in pediatric BCP-ALL. This translocation results in the formation of the TCF3/PBX1 fusion transcript, which disrupt the maturation of lymphoid lineages and expand undifferentiated progenitor populations, thus contributing to the leukemogenesis process. Interestingly, we found the TCF3/PBX1 fusion transcript in EVs isolated from 697 cells stimulated or not with ActivinA. Of note, the t(1;19) expression in leukemia-derived EVs implicates the this fusion transcript could be delivered to other cell types to mediate malignant transformation. Future experiments are needed to understand whether this fusion transcript is delivered to other cell types of the leukemic BM microenvironment and the biological effects. Recently, a considerable interest in the cancer field has focused on the role of EVs in regulating the drug resistance of leukemic cells. In order to study the biological effects in which can be involved leukemia-derived EVs obtained after ActivinA stimulation, we investigated whether they could participate to chemoprotection. For this purpose, we used Asparaginase which is an anti-leukemic drug used in current BCP-ALL protocols. Firstly, we performed chemoresistance assays on cells to evaluate ActivinA effect, and we demonstrated that the molecule was able to decrease the sensitivity of leukemic cells to the drug-induced apoptosis. Thereafter, to confirm the specificity of this effect, we blocked

ActivinA signaling through the use of SB-431542, which acts as a potent inhibitor of Activin receptors ALK4, ALK5 and ALK7. Interestingly, by blocking Activin/ActivinA receptors axis by using SB-431542, we observed a significant reduction of viability in ActivinA-stimulated cells treated with ASNase, thus demonstrating that chemoprotection could be reverted by ActivinA blocking. We then investigated whether leukemia-derived EVs, obtained after ActivinA stimulation, could mediate drug resistance. Surprisingly, our preliminary results showed that ActivinA-induced 697 EVs were specifically able to protect 697 unstimulated cells from Asparaginase-dependent apoptosis. This effect was not observed when EVs from unstimulated 697 cells were used. Therefore, we can hypothesize that, within the leukemic BM niche, ActivinA could induce the release of EVs that could increase in a paracrine manner the chemoresistance of the leukemic bulk. To understand the mechanisms by which EVs released from ActivinA stimulated BCP-ALL cells can mediate the protective effect against ASNase treatment, we explored their miRNA cargo. MicroRNAs, as one of the most important post-transcription regulatory elements, are transferred among the cells by EVs and affect them based on the information of the cell origin[12]. Notably, we observed the existence of a different microRNA signature in ActivinA-induced 697 EVs compared to EVs from unstimulated cells. We found dysregulation of miR-491-5p and miR-1236-3p expression after ActivinA stimulation for 24 hours and 48 hours, respectively. Of these, downregulation of miR-1236-3p has been reported to be associated with

promotion of cell motility and invasive properties[13], while upregulation of miR-491-5p has been demonstrated to be linked to ASNase resistance in childhood BCP-ALL[14]. Interestingly, by using the online tool DIANA-mirPath v.3[15], we found that miR-491-5p and miR-1236-3p are implicated in the “adherence junction” pathway which previously was associated to other EV-miRNA from AML cells[16] and it is known to contribute to quiescence, apoptosis and drug resistance via HIPPO signaling pathway. More importantly, KEGG pathway results revealed that between the target genes of these two miRNAs there is TCF7[17] which is a transcription factor involved in the activation of Wnt signaling. Hinze et al. found that, in acute leukemias, Wnt signaling induces asparaginase sensitivity by limiting Asparagine availability[18]. Future studies will provide whether EV chemoprotection could occur through these pathways.

Moreover, we will also investigate the possible involvement of miR-1236-5p in ActivinA-mediated effect on BCP-ALL cell motility and invasiveness.

In conclusion, we demonstrated that ActivinA modulates leukemic B cell vesiculation and their cargo in terms of miRNAs, protects leukemic cells from drug-induced apoptosis and ActivinA-induced EVs participate to this chemoprotective process. Targeting EV-directed communication between leukemic cells and their supportive niche may be a promising new approach to kill leukemic cells and prevent drug resistance.

# References


1. Chiarini F, Lonetti A, Evangelisti C, et al. Advances in understanding the acute lymphoblastic leukemia bone marrow microenvironment: From biology to therapeutic targeting. Biochimica et Biophysica Acta - Molecular Cell Research 2016;1863(3):449–463.
2. Bhojwani D, Yang JJ, Pui CH. Biology of childhood acute lymphoblastic leukemia. *Pediatric Clinics of North America* 2015;62(1):47–60.
3. Alvarnas JC, Co-Chair /, Hopkins J, et al. Acute Lymphoblastic Leukemia NCCN Guidelines ® NCCN Acute Lymphoblastic Leukemia Panel Members. 2015. 1258 p.
4. Preston DL, Kusumi S, Tomonaga M, et al. Supplement: Cancer Incidence in Atomic Bomb Survivors. Radiation Effects Research Foundation, Hiroshima and Nagasaki. 68–97 p.
5. O'Connor D, Bate J, Wade R, et al. Infection-related mortality in children with acute lymphoblastic leukemia: An analysis of infectious deaths on UKALL2003. Blood 2014;124(7):1056–1061.
6. Roberts KG, Mullighan CG. Genomics in acute lymphoblastic leukaemia: insights and treatment implications. Nature Reviews Clinical Oncology 2015;12(6):344–357.
7. Hong D, Gupta R, Ancliff P, et al. Initiating and Cancer-Propagating Cells in TEL-AML1-Associated Childhood Leukemia. Source: Science, New Series 2008;319(5861):336–339.
8. Ren R. Mechanisms of BCR-ABL in the pathogenesis of chronic myelogenous leukaemia. *Nature Reviews Cancer* 2005;5(3):172–183.
9. Kamps MP. E2A-Pbxl Induces Growth, Blocks Differentiation, and Interacts with Other Homeodomain Proteins Regulating Normal Differentiation.
10. Vrooman LM, Silverman LB. Treatment of Childhood Acute Lymphoblastic Leukemia: Prognostic Factors and Clinical Advances. *Current Hematologic Malignancy Reports* 2016;11(5):385–394.
11. Holmfeldt L, Wei L, Diaz-Flores E, et al. The genomic landscape of hypodiploid acute lymphoblastic leukemia. Nature Genetics 2013;45(3):242–252.
12. Mullighan CG, Goorha S, Radtke I, et al. Genome-wide analysis of genetic alterations in acute lymphoblastic leukaemia. Nature 2007;446(7137):758–764.
13. Roberts KG, Morin RD, Zhang J, et al. Genetic Alterations Activating Kinase and Cytokine Receptor Signaling in High-Risk Acute Lymphoblastic Leukemia. Cancer Cell 2012;22(2):153–166.
14. Cooper SL, Brown PA. Treatment of pediatric acute lymphoblastic leukemia. *Pediatric Clinics of North America* 2015;62(1):61–73.
15. Heikamp EB, Pui CH. Next-Generation Evaluation and Treatment of Pediatric Acute Lymphoblastic Leukemia. Journal of Pediatrics 2018;20314-24.e2.
16. R Shofield. The relationship between the spleen colony-forming cell and the haemopoietic stem cell. Blood Cells [Epub ahead of print].

17. Bakker ST, Passegué E. Resilient and resourceful: Genome maintenance strategies in hematopoietic stem cells. *Experimental Hematology* 2013;41(11):915–923.
18. Pietras EM, Warr MR, Passegué E. Cell cycle regulation in hematopoietic stem cells. Journal of Cell Biology 2011;195(5):709–720.
19. Perry JM, Li L. Disrupting the Stem Cell Niche: Good Seeds in Bad Soil. *Cell* 2007;129(6):1045–1047.
20. Kiel MJ, Yilmaz ÖH, Iwashita T, Yilmaz OH, Terhorst C, Morrison SJ. SLAM family receptors distinguish hematopoietic stem and progenitor cells and reveal endothelial niches for stem cells. Cell 2005;121(7):1109–1121.
21. Winkler IG, Barbier V, Nowlan B, et al. Vascular niche E-selectin regulates hematopoietic stem cell dormancy, self renewal and chemoresistance. Nature Medicine 2012;18(11):1651–1657.
22. Poulos MG, Guo P, Kofler NM, et al. Endothelial Jagged-1 Is necessary for homeostatic and regenerative hematopoiesis. Cell Reports 2013;4(5):1022–1034.
23. Yamazaki S, Ema H, Karlsson G, et al. Nonmyelinating schwann cells maintain hematopoietic stem cell hibernation in the bone marrow niche. Cell 2011;147(5):1146–1158.
24. Yamazaki S, Iwama A, Takayanagi S, Eto K, Ema H, Nakauchi H. TGF-β as a candidate bone marrow niche signal to induce hematopoietic stem cell hibernation. Blood 2009;113(6):1250–1256.
25. Bruns I, Lucas D, Pinho S, et al. Megakaryocytes regulate hematopoietic stem cell quiescence through CXCL4 secretion. Nature Medicine 2014;20(11):1315–1320.
26. Zhao M, Perry JM, Marshall H, et al. Megakaryocytes maintain homeostatic quiescence and promote post-injury regeneration of hematopoietic stem cells. Nature Medicine 2014;20(11):1321–1326.
27. Kiel MJ, Morrison SJ. Uncertainty in the niches that maintain haematopoietic stem cells. *Nature Reviews Immunology* 2008;8(4):290–301.
28. Frisch BJ, Porter RL, Calvi LM. Hematopoietic niche and bone meet.
29. Tie2/Angiopoietin-1 Signaling Regulates Hematopoietic Stem Cell Quiescence in the Bone Marrow Niche.
30. Tzeng YS, Li H, Kang YL, Chen WG, Cheng W, Lai DM. Loss of Cxcl12/Sdf-1 in adult mice decreases the quiescent state of hematopoietic stem/progenitor cells and alters the pattern of hematopoietic regeneration after myelosuppression. Blood 2011;117(2):429–439.
31. Zhang J, Niu C, Ye L, et al. Identification of the haematopoietic stem cell niche and control of the niche size. Nature 2003;425(6960):836–841.
32. Calvi LM, Adams GB, Weibrecht KW, et al. Osteoblastic cells regulate the haematopoietic stem cell niche. Nature 2003;425(6960):841–846.
33. Weber JM, Calvi LM. Notch signaling and the bone marrow hematopoietic stem cell niche. *Bone* 2010;46(2):281–285.

34. Stier S, Ko Y, Forkert R, et al. Osteopontin is a hematopoietic stem cell niche component that negatively regulates stem cell pool size. Journal of Experimental Medicine 2005;201(11):1781–1791.
35. Fox N, Priestley G, Papayannopoulou T, Kaushansky K. Thrombopoietin expands hematopoietic stem cells after transplantation. Journal of Clinical Investigation 2002;110(3):389–394.
36. Kollet O, Dar A, Shivtiel S, et al. Osteoclasts degrade endosteal components and promote mobilization of hematopoietic progenitor cells. Nature Medicine 2006;12(6):657–664.
37. Adams GB, Chabner KT, Alley IR, et al. Stem cell engraftment at the endosteal niche is specified by the calcium-sensing receptor. Nature 2006;439(7076):599–603.
38. Naveiras O, Nardi V, Wenzel PL, Hauschka P v., Fahey F, Daley GQ. Bone-marrow adipocytes as negative regulators of the haematopoietic microenvironment. Nature 2009;460(7252):259–263.
39. Zhou BO, Yu H, Yue R, et al. Bone marrow adipocytes promote the regeneration of stem cells and haematopoiesis by secreting SCF. Nature Cell Biology 2017;19(8):891–903.
40. Claycombe K, King LE, Fraker PJ. A role for leptin in sustaining lymphopoiesis and myelopoiesis.
41. Mercier FE, Ragu C, Scadden DT. The bone marrow at the crossroads of blood and immunity. *Nature Reviews Immunology* 2012;12(1):49–60.
42. Degliantoni G, Murphy M, Kobayashi M, Francis MK, Perussia B, Trinchieri G. NATURAL KILLER (NK) CELL-DERIVED HEMATOPOIETIC COLONY-INHIBITING ACTIVITY AND NK CYTOTOXIC FACTOR Relationship with Tumor Necrosis Factor and Synergism with Immune Interferon.
43. Sharara LI, Andersson Å, Guy-Grand D, Fischer A, Disanto JP. Deregulated TCRαβ T cell population provokes extramedullary hematopoiesis in mice deficient in the common γ chain. European Journal of Immunology 1997;27(4):990–998.
44. Urbieta M, Barao I, Jones M, et al. Hematopoietic progenitor cell regulation by CD4+CD25+ T cells. Blood 2010;115(23):4934–4943.
45. Fujisaki J, Wu J, Carlson AL, et al. In vivo imaging of T reg cells providing immune privilege to the haematopoietic stem-cell niche. Nature 2011;474(7350):216–220.
46. Chow A, Lucas D, Hidalgo A, et al. Bone marrow CD169+ macrophages promote the retention of hematopoietic stem and progenitor cells in the mesenchymal stem cell niche. Journal of Experimental Medicine 2011;208(2):761–771.
47. Albiero M, Poncina N, Ciciliot S, et al. Bone marrow macrophages contribute to diabetic stem cell mobilopathy by producing oncostatin M. Diabetes 2015;64(8):2957–2968.
48. Ludin A, Itkin T, Gur-Cohen S, et al. Monocytes-macrophages that express α-smooth muscle actin preserve primitive hematopoietic cells in the bone marrow. Nature Immunology 2012;13(11):1072–1082.

49. Hoggatt J, Singh P, Sampath J, Pelus LM. Prostaglandin E2 enhances hematopoietic stem cell homing, survival, and proliferation. Blood 2009;113(22):5444–5455.
50. Kawano Y, Fukui C, Shinohara M, et al. G-CSF-induced sympathetic tone provokes fever and primes antimobilizing functions of neutrophils via PGE 2 Key Points • G-CSF-induced sympathetic tone provokes fever and modulates microenvironment via PGE 2 production by bone marrow Gr-1 high neutrophils [Epub ahead of print].
51. Frisch BJ, Porter RL, Gigliotti BJ, et al. In vivo prostaglandin E2 treatment alters the bone marrow microenvironment and preferentially expands short-term hematopoietic stem cells. Blood 2009;114(19):4054–4063.
52. Casanova-Acebes M, Pitaval C, Weiss LA, et al. XRhythmic modulation of the hematopoietic niche through neutrophil clearance. Cell 2013;153(5):1025.
53. Mesenchymal progenitor cells localize within hematopoietic sites throughout ontogeny [Epub ahead of print].
54. Friedenstein A, Petrakova K, Kurolesova A, Frolova G. Heterotopic of bone marrow. Analysis of precursor cells for osteogenic and hematopoietic tissues. Transplantation [Epub ahead of print].
55. Greenbaum A, Hsu YMS, Day RB, et al. CXCL12 in early mesenchymal progenitors is required for haematopoietic stem-cell maintenance. Nature 2013;495(7440):227–230.
56. Méndez-Ferrer S, Michurina T v., Ferraro F, et al. Mesenchymal and haematopoietic stem cells form a unique bone marrow niche. Nature 2010;466(7308):829–834.
57. Meisel R, Zibert A, Laryea M, Göbel U, Däubener W, Dilloo D. Human bone marrow stromal cells inhibit allogeneic T-cell responses by indoleamine 2,3-dioxygenase–mediated tryptophan degradation. Blood 2004;103(12):4619–4621.
58. Aggarwal S, Pittenger MF. Human mesenchymal stem cells modulate allogeneic immune cell responses [Epub ahead of print].
59. Waterman RS, Tomchuck SL, Henkle SL, Betancourt AM. A new mesenchymal stem cell (MSC) paradigm: Polarization into a pro-inflammatory MSC1 or an immunosuppressive MSC2 phenotype. PLoS ONE;5(4):.
60. Kreso A, Dick JE. Evolution of the cancer stem cell model. *Cell Stem Cell* 2014;14(3):275–291.
61. Schepers K, Campbell TB, Passegué E. Normal and leukemic stem cell niches: Insights and therapeutic opportunities. *Cell Stem Cell* 2015;16(3):254–267.
62. Hanoun M, Zhang D, Mizoguchi T, et al. Acute myelogenous leukemia-induced sympathetic neuropathy promotes malignancy in an altered hematopoietic stem cell Niche. Cell Stem Cell 2014;15(3):365–375.
63. Arranz L, Sánchez-Aguilera A, Martín-Pérez D, et al. Neuropathy of haematopoietic stem cell niche is essential for myeloproliferative neoplasms. Nature 2014;512(1):78–81.

64. Schepers K, Pietras EM, Reynaud D, et al. Myeloproliferative neoplasia remodels the endosteal bone marrow niche into a self-reinforcing leukemic niche. Cell Stem Cell 2013;13(3):285–299.
65. Jacamo R, Chen Y, Wang Z, et al. Reciprocal leukemia-stroma VCAM-1/VLA-4-dependent activation of NF-κB mediates chemoresistance. Blood 2014;123(17):2691–2702.
66. Døsen-Dahl G, Munthe E, Nygren MK, Stubberud H, Hystad ME, Rian E. Bone marrow stroma cells regulate TIEG1 expression in acute lymphoblastic leukemia cells: Role of TGFβ/BMP-6 and TIEG1 in chemotherapy escape. International Journal of Cancer 2008;123(12):2759–2766.
67. Juarez J, Baraz R, Gaundar S, Bradstock K, Bendall L. Interaction of interleukin-7 and interleukin-3 with the CXCL12-induced proliferation of B-cell progenitor acute lymphoblastic leukemia. Haematologica 2007;92(4):450–459.
68. Frolova O, Samudio I, Benito J, et al. Regulation of HIF-1α signaling and chemoresistance in acute lymphocytic leukemia under hypoxic conditions of the bone marrow microenvironment. Cancer Biology and Therapy 2012;13(10):858–870.
69. Iwamoto S, Mihara K, Downing JR, Pui CH, Campana D. Mesenchymal cells regulate the response of acute lymphoblastic leukemia cells to asparaginase. Journal of Clinical Investigation 2007;117(4):1049–1057.
70. Colmone A, Amorim M, Pontier AL, Wang S, Jablonski E, Sipkins DA. Leukemic Cells Create Bone Marrow Niches That Disrupt the Behavior of Normal Hematopoietic Progenitor Cells. Science 2008;322(5909):1861–1865.
71. Duan C-W, Shi J, Chen J, et al. Leukemia Propagating Cells Rebuild an Evolving Niche in Response to Therapy. Cancer Cell 2014;25(6):778–793.
72. de Rooij B, Polak R, van den Berk LCJ, Stalpers F, Pieters R, den Boer ML. Acute lymphoblastic leukemia cells create a leukemic niche without affecting the CXCR4/CXCL12 axis. *Haematologica* 2017;102(10):e389–e393.
73. Zhang B, Ho YW, Huang Q, et al. Altered Microenvironmental Regulation of Leukemic and Normal Stem Cells in Chronic Myelogenous Leukemia. Cancer Cell 2012;21(4):577–592.
74. Li Z-W, Dalton WS. Tumor microenvironment and drug resistance in hematologic malignancies. Blood Reviews 2006;20(6):333–342.
75. Kim J-A, Shim J-S, Lee G-Y, et al. Microenvironmental Remodeling as a Parameter and Prognostic Factor of Heterogeneous Leukemogenesis in Acute Myelogenous Leukemia. Cancer Research 2015;75(11):2222–2231.
76. Manabe A, Coustan-Smith E, Behm F, Raimondi S, Campana D. Bone marrow-derived stromal cells prevent apoptotic cell death in B-lineage acute lymphoblastic leukemia. Blood [Epub ahead of print].
77. Vilchis-Ordoñez A, Contreras-Quiroz A, Vadillo E, et al. Bone Marrow Cells in Acute Lymphoblastic Leukemia Create a Proinflammatory

Microenvironment Influencing Normal Hematopoietic Differentiation Fates. BioMed Research International 2015;20151–14.
78. Enciso J, Mayani H, Mendoza L, Pelayo R. Modeling the pro-inflammatory tumor microenvironment in acute lymphoblastic leukemia predicts a breakdown of hematopoietic-mesenchymal communication networks. Frontiers in Physiology;7(AUG):
79. Tabe Y, Konopleva M. Role of Microenvironment in Resistance to Therapy in AML. Current Hematologic Malignancy Reports 2015;10(2):96–103.
80. Doepfner KT, Spertini O, Arcaro A. Autocrine insulin-like growth factor-I signaling promotes growth and survival of human acute myeloid leukemia cells via the phosphoinositide 3-kinase/Akt pathway. Leukemia 2007;21(9):1921–1930.
81. Huan J, Hornick NI, Goloviznina NA, et al. Coordinate regulation of residual bone marrow function by paracrine trafficking of AML exosomes. Leukemia 2015;29(12):2285–2295.
82. Huan J, Hornick NI, Shurtleff MJ, et al. RNA Trafficking by Acute Myelogenous Leukemia Exosomes. Cancer Research 2013;73(2):918–929.
83. Chen W, ten Dijke P. Immunoregulation by members of the TGFβ superfamily. Nature Reviews Immunology 2016;16(12):723–740.
84. Harrison CA, Gray PC, Vale WW, Robertson DM. Antagonists of activin signaling: Mechanisms and potential biological applications. *Trends in Endocrinology and Metabolism* 2005;16(2):73–78.
85. Antsiferova M, Werner S. The bright and the dark sides of activin in wound healing and cancer. *Journal of Cell Science* 2012;125(17):3929–3937.
86. Robson NC, Phillips DJ, Mcalpine T, et al. Activin-A: a novel dendritic cell-derived cytokine that potently attenuates CD40 ligand-specific cytokine and chemokine production [Epub ahead of print].
87. Ogawa K, Funaba M, Chen Y, Tsujimoto M. Activin A Functions as a Th2 Cytokine in the Promotion of the Alternative Activation of Macrophages. The Journal of Immunology 2006;177(10):6787–6794.
88. Mantovani A, Sozzani S, Locati M, Allavena P, Sica A. Macrophage polarization: tumor-associated macrophages as a paradigm for polarized M2 mononuclear phagocytes.
89. Robson NC, Wei H, McAlpine T, Kirkpatrick N, Cebon J, Maraskovsky E. Activin-A attenuates several human natural killer cell functions. Blood 2009;113(14):3218–3225.
90. Shiozaki M, Sakai R, Tabuchi M, Eto Y, Kosaka M, Shibai H. Invivo treatment with erythroid differentiation factor (EDF / activin a) increases erythroid precursors (CFU-E and BFU-E) in mice. Biochemical and Biophysical Research Communications 1989;165(3):1155–1161.
91. Shav‐Tal Y, Zipori D. The Role of Activin A in Regulation of Hemopoiesis. Stem Cells 2002;20(6):493–500.
92. SHOHAM T, PARAMESWARAN R, SHAV-TAL Y, BARDA-SAAD M, ZIPORI D. The Mesenchymal Stroma Negatively Regulates B Cell

Lymphopoiesis through the Expression of Activin A. Annals of the New York Academy of Sciences 2003;996(1):245–260.
93. Burdette JE, Jeruss JS, Kurley SJ, Lee EJ, Woodruff TK. Activin A mediates growth inhibition and cell cycle arrest through Smads in human breast cancer cells. Cancer Research 2005;65(17):7968–7975.
94. Hempen PM, Zhang L, Bansal RK, et al. Evidence of Selection for Clones Having Genetic Inactivation of the Activin A Type II Receptor (ACVR2) Gene in Gastrointestinal Cancers 1. 994–999 p.
95. Grusch M, Drucker C, Peter-Vörösmarty B, et al. Deregulation of the activin/follistatin system in hepatocarcinogenesis. Journal of Hepatology 2006;45(5):673–680.
96. Bufalino A, Cervigne NK, de Oliveira CE, et al. Low miR-143/miR-145 Cluster Levels Induce Activin A Overexpression in Oral Squamous Cell Carcinomas, Which Contributes to Poor Prognosis. PLOS ONE 2015;10(8):e0136599.
97. Taylor C, Loomans HA, le Bras GF, et al. Activin a signaling regulates cell invasion and proliferation in esophageal adenocarcinoma. Oncotarget 2015;6(33):34228–34244.
98. Loumaye A, de Barsy M, Nachit M, et al. Circulating Activin A predicts survival in cancer patients. Journal of Cachexia, Sarcopenia and Muscle 2017;8(5):768–777.
99. Hoda MA, Rozsas A, Lang E, et al. High circulating activin A level is associated with tumor progression and predicts poor prognosis in lung adenocarcinoma. Oncotarget 2016;7(12):13388–13399.
100. Bashir M, Damineni S, Mukherjee G, Kondaiah P. Activin-a signaling promotes epithelial–mesenchymal transition, invasion, and metastatic growth of breast cancer. npj Breast Cancer;1.
101. Ramirez MI, Amorim MG, Gadelha C, et al. Technical challenges of working with extracellular vesicles. *Nanoscale* 2018;10(3):881–906.
102. Pan B-T, Johnstone RM. Fate of the transferrin receptor during maturation of sheep reticulocytes in vitro: Selective externalization of the receptor. Cell 1983;33(3):967–978.
103. Harding C, Heuser J, Stahl P. Receptor-mediated endocytosis of transferrin and recycling of the transferrin receptor in rat reticulocytes. Journal of Cell Biology 1983;97(2):329–339.
104. Mathivanan S, Ji H, Simpson RJ. Exosomes: Extracellular organelles important in intercellular communication. *Journal of Proteomics* 2010;73(10):1907–1920.
105. Cocucci E, Meldolesi J. Ectosomes and exosomes: Shedding the confusion between extracellular vesicles. *Trends in Cell Biology* 2015;25(6):364–372.
106. Mathivanan S, Ji H, Simpson RJ. Exosomes: Extracellular organelles important in intercellular communication. *Journal of Proteomics* 2010;73(10):1907–1920.
107. Soler N, Marguet E, Verbavatz J-M, Forterre P. Virus-like vesicles and extracellular DNA produced by hyperthermophilic archaea of the order Thermococcales. Research in Microbiology 2008;159(5):390–399.

108. Knox KW, Vesk M, Work E. Relation Between Excreted Lipopolysaccharide Complexes and Surface Structures of a Lysine-Limited Culture of Escherichia coli. Journal of Bacteriology 1966;92(4):1206–1217.
109. Lee E-Y, Choi D-Y, Kim D-K, et al. Gram-positive bacteria produce membrane vesicles: Proteomics-based characterization of Staphylococcus aureus-derived membrane vesicles. PROTEOMICS 2009;9(24):5425–5436.
110. Tatischeff I, Bomsel M, de Paillerets C, et al. Dictyostelium discoideum cells shed vesicles with associated DNA and vital stain Hoechst 33342. Cellular and Molecular Life Sciences (CMLS) 1998;54(5):476–487.
111. Albuquerque PC, Nakayasu ES, Rodrigues ML, et al. Vesicular transport in *Histoplasma capsulatum* : an effective mechanism for trans-cell wall transfer of proteins and lipids in ascomycetes. Cellular Microbiology 2008;10(8):1695–1710.
112. Rodrigues ML, Nimrichter L, Oliveira DL, et al. Vesicular Polysaccharide Export in Cryptococcus neoformans Is a Eukaryotic Solution to the Problem of Fungal Trans-Cell Wall Transport. Eukaryotic Cell 2007;6(1):48–59.
113. Regente M, Corti-Monzón G, Maldonado AM, Pinedo M, Jorrín J, de la Canal L. Vesicular fractions of sunflower apoplastic fluids are associated with potential exosome marker proteins. FEBS Letters 2009;583(20):3363–3366.
114. Wolf P. The Nature and Significance of Platelet Products in Human Plasma. British Journal of Haematology 1967;13(3):269–288.
115. Gangoda L, Boukouris S, Liem M, Kalra H, Mathivanan S. Extracellular vesicles including exosomes are mediators of signal transduction: Are they protective or pathogenic? *Proteomics* 2015;15(2–3):260–271.
116. Raposo G, Stoorvogel W. Extracellular vesicles: Exosomes, microvesicles, and friends. *Journal of Cell Biology* 2013;200(4):373–383.
117. Keerthikumar S, Gangoda L, Liem M, et al. Proteogenomic analysis reveals exosomes are more oncogenic than ectosomes.
118. Balaj L, Lessard R, Dai L, et al. Tumour microvesicles contain retrotransposon elements and amplified oncogene sequences. Nature Communications 2011;2(1):180.
119. Thakur BK, Zhang H, Becker A, et al. Double-stranded DNA in exosomes: A novel biomarker in cancer detection. *Cell Research* 2014;24(6):766–769.
120. Guescini M, Genedani S, Stocchi V, Agnati LF. Astrocytes and Glioblastoma cells release exosomes carrying mtDNA. Journal of Neural Transmission 2010;117(1):1–4.
121. Ratajczak J, Wysoczynski M, Hayek F, Janowska-Wieczorek A, Ratajczak MZ. Membrane-derived microvesicles: Important and underappreciated mediators of cell-to-cell communication. *Leukemia* 2006;20(9):1487–1495.

122. Kunz F, Kontopoulou E, Reinhardt K, et al. Detection of AML-specific mutations in pediatric patient plasma using extracellular vesicle–derived RNA. Annals of Hematology 2019;98(3):595–603.
123. Reclusa P, Laes JF, Malapelle U, et al. EML4-ALK translocation identification in RNA exosomal cargo (ExoALK) in NSCLC patients: A novel role for liquid biopsy. *Translational Cancer Research* 2019;8S76–S78.
124. Nolte'T Hoen ENM, Buermans HPJ, Waasdorp M, Stoorvogel W, Wauben MHM, 'T Hoen PAC. Deep sequencing of RNA from immune cell-derived vesicles uncovers the selective incorporation of small non-coding RNA biotypes with potential regulatory functions. Nucleic Acids Research 2012;40(18):9272–9285.
125. Yang Q, Diamond MP, Al-Hendy A. The emerging role of extracellular vesicle-derived miRNAs: implication in cancer progression and stem cell related diseases.
126. Zhang B, Pan X, Cobb GP, Anderson TA. microRNAs as oncogenes and tumor suppressors. Developmental Biology 2007;302(1):1–12.
127. Fong MY, Zhou W, Liu L, et al. Breast-cancer-secreted miR-122 reprograms glucose metabolism in premetastatic niche to promote metastasis. Nature Cell Biology 2015;17(2):183–194.
128. Lunavat TR, Cheng L, Einarsdottir BO, et al. BRAFV600 inhibition alters the microRNA cargo in the vesicular secretome of malignant melanoma cells. Proceedings of the National Academy of Sciences of the United States of America 2017;114(29):E5930–E5939.
129. Liu Y, Luo F, Wang B, et al. STAT3-regulated exosomal miR-21 promotes angiogenesis and is involved in neoplastic processes of transformed human bronchial epithelial cells. Cancer Letters 2016;370(1):125–135.
130. Liao J, Liu R, Shi YJ, Yin LH, Pu YP. Exosome-shuttling microRNA-21 promotes cell migration and invasion-targeting PDCD4 in esophageal cancer. International Journal of Oncology 2016;48(6):2567–2579.
131. Qin X, Yu S, Zhou L, et al. Cisplatin-resistant lung cancer cell–derived exosomes increase cisplatin resistance of recipient cells in exosomal miR-100–5p-dependent manner. International Journal of Nanomedicine 2017;123721–3733.
132. Yeh Y-Y, Ozer HG, Lehman AM, et al. Characterization of CLL exosomes reveals a distinct microRNA signature and enhanced secretion by activation of BCR signaling [Epub ahead of print].
133. Paggetti J, Haderk F, Seiffert M, et al. Exosomes released by chronic lymphocytic leukemia cells induce the transition of stromal cells into cancer-associated fibroblasts. Blood 2015;126(9):1106–1117.
134. Bouvy C, Wannez A, Laloy J, Chatelain C, Dogné JM. Transfer of multidrug resistance among acute myeloid leukemia cells via extracellular vesicles and their microRNA cargo. Leukemia Research 2017;6270–76.
135. Mirzaei H, Sahebkar A, Jaafari MR, Goodarzi M, Mirzaei HR. Diagnostic and Therapeutic Potential of Exosomes in Cancer: The

Beginning of a New Tale? *Journal of Cellular Physiology* 2017;232(12):3251–3260.

136. Pant S, Hilton H, Burczynski ME. The multifaceted exosome: Biogenesis, role in normal and aberrant cellular function, and frontiers for pharmacological and biomarker opportunities. *Biochemical Pharmacology* 2012;83(11):1484–1494.

# 5. Publications

Dander E, Fallati A, Gulic T, Pagni F, Gaspari S, Silvestri D, **Cricrì Giulia**, Bedini G, Portale F, Buracchi C, Brizzolara L, Maglia O, Mantovani A, Garlanda C, Valsecchi MG, Locatelli F, Biondi A, Bottazza B, Allavena P, D'Amico. "*Altered monocyte and macrophage compartments are part of the extensive remodeling of the immune microenvironment in B-ALL pathology*". Under revision for the British Journal of Hematology.

Portale F. **Cricrì Giulia**, Bresolin S, Lupi M, Gaspari S, Silvestri D, Russo B, Marino N, Ubezio P, Pagni F, Vergani P, Te Kronnie G, Valsecchi MG, Locatelli F, Rizzari C, Biondi A, Dander E, D'Amico G. "*ActivinA: a new leukemia-promoting factor conferring migratory advantage to B-cell precursor-acute* lymphoblastic leukemic cells". Haematologica, 2019,104(3):533-545. (https://doi.org/10.3324/haematol.2018.188664)